

UC Santa Cruz

UC Santa Cruz Electronic Theses and Dissertations

Title

Impacts of Global Environmental Change on Fish and Fisheries of the Northeastern Pacific Ocean

Permalink

<https://escholarship.org/uc/item/7d53h7c9>

Author

Willis-Norton, Ellen Margaret

Publication Date

2022

Copyright Information

This work is made available under the terms of a Creative Commons Attribution-NonCommercial-NoDerivatives License, available at <https://creativecommons.org/licenses/by-nc-nd/4.0/>

Peer reviewed|Thesis/dissertation

UNIVERSITY OF CALIFORNIA
SANTA CRUZ

**IMPACTS OF GLOBAL ENVIRONMENTAL CHANGE ON FISH AND
FISHERIES OF THE NORTHEASTERN PACIFIC OCEAN**

A dissertation submitted in partial satisfaction of
the requirements for the degree of

DOCTOR OF PHILOSOPHY

In

ECOLOGY & EVOLUTIONARY BIOLOGY

By

Ellen Willis-Norton

September 2022

The Dissertation of Ellen Willis-Norton is approved:

Professor Mark H. Carr, chair

Elliott Hazen, Ph.D.

Professor Kristy J Kroeker

Steven J. Bograd, Ph.D.

Peter Biehl
Vice Provost and Dean of Graduate Studies

Copyright © by

Ellen Willis-Norton 2022

Table of Contents

List of Figures and Tables	iv
Abstract	xix
Acknowledgements	xxi
Introduction	1
Chapter 1: Multistressor global change drivers reduce successful hatch and viability of Lingcod embryos (<i>Ophiodon elongatus</i>), a benthic egg layer in the California Current System	5
Chapter 2: Climate-driven shifts in predator-prey interactions for commercially and ecologically important Eastern Bering Sea fishes	45
Chapter 3: Market squid fishery participant responses to past climate perturbations: Implications for a socio-ecological fishery network as climate change progresses	95
Conclusions and Future Directions	128
Bibliography:	131

List of Figures and Tables

Figure 1.1: Conceptual figure illustrating the flow-through experimental mesocosm. Blue represents the year 2020 treatment, yellow represents year 2050, and red represents year 2100. The ambient and climate change sump tank water (cylinders) is mixed as it flows to the header tanks (circles) to attain the setpoints for each treatment. There are two replicate header tanks for each treatment and each header tank supplies water to three replicate aquaria (squares), for a total of six replicate aquaria for each treatment.

Figure 1.2: Temperature, pH, and DO values measured over the duration of the experiment for the year 2020 (blue), year 2050 (yellow), and year 2100 (red) treatments. Temperature and pH values were measured every 15 seconds by Durafet sensors in the header tanks (lines) and once daily by YSI sensors in the replicate aquaria (triangles). DO concentration was measured by Vernier sensors every 15 minutes in the header tanks (lines) and once daily by YSI sensors in the replicate aquaria (triangles).

Table 1.1: Mean and standard deviation of the temperature, pH, and DO conditions measured by YSI sensors in the replicate aquaria over the duration of the experiment.

Figure 1.3: Illustration of the 10 measurements taken for each larval image using ImageJ.

Table 1.2: Mean and standard deviation of degree days and calendar days to first hatch, degree and calendar days to 50% hatch, and total number of hatch days for the year 2020, year 2050, and year 2100 treatments. Nested mixed model ANOVAs were run to determine statistical significance. Pairwise comparisons for degree days to first hatch ($p_{2020,2050}<1\times 10^{-4}$, $p_{2050,2100}<1\times 10^{-4}$, $p_{2020,2100}=0$), degree days to 50% hatch ($p_{2020,2050}<1\times 10^{-4}$, $p_{2050,2100}<1\times 10^{-4}$, $p_{2020,2100}=0$), and total number of hatch days ($p_{2020,2050}=3.7\times 10^{-3}$, $p_{2050,2100}<1\times 10^{-4}$, $p_{2020,2100}=0$) were significantly different. Calendar days to first hatch ($p_{2020,2050}=0.11$, $p_{2050,2100}=0.02$, $p_{2020,2100}=0.29$) and calendar days to 50% hatch ($p_{2020,2050}=0.01$, $p_{2050,2100}=0.15$, $p_{2020,2100}=1$) were not significantly different.

Figure 1.4: Boxplots illustrating the median, upper and lower quartile, and interquartile range of percent total hatch for the year 2020 (blue), year 2050 (yellow), and year 2100 (red) treatments. The average percent hatch was 19% for the year 2020 treatment, 9% for the year 2050 treatment, and 0.6% for the year 2100 treatment. Nested mixed model ANOVAs were run to determine statistical significance, letters indicate significant differences ($p_{2020,2050}=3\times 10^{-4}$, $p_{2050,2100}=4\times 10^{-3}$, $p_{2020,2100}<1\times 10^{-4}$).

Figure 1.5: Linear regression for Lingcod larvae weight (μg) as the hatch period progresses for the year 2020 (blue), year 2050 (yellow), and year 2100 (red)

treatment. A nested mixed model ANOVA was run to determine statistical significance ($p_{2020,2050}=0.21$, $p_{2050,2100}<1 \times 10^{-4}$, $p_{2020,2100}<1 \times 10^{-4}$).

Table 1.3: Mean and standard deviations of morphometric data for Lingcod larvae samples from year 2020, year 2050, and year 2100 treatments. Count (n=) represents the number of larvae measured using ImageJ for each treatment, not the total hatch number. Treatments with different letters for each response variable were significantly different (nested mixed model ANOVAs; $p < 0.01$).

Table 1.4: Mean and standard deviation for the percent of larvae from each 1g Lingcod egg mass that had a deformity in the seven deformity categories for the year 2020, year 2050, and year 2100 treatments. N represents the number of images analyzed for each treatment. Nested mixed model ANOVAs were run to determine statistical significance, letters indicate significant differences ($p < 0.01$).

Figure 1.6: A) Boxplots illustrating the median, upper and lower quartile, and interquartile range of the C:N ratio for the year 2020 (blue), year 2050 (yellow), and year 2100 (red) treatments ($p_{2020,2050}=0.27$, $p_{2050,2100}<1 \times 10^{-4}$, $p_{2020,2100}<1 \times 10^{-4}$). B) fraction of total weight (μg) comprised of total N and total C for each treatment. C) Boxplots illustrating the median, upper and lower quartile, and interquartile range of the concentration (per mille) of nitrogen-15 in each treatment ($p_{2020,2050}=0.57$,

$p_{2050,2100} < 1 \times 10^{-4}$, $p_{2020,2100} < 1 \times 10^{-4}$). Nested mixed model ANOVAs were run to determine statistical significance, letters indicate significant differences.

Supplementary Figure 1.1: Map of Monterey Bay, CA (black rectangle) showing location of lingcod egg mass collection (blue circle).

Supplementary Table 1.1: Discrete water samples were collected at three time points (2/12, 2/21, 3/2) from each replicate aquaria (n=6 per treatment) during the experiment. Tris buffer-calibrated YSI sensors measured pH, temperature, DO, and salinity at the time of discrete water sample collection. Total alkalinity from these discrete samples was measured using a Metrohm 815 Robotic USB Sample Processor XL and Titrando 905. The CO2SYS package was used to obtain the detailed state of the carbonate system.

Supplementary Figure 1.2: Boxplots illustrating the median, upper and lower quartile, and interquartile range of mass specific respiration rates ($\mu\text{mol}/\text{min}/\text{g}$) for Lingcod embryos placed in the year 2020 (blue), year 2050 (yellow), and year 2100 (red) treatments. $P > 0.01$ for all pairwise comparisons ($p_{2020,2050} = 0.85$, $p_{2050,2100} = 0.98$, $p_{2020,2100} = 0.93$).

Supplementary Figure 1.3: Boxplots illustrating the median, upper and lower quartile, and interquartile range of percent total hatch, percent hatch of larvae with oil

globules, and percent hatch of larvae without deformities for the year 2020 (blue), year 2050 (yellow), and year 2100 (red) treatments. Nested mixed model ANOVAs were run to determine statistical significance. The percent of larvae with oil globules was significantly lower in the future condition treatments compared to the year 2020 treatment ($p_{2020,2050}<0.001$, $p_{2050,2100}=0.06$, $p_{2020,2100}<0.001$). The percent of larvae with deformities was statistically similar between the year 2020 and year 2050 treatment; the percent of larvae with deformities significantly increased in year 2100 conditions ($p_{2020,2050}=0.1$, $p_{2050,2100}=0.01$, $p_{2020,2100}<1 \times 10^{-4}$).

Figure 2.1: The four predator species of interest and their focal prey species in the EBS (percent weight in predator diet listed on right-hand side).

Figure 2.2: Bottom temperature projections from SODA's ocean reanalysis that were statistically downscaled for the Eastern Bering Sea. A) Projections from the modeled baseline period (1982-2014). B) RCP 8.5 projections for 2081-2100. Projections are the average across 18 earth system models from CMIP5, missing grid cells are locations not adequately sampled by the Eastern Bering Sea trawl survey.

Figure 2.3: Area overlap between predator-prey pairs during the historical period (1982-2019) and for the projected period (2021-2040 through 2081-2100). Each panel shows the proportion of the study area where the predator co-occurs with its prey (0-1 scale) within the Eastern Bering Sea trawl survey region for predators: A) Pacific

Cod, B) Arrowtooth Flounder, C) Pacific Halibut, and D) Adult Walleye Pollock. Each line in the figures represents the predator's overlap with a single prey species: Juvenile Walleye Pollock (blue), Alaskan Pink Shrimp (pink), Tanner Crab (green), and Snow Crab (purple). Shaded regions in the projections represent the 95% confidence interval from the ensemble of 18 earth system models

Figure 2.4: Pacific Cod's spatial overlap, calculated using Hurlbert's Index, with A) juvenile Walleye Pollock, B) Alaskan Pink Shrimp, C) Tanner Crab, and D) Snow Crab for 2007-2020 projections (left), 2081-2100 projections (center), and the change in overlap between the current and future projections (right). Hurlbert's Index was used to illustrate the spatial overlap projections because it is the only encounter metric that explicitly accounts for the size of the area occupied by each species (shared legend in bottom center panel; Carroll et al. 2019). Change in overlap was calculated by subtracting the 2081-2100 from the 2007-2020 overlap projections for each grid cell and then calculating the z-score for each grid cell. Blue represents a likely decrease in future predator-prey overlap, red represents a likely increase in predator-prey overlap (shared legend in bottom right panel).

Figure 2.5: Arrowtooth Flounder's projected spatial overlap, calculated using Hurlbert's Index, with A) juvenile Walleye Pollock and B) Alaskan Pink Shrimp for SODA's 2007-2020 projections (left), 2081-2100 projections (center), and the change in overlap between the current and future projections (right).

Figure 2.6: Pacific Halibut's projected spatial overlap, calculated using Hurlbert's Index, with A) juvenile Walleye Pollock, B) Tanner Crab, and C) Snow Crab for SODA's 2007-2020 projections (left), 2081-2100 projections (center), and the change in overlap between the current and future projections (right).

Figure 2.7: Adult Walleye Pollock's projected spatial overlap, calculated using Hurlbert's Index, with juvenile Walleye Pollock for SODA's 2007-2020 projections (left), 2081-2100 projections (center), and the change in overlap between the current and future projections (right).

Figure 2.8: Shifts in the global index of collocation between predator-prey pairs during the historical period (1982-2019) and for the projected period (2030 through 2100). Each panel shows the geographical distinctness between a predator and their prey's centres of gravity within the Eastern Bering Sea trawl survey region (0 is completely distinct and 1 is coincident) for predators: A) Pacific Cod, B) Arrowtooth Flounder, C) Pacific Halibut, and D) Adult Walleye Pollock. Each line in the figures represents the predator's overlap with a single prey species: Juvenile Walleye Pollock (blue), Alaskan Pink Shrimp (pink), Tanner Crab (green), and Snow Crab (purple).

Supplementary Table 2.1: Deviance explained, AUC, and AIC of the selected presence/absence and abundance GAM for the predator and prey species.

Supplementary Table 2.2: Table adapted from Carroll et al. 2019 showing the three spatial predator-prey overlap metrics used for my historical and future projections of changes in species overlap in the Eastern Bering Sea. $A_{pred, prey}$ is the area occupied by both species, A_{total} is the total size of the study area, $A_{occupied}$ is the total area occupied by at least one of the species. p_{pred_i} and p_{prey_i} are the proportions of the total number of predator and prey in grid cell i . $CG_{pred,l}$ is the latitude or longitude (l) centre of gravity for the predator (same formula for prey). I is Inertia.

Supplementary Figure 2.1: Generalized additive model response curves for sea bottom temperature from binary presence/absence models for species A-H. Solid black lines are the fitted relationships between sea bottom temperatures and the partial responses, with the gray shaded area representing the 95% confidence interval. The predicted probability of occurrence is <0 below the dashed horizontal line and >0 above the dashed horizontal line. Black dashes along the x axis show the density of sea bottom temperature values observed in the survey. The vertical scale is the same for species A-D (-10 to 5) and the same for species E-H (-4 to 2).

Supplementary Figure 2.2: Generalized additive model response curves for sea surface temperature from binary presence/absence models for species A-G. Sea surface temperature was not significant for the juvenile Walleye Pollock GAM. Solid black lines are the fitted relationships between sea surface temperatures and the

partial responses, with the gray shaded area representing the 95% confidence interval. The predicted probability of occurrence is <0 below the dashed horizontal line and >0 above the dashed horizontal line. Black dashes along the x axis show the density of sea surface temperature values observed in the survey. The vertical scale is the same for species A-B (-4 to 8) and the same for species C-G (-4 to 4).

Supplementary Figure 2.3: Generalized additive model response curves for delta temperature (the difference between sea surface temperature and sea bottom temperature) from binary presence/absence models for species A-F. Delta temperature was not significant for the adult and juvenile Walleye Pollock GAMs. Solid black lines are the fitted relationships between delta temperatures and the partial responses, with the gray shaded area representing the 95% confidence interval. The predicted probability of occurrence is <0 below the dashed horizontal line and >0 above the dashed horizontal line. Black dashes along the x axis show the density of delta temperature values observed in the survey. The vertical scale is the same for species A-B (-7.5 to 5) and the same for species C-G (-4 to 2).

Supplementary Figure 2.4: Generalized additive model response curves for depth from binary presence/absence models for species A-F. Depth was not significant for the Pacific Cod and juvenile Walleye Pollock GAMs. Solid black lines are the fitted relationships between depth and the partial responses, with the gray shaded area representing the 95% confidence interval. The predicted probability of occurrence is

<0 below the dashed horizontal line and >0 above the dashed horizontal line. Black dashes along the x axis show the density of depths observed in the survey.

Supplementary Figure 2.5: Generalized additive model response curves for grain size from binary presence/absence models for species A-H. Solid black lines are the fitted relationships between depth and the partial responses, with the gray shaded area representing the 95% confidence interval. The predicted probability of occurrence is <0 below the dashed horizontal line and >0 above the dashed horizontal line. Black dashes along the x axis show the density of squared grain sizes observed in the survey. The vertical scale is the same for species A-D (-2 to 2) and same for species C-G (-4 to 2).

Supplementary Figure 2.6: Generalized additive model response curves for rugosity from binary presence/absence models for species A-G. Rugosity was not significant for the Arrowtooth Flounder abundance GAM. Solid black lines are the fitted relationships between depth and the partial responses, with the gray shaded area representing the 95% confidence interval. The predicted probability of occurrence is <0 below the dashed horizontal line and >0 above the dashed horizontal line. Black dashes along the x axis show the density of rugosities observed in the survey.

Supplementary Figure 2.7: Generalized additive model response curves for sea bottom temperature from log catch per unit effort models assuming presence for

species A-H. Solid black lines are the fitted relationships between sea bottom temperature and the partial abundance responses, with the gray shaded area representing the 95% confidence interval. Black dashes along the x axis show the density of sea bottom temperatures observed in the survey.

Supplementary Figure 2.8: Generalized additive model response curves for sea surface temperature from log catch per unit effort models assuming presence for species A-H. Solid black lines are the fitted relationships between sea bottom temperature and the partial abundance responses, with the gray shaded area representing the 95% confidence interval. Black dashes along the x axis show the density of sea surface temperatures observed in the survey. The vertical scale is the same for species A-G (-2 to 2) and changes for species H (-6 to 6).

Supplementary Figure 2.9: Generalized additive model response curves for delta temperature (the difference between sea surface temperature and sea bottom temperature) from log catch per unit effort models assuming presence for species A-H. Solid black lines are the fitted relationships between delta temperature and the partial abundance responses, with the gray shaded area representing the 95% confidence interval. Black dashes along the x axis show the density of delta temperatures observed in the survey.

Supplementary Figure 2.10: Generalized additive model response curves for depth from log catch per unit effort models assuming presence for species A-E. Depth was not significant for the Pacific Cod, adult Walleye Pollock, and juvenile Walleye Pollock abundance GAMs. Solid black lines are the fitted relationships between depth and the partial abundance responses, with the gray shaded area representing the 95% confidence interval. Black dashes along the x axis show the density of depths observed in the survey.

Supplementary Figure 2.11: Generalized additive model response curves for grain size from log catch per unit effort models assuming presence for species A-H. Solid black lines are the fitted relationships between depth and the partial abundance responses, with the gray shaded area representing the 95% confidence interval. Black dashes along the x axis show the density of squared grain sizes observed in the survey.

Supplementary Figure 2.12: Generalized additive model response curves for rugosity from log catch per unit effort models assuming presence for species A-H. Solid black lines are the fitted relationships between depth and the partial abundance responses, with the gray shaded area representing the 95% confidence interval. Black dashes along the x axis show the density of rugosities observed in the survey. The vertical scale is the same for species A-E (-0.50 to 0.50) and the same for species F-H (-2 to 1).

Supplementary Figure 2.13: Maps of historical (2007-2020) and future (2081-2100) biomass for each grid cell of the Eastern Bering Sea trawl survey region for the four predator species: A) adult Walleye Pollock, B) Arrowtooth Flounder, C) Pacific Cod, and D) Pacific Halibut. Projections are the average across 18 earth system models (CMIP5; RCP8.5). Range extent was defined as the mean presence/absence probability for the entire trawl area. The projected CPUE for each grid cell was summed throughout the trawl region to obtain the total biomass estimate.

Supplementary Figure 2.14: Maps of current (2007-2020) and future (2081-2100) projected biomass for each grid cell of the Eastern Bering Sea trawl survey region for the four prey species: A) juvenile Walleye Pollock, B) Alaskan Pink Shrimp, C) Tanner Crab, and D) Snow Crab. Range extent was defined as the mean presence/absence probability for the entire trawl area. The projected CPUE for each grid cell was summed throughout the trawl region to obtain the total biomass estimate.

Supplementary Figure 2.15: Yearly temperature anomaly for the Eastern Bering Sea based on the average observed temperature from 1982-2019.

Figure 3.1: Total pounds caught (left) and number of participating vessels (right) per year (2005-2021) for vessels that use brail and purse/drum seine gear with home ports north of 35° lat (blue) and south of 35° lat (red). Dashed vertical lines indicate the

strongest La Niña (2010-2011; blue), strongest El Niño (2015-2016; red), and the neutral period in-between (gray).

Figure 3.2: Total pounds purchased (left) and number of participating buyers (right) per year (2005-2021) for buyers with plant locations north of 35° lat (blue), south of 35° lat (red), and in both the north and south of California (purple). Dashed vertical lines indicate the strongest La Niña (2010-2011; blue), strongest El Niño (2015-2016; red), and the neutral period in-between (gray).

Figure 3.3: Proportion of squid landed in northern ports (>35° lat; blue) versus southern ports (<35° lat; red).

Figure 3.4: Average distance traveled between fishing location (centroid of reported fishing block) and A) Northern California landings ports and B) Southern California landing ports. Vessels were separated based on gear type and home port location, north of 35° lat (blue) and south of 35° lat (red). Brail vessels were not included for Northern California landing ports to adhere to confidentiality requirements. Dashed vertical lines indicate the strongest La Niña (2010-2011; blue), strongest El Niño (2015-2016; red), and the neutral period in-between (gray).

Figure 3.5: A) Network between squid vessels and buyers, B) network between vessels using purse/drum seines and landing port (center), and C) network between

vessels using brail gear and landing port (right) for the strongest El Niño (2015-2016), La Niña (2010-2011), and a neutral year (2012-2013).

Figure 3.6: Matrix showing vessel-buyer interactions for 2015-2016 El Niño, 2010-2011 La Niña, and 2012-2013 (a neutral year). Darker colors represent a greater number of interactions. Boxes created with blue lines represent vessel-buyer communities identified using the Louvain method.

Figure 3.7: Projected center of gravity by latitude from 1980-2100 for the three GCMs (ROMs-GFDL; ROMs-HAD and ROMs-IPSL). Gray bounding box shows the 2005-2021 time period (the start of the Market Squid fishery management plan).

Figure 3.8: Projected habitat suitability (probability of occurrence between 0-1) for 1985-2015 (left) and 2070-2100 (right) for the three GCMs: A) ROMs-GFDL, B) ROMs-HAD, and C) ROMs-IPSL.

Supplementary Table 3.1: Fields used to run my analyses for each CDFW acquired data set.

Supplementary Table 3.2: Number of landings receipts for the entire study period (2005-2021), the El Niño period (2015-2016), the La Niña period (2010-2011), and the neutral period (2012-2013).

**IMPACTS OF GLOBAL ENVIRONMENTAL CHANGE ON
FISH AND FISHERIES OF THE NORTHEASTERN
PACIFIC OCEAN**

by

Ellen Willis-Norton

Abstract

Marine fishes' intolerance to global change conditions can affect the abundance and distribution of ecologically and economically important species, reshape the structure of trophic webs, and profoundly impact the human communities that rely on fished species for their livelihood and culture. Only by understanding the vulnerability of fished species and fishing communities to global change can we take effective adaptive action and implement climate-ready fisheries management. In this dissertation, I investigate the vulnerability of eight commercially important fished species and one fishing community to global change in the Northeastern Pacific Ocean. In chapter one, I expose Lingcod (*Ophiodon elongatus*), a benthic egg layer, to temperature, oxygen, and pH conditions we expect to see in the Central California Current System (CCS) by the year 2050 and 2100. I examine both the lethal and sublethal effects of these two multistressor climate change scenarios by measuring differences in metabolic rate, hatching success, and larval quality between treatments. In chapter two, I use a species distribution modeling approach to evaluate how historical (1982-2019) and projected (2030 through end-of-century) warming in the

Eastern Bering Sea (EBS), Alaska, affects predator-prey interactions for some of the most commercially valuable fisheries in the U.S. These species include: 1) Pacific Cod (*Gadus macrocephalus*), 2) Pacific Halibut (*Hippoglossus stenolepis*), 3) Arrowtooth Flounder, 4) Walleye Pollock (*Gadus chalcogrammus*), 5) Tanner Crab (*Chionoecetes bairdi*), 6) Snow Crab (*Chionoecetes opilio*), and 7) Alaskan Pink Shrimp (*Pandalus eous*). In chapter three, I use social network analyses to depict the resilience and adaptability of the California Market Squid fishery (*Doryteuthis opalescens*), the most valuable in the state, to climate perturbations and project changes in habitat suitability by the year 2100 in the CCS. By using all of these vulnerability assessment tools, we can begin to prepare U.S. west coast fisheries for global environmental change.

Acknowledgements

I am profoundly grateful for my dissertation committee, they are all engaged, encouraging, and deeply kind people. They have made my PhD experience one I will look back on with fondness and I am incredibly lucky. Elliott Hazen has been my mentor since I was an undergraduate. From spending every day in his office at 20 years-old peppering him with questions; to encouraging me to publish my first paper while I was working in San Francisco; to being my PhD advisor for seven long years. He is one of the most productive people I know and manages so many commitments, but he has always known when to support me when I've needed it or when to give me space when I've needed it. He has provided me with a network of scientists (many of whom are co-authors and mentors themselves) that will last a lifetime. Mark Carr welcomed me to his lab and ever since has shown enthusiasm and curiosity for my research, helping me generate ideas and making sure I had the resources to do the research that excited me. Mark has always made himself available, getting me through working from home during the pandemic with our weekly check-ins and allowing me to pop into his office any time for a myriad of questions.

Kristy Kroeker is a scientist and person I have looked up to since I started at UCSC, and I am so lucky she adopted me into her lab. I knew I wanted to explore the field of global change biology outside of modeling work and Kristy gave me the support, connections, and resources I needed to learn about a field I had no experience in as a later-stage PhD student. She has generated a lab full of people I call my friends,

creating a community that is welcoming, fun, and hard-working. I am so grateful to everyone in the Kroeker Lab that took the time to teach me all about mesocosm experiments. Steven Bograd was the first person to sit me down and on a pad of paper teach me the basics of oceanography. He is an excellent scientist, who somehow manages to run a lab while remaining thoughtful and gentle, cultivating curiosity. I'm continually impressed by every comment or idea he provides, they are always extremely valuable. Carrie Pomeroy has introduced me to the world of the human dimensions of fisheries. She has taught me to pause in my rush to crunch data, to think about the strength of fishing identities and relationships that form social systems that allow communities to be resilient in the face of global change. I am grateful she was there at the beginning of what I hope is a career spent researching fishing communities.

There are too many undergraduate volunteers, lab members, and departmental colleagues to thank. Know that I have chosen to continue in academia because of your excitement for learning, your support of my research, and just being fun to work in the same building as. I am also grateful for the funding I have received that has allowed me to finish my dissertation including the NSF Graduate Research Fellowship Program, the Earl and Ethel Myers Oceanographic and Marine Biology Trust, and UCSC's Ecology and Evolutionary Biology Department.

Introduction

As global environmental change progresses, marine species are being exposed to novel environmental conditions (IPCC 2021; Doney et al. 2012; Poloczanska 2016; Song et al. 2021). Physiological intolerance to future ocean conditions can affect development, growth, survival, the timing of ontogenetic transitions, and reproductive success (Harley et al. 2006; Cheung et al. 2010; Doney et al. 2012; Free et al. 2019). These demographic effects cause population level shifts in abundance and distribution; and these shifts may differ between species in adapted trophic relationships, reshaping ecological relationships (Brander 2010; Doney et al. 2012). For many marine fishes, changes in their abundance and distribution will not only impact the structure, dynamics and resilience of ecological communities, but also the human communities that rely on these resources.

Climate-ready fisheries management is a top priority for U.S. management and governance bodies that seek to prepare for and build resilience to global environmental change. Successful climate-ready management requires a foundation of knowledge on both the vulnerabilities and likely responses to future ocean conditions (Bell et al. 2020). There are many different approaches to evaluate ecological and socio-economic vulnerability to climate change. Trait-based climate vulnerability assessments rank species' and community's exposure, sensitivity, and adaptive capacity to climate change (Pacifci et al. 2015; Dudley et al. 2021); species distribution models predict future suitable habitat (Elith and Leathwick 2009); mesocosm experiments expose species to projected future conditions and examine

changes in development, growth, and survival(Stewart et al. 2013); hindcasts show how species and communities have responded to past environmental change as a prediction of future behavior (Pinsky et al. 2013); network analyses examine the adaptability and resilience of fishing communities to past climate perturbations (Fisher 2021).

In this dissertation, I improve our current understanding of the impact of climate change on 10 fished species and one fishing community in the highly productive waters off the U.S. West Coast (Alaska and California). Commercial fisheries in the region are managed by the Pacific Fisheries Management Council (California), California Department of Fish and Wildlife, the North Pacific Fisheries Management Council (Alaska), and Alaska Department of Fish and Game. Over half of the nation's commercially harvested fish come from Alaska; combined the commercial and recreational fishing industry in Alaska supports a \$8.7 billion industry and 52,500 jobs annually (NMFS 2022). Commercial and recreational fisheries support a \$1.5 billion industry and 10,000 jobs in California (NMFS 2022). There is a substantial amount of literature modeling the impact of climate change on the adult life stage of commercially fished species along the U.S. West Coast. However, there is a critical data gap for how climate change will impact early life history stages, species interactions, and fishing communities.

In **chapter one**, I examined how the earliest life history stage of Lingcod (*Ophiodon elongatus*), a commercially and recreationally important species and an ecologically significant predator, will be impacted by future warming, acidification,

and deoxygenation. I ran a flow-through mesocosm experiment that exposed Lingcod eggs collected from Monterey Bay, CA to conditions we expect to see in central California by the year 2050 and 2100. I measured differences in metabolic rate, hatching success, and larval quality to assess if recruitment rates will shift with climate change. This experiment is the first to expose marine benthic eggs to future temperature, pH, and dissolved oxygen conditions in concert.

In **chapter two**, I evaluated how projected warming in the Eastern Bering Sea, the largest marine ecosystem in Alaska, will impact predator-prey relationships for some of the most commercially valuable fisheries in the U.S. Shifts in predator-prey interactions can alter the size and location of prey refuges, reduce predator biomass more than individual model results anticipate, and shift the relative importance of prey species in predator diets. I use a species distribution modeling approach to project changes in the distribution, abundance, and predator-prey overlap for 1) adult Walleye Pollock (*Gadus chalcogrammus*), 2) Pacific Cod (*Gadus macrocephalus*), 3) Pacific Halibut (*Hippoglossus stenolepis*), 4) Arrowtooth Flounder and their prey species: 1) juvenile Walleye Pollock, 2) Tanner Crab (*Chionoecetes bairdi*), 3) Snow Crab (*Chionoecetes opilio*), and 4) Alaskan Pink Shrimp (*Pandalus eous*).

In **chapter three**, I moved beyond looking at species-level climate change impacts and examined how fishing communities may be affected by global environmental change. Market squid (*Doryteuthis opalescens*) is routinely ranked as the top commercial fishery in California (NMFS 2018). I first used a species distribution model to examine historical variability in the distribution and abundance

of market squid. I then used a network analysis approach to determine if changes in the distribution and abundance of market squid impacted the spatial and social network between fishing community participants. For example, I examined whether El Niño conditions (i.e., a warm year) affected relationships between fishing vessels and California ports, vessels and seafood buyers, and seafood buyers and ports.

Projecting how global environmental change will impact marine fishes and fishing communities is complex. It is important to understand how the most vulnerable life stages will be impacted by multiple stressors and how species' varying physiological limits will impact species interactions and thus ecosystem stability. If we can project the impacts of global environmental change on marine fishes, we can assess the vulnerability and adaptability of communities that rely on these resources.

Chapter 1: Multistressor global change drivers reduce successful hatch and viability of Lingcod embryos (*Ophiodon elongatus*), a benthic egg layer in the California Current System

Abstract

Early life history stages of marine fishes are often more susceptible to environmental stressors than the adult stage. This vulnerability is likely exacerbated for species that lay benthic egg masses bound to substrate because the embryos cannot evade locally unfavorable environmental conditions. As global change progresses, we need to assess the lethal and sublethal effects of exposing this sensitive life stage to future warming, acidification, and deoxygenation so we can manage for the resilience of species, communities, and the fisheries they support. Lingcod (*Ophiodon elongatus*), a benthic egg layer, is an abundant and ecologically significant predator, and contributes to economically important recreational and commercial fisheries in the highly-productive California Current System (CCS). Here I ran a flow-through mesocosm experiment that exposed Lingcod eggs collected from Monterey Bay, CA to conditions I expect to see in the central CCS by the year 2050 and 2100. Throughout the month-long experiment I measured differences in metabolic rate, hatching success, and larval quality between treatments. Exposure to temperature, pH, and dissolved oxygen concentrations projected by the year 2050 halved the successful hatch of Lingcod embryos and significantly reduced the size of day-1 larvae. In the year 2100 treatment, viable hatch plummeted (3% of normal), larvae were undersized (83% of normal), yolk reserves were exhausted (38% of normal), and deformities were widespread (94% of individuals). The size and persistence of Lingcod populations is dependent on acclimation or adaptation to these future conditions as well as on the adoption of “climate-ready” fisheries management. This experiment is

the first to expose marine benthic eggs to future temperature, pH, and dissolved oxygen conditions in concert based on the tight coupling of these conditions in nature. Lingcod are a potential indicator species for other benthic egg layers that global change conditions may significantly diminish recruitment rates.

I. Introduction

As global environmental change progresses, species are being exposed to novel environmental conditions, creating unprecedented risks (IPCC 2021; Doney et al. 2012; Poloczanska 2016; Song et al. 2021). Physiological intolerance to future conditions can affect survival, reproductive capacity, growth and development rates, and the timing of ontogenetic transitions (Harley et al. 2006; Cheung et al. 2010; Doney et al. 2012; Free et al. 2019). Our ability to manage for the resilience of species and the ecosystems and services many of these species support requires understanding how species will respond to likely changes in their environment. For the many marine species with complex life histories, not only do physiological susceptibilities differ markedly among life stages (Dahlke et al. 2020; Harley et al. 2006; Hodgson et al. 2016; Pörtner & Peck 2010, Peck et al. 2013; Tsoukali et al. 2016; Helaouët & Beaugrand 2009), but so does mobility and the ability to move to avoid physiological stressful conditions. Predicting the consequences of changing environmental conditions for individual organisms, and the populations and communities they constitute, requires knowledge of how environmental stressors impact the physiological rates and tolerance of each lifestage of a species.

The first lifestage for many fish is as developing fish embryos, which are passive recipients of their environment. Embryos rely on diffusion across their membrane and do not possess fully developed regulatory processes (Pankhurst and Munday 2011; Brauner 2008; Kamler, 2008; Dahlke et al. 2017). The vulnerability of this susceptible life stage is exacerbated for benthic egg masses that are bound to geologic or biogenic substrates and cannot evade locally unfavorable environmental conditions. Most freshwater and brackish fishes lay benthic eggs (e.g. sturgeon and salmon; Shelbourne 1955). Marine fish typically produce pelagic eggs because of saltwater's buoyancy (Sundby and Kristiansen 2015). However, small demersal fishes are often benthic egg layers, including over half of the species in the ornamental fish trade (e.g. blennies, gobies, damselfish; Shei et al. 2017). Well known, commercially important marine benthic egg layers also include Lingcod (*Ophiodon elongatus*), Cabezon (*Scorpaenichthys marmoratus*), Herring (*Clupea pallasii*), and Capelin (*Mallotus villosus*; Sundby and Kristiansen 2015; Olsen et al. 2010; Lønning et al. 1988; Wilson et al. 2008). Given the considerable vulnerability of benthic egg masses to changing environmental conditions, it is important to understand the lethal and sublethal effects of global change for this most sensitive life history stage (Dahlke et al. 2017; Pörtner & Farrell, 2008; Pörtner & Peck, 2010).

Here, I conducted a flow-through mesocosm experiment that exposed Lingcod eggs to temperature, pH, and dissolved oxygen (DO) conditions projected for the central California Current System (CCS) by the year 2050 and 2100. Lingcod are high

trophic level, voracious predators in northeast Pacific that lay benthic egg masses in shallow reef ecosystems (Beaudreau 2009). Many Lingcod populations are found in coastal upwelling zones within the CCS from 29°N to 58°N north (Love 2011). In these highly productive zones, upwelling-favorable winds push surface waters offshore, which are then replaced with deep, nutrient-rich waters. Nearly 20% of global fish catch occurs in upwelling regions, despite representing less than 1% of the global ocean (Mote et al., 2002; Pauly and Christensen 1995). Temperature, pH, and DO covary in upwelling zones, as upwelled waters are cooler and have lower pH and DO concentrations than the surface waters they replace (Baumann and Smith 2018; Cheresh and Fiechter 2020; Reum et al. 2016; Alin et al. 2012). As global change progresses, temperature in the central CCS will increase while pH and DO concentrations of upwelled waters are expected to continue to decrease due to ocean acidification and deoxygenation (Gruber et al. 2012; Hauri et al 2013). Lingcod's ecological and economic importance in a highly-productive ecosystem with already depressed pH and DO conditions makes this experiment an important case study for how a benthic egg layers' metabolism, growth, survival, and larval quality could be impacted by global environmental change.

Temperature is the most well-studied environmental variable and is often considered the dominant stressor that has a clear impact on developing embryos. Previous experiments exposing pelagic eggs and larval stage fish to temperature increases found that development time tends to decrease, metabolic rate increases, and hatch

success decreases (Pepin 1991; Laurel and Blood 2011; Guevara-Fletcher et al. 2016; Pankhurst and Munday 2011; Collins and Nelson 1993). Additionally, larval quality (e.g. length, weight, yolk-sac volume, presence of deformities) is affected by the temperature eggs are exposed to, with evidence for decreased fitness (Cook et al. 2005; Pörtner 2012; Dahlke et al. 2017; Laurel et al. 2018; Guevara-Fletcher et al. 2016; Blacter 1988; Jordaan et al. 2006; Pena et al. 2014; Llanos-Rivera et al 2006; Watson et al. 2018; Somero 2010). Fish eggs can have higher DO requirements than adults and cannot avoid low oxygen environments (Breitburg 2002). In contrast to warming, reduced DO levels can slow development and metabolic rates, as well as reduce embryo survival, decrease size at hatch, and increase morphological abnormalities (Hassell et al. 2008; Giorgi 1981; Silver et al. 1963; Shumway 1964; Alderdice and Forrester 1971; Oseid and Smith 1971; Siefert et al. 1974; Siefert and Spoor 1974). The story for ocean acidification is more complicated. Previous studies have found contradicting results regarding the effect of decreasing pH on fish eggs. Some studies have reported detrimental effects, such as reduced survival and larval quality (Baumann et al. 2012; Faria et al. 2017; Frommel et al. 2012; Leo et al. 2018) whereas others have failed to find any effect (Munday et al. 2009; Hurst et al. 2013; Munday et al. 2016) and many studies show minor effects (Wang et al. 2017; Franke and Clemmesen 2011; Forsgren et al. 2013; Bromhead et al. 2015). Understanding how the combined effects of warming, acidification and deoxygenation will affect fish eggs and embryos remains a critical next step for global change studies.

While these previous studies examined the physiological response to individual stressors – global change will cause simultaneous shifts in all three, potentially interacting, stressors in the California Current and globally. Experimental studies examining the impact of changing temperature, pH, and DO (known as the “deadly trio”) are scarce and are urgently needed to provide more accurate predictions of biological responses to environmental change (Sampaio et al . 2021). This study is the first to expose marine benthic eggs to future temperature, pH, and DO conditions in concert.

Predictions for how benthic eggs will be impacted by future conditions are difficult because of potential synergies between temperature, pH, and DO (Crain et al. 2008). The addition of acidification and hypoxia as stressors could enhance sensitivity to the temperature signal (Pörtner et al. 2005; Pörtner 2012). Or the three stressors operating together could cause effects contrary to what might be predicted (Piggott 2015; Paine et al. 1998). Lingcod embryos may already be physiologically stressed and even small decreases in pH and DO could be detrimental to development, or as benthic spawners in upwelling zones, Lingcod eggs may be adapted to cope with low DO and pH conditions (Baumann et al. 2012; Crain et al. 2008). To assess the biological ramifications of these global change conditions, experiments can take a full-factorial approach, providing a mechanistic understanding of all possible stressor interactions; or experiments can take a scenario-based approach, where multistressor treatments are based on projected future conditions (Boyd et al. 2018). I chose to employ a

scenario-based approach because it permits robust replication, increasing statistical power, and allows for hypotheses about the combined impact of the “deadly trio” that are relevant to managers and policy makers.

I hypothesize that temperature will be the dominant stressor impacting the viability of Lingcod eggs in 2050 and 2100 because of Lingcod’s likely adaptation to existing pulses of low pH and DO conditions associated with coastal upwelling. Based on results of the studies cited above, I hypothesize that conditions expected in Monterey Bay by the year 2050 and 2100 will 1) increase metabolic rate; 2) decrease time to hatch and reduce percent viable hatch; and 3) decrease capacity for growth and diminish larval quality. If metabolism, successful hatch, and larval quality is unaffected by the predicted environmental conditions evaluated in this experiment, it suggests that Lingcod may currently have the genetic and physiological scope to tolerate global environmental change. If the earliest life history stage is unable to cope with predicted future conditions, then the persistence of this benthic egg laying species in a changing ocean is uncertain (Pimentel et al. 2014).

II. Methods

2.1 Study System and Egg Collection

Study species

Lingcod are distributed along the west coast of North America from Southeast Alaska to Baja California, Mexico and are caught in both commercial and recreational

fisheries across its entire range (Miller and Geibel 1973; Giorgi 1981). In Monterey Bay, a diverse and productive ecosystem of the central California Current System (CCS), Lingcod is an ecologically significant predator that contributes to economically important recreational and commercial fisheries. Spawning occurs from November through early spring with females depositing eggs in shallow rocky reefs with swift flow to provide adequate ventilation for the benthic egg masses (Lam 2019; Lynn 2008; Miller and Geibel 1973; Hart, 1973; Low & Beamish, 1978; Jewell 1968; Giorgi 1984). One Lingcod egg mass is sired by one mother and between one and five fathers (King and Withler 2005). Males guard and fan the mass from fertilization until hatch, approximately six to seven weeks in the central CCS, and hatching takes place over three to seven days (Wilby 1937; Miller and Geibel 1973). After a pelagic larval stage, male Lingcod become relatively sedentary with high nest site fidelity, living to a maximum age of 25 years (King and Withler 2005).

Study area and field sampling

Lingcod benthic egg masses were collected from rocky reefs along the northern coast of the Monterey Peninsula, at the southern end of Monterey Bay, central California (36°38.4'N, 121°56'W; Supplementary Figure 1). Male Lingcod guarding and tending benthic egg masses are often associated with high relief, nearshore kelp forests during spawning season. To obtain egg masses, I searched for male Lingcod with SCUBA at depths of 5 to 15m bottom depth starting in early January, 2020. Once on the vessel, egg masses were placed in large coolers filled with aerated seawater, transported to

the NOAA Fisheries Santa Cruz laboratory on the University of California's Coastal Science Campus, and placed in a flow-through seawater system.

Once in the laboratory, the developmental stage of the eggs was evaluated. I required eggs at an early stage of development to ensure that exposure to future conditions could continue throughout their embryonic development. On February 7th, 2020 a ~8 kg egg mass was collected at a reef off of Point Pinos, Pacific Grove that was fertilized approximately 1.5 weeks prior to collection based on examination of the developmental stage of a subset of eggs with a microscope. Stable isotope analyses indicated that the mother's diet included piscivorous fish, suggesting high maternal provisioning. Similar to Cook et al. (2005), I assumed the egg mass was uniformly fertilized. The egg mass was placed in a well-aerated holding container for three days to acclimate to the laboratory environment before being exposed to the experimental treatments.

2.2 Experimental Design

The flow-through mesocosm was designed to simultaneously manipulate temperature, pH, and DO levels of the incoming seawater to create three treatment levels: 1) year 2020 conditions, 2) projected year 2050 conditions, and 3) projected year 2100 conditions (Figure 1). The setpoints for these three treatments were based on an ensemble of climate change models assembled by the Coupled Model Intercomparison Project (CMIP5) and nearshore ocean acidification projections for

the California Current (ESRL 2019; Hauri et al. 2013; Gruber et al. 2012; Feely et al. 2010; Frieder et al. 2012). Based on the literature, I assumed that the average depth of Lingcod egg masses was 10 m, and adjusted the future temperature, pH, and DO setpoints accordingly (based on observations from Monterey Bay moorings; Frieder et al. 2012). The setpoints for the three treatments were:

- 1) Year 2020 — Temperature: 13°C; pH: 7.9; DO: 9 mg/l
- 2) Year 2050 — Temperature: 14.5°C; pH: 7.7; DO: 7 mg/l
- 3) Year 2100 — Temperature: 15.8°C; pH: 7.5; DO: 5 mg/l

The experimental system was fed with raw seawater pumped through a UV filter into two large sump tanks (~ 350 l). Sump tank 1 (“ambient sump”) had a chilled seawater line to maintain an average water temperature of 12.5°C. pH and DO levels were unmanipulated. Sump tank 2 (“global change sump”) had four 1000-watt heaters to maintain temperatures between 17 and 21°C, the range mimicking the diel temperature cycle. The global change sump also had a CO₂ gas line flowing at 0.5 sl/min to reduce pH levels to 7.2, and a N₂ gas line bubbled at 3 sl/min to reduce DO levels to 5 mg/l.

To achieve the three treatment setpoints, controllers (Universal Dual Analyzer, Honeywell) connected to tris buffer-calibrated sensors (Durafet, Honeywell) monitored pH and temperature in six 20 l header barrels (two headers per treatment) that were receiving a mix of water from the ambient and global change sump tanks

through a distribution manifold. If pH exceeded the desired setpoint for a header tank, the corresponding solenoid valve opened to release water from the global change sump tank; if pH fell below the setpoint the solenoid valve closed. Water from the header tanks gravity-fed three replicate aquaria each, resulting in a total of six 14 l replicate aquaria per treatment (n=18). Sections of the collected egg mass were ultimately placed in these 18 replicate aquaria.

Aquarium pumps in sump tanks, header barrels, and replicate aquaria ensured adequate mixing and water flow over the eggs; and timers controlled light levels to mimic the day-night cycle. Durafet sensors measured pH and temperature every 15 s and dissolved oxygen probes (GoDirect, Vernier) measured DO every 15 m in the sump tanks and header barrels. In the replicate aquaria, tris buffer-calibrated handheld sensors (YSI, Oakton Instruments) were used daily to measure pH, temperature, DO, and salinity. Discrete water samples were collected at three timepoints from the replicate aquaria to calculate additional carbonate chemistry parameters (Supplementary Table 1). Total alkalinity from these discrete samples was measured using a Metrohm 815 Robotic USB Sample Processor XL and Titrand 905. Throughout the month-long experiment, the average pH, temperature, and DO recorded in the headers and replicate aquaria were comparable to the three treatments' setpoints (Figure 2 & Table 1).

The egg mass was separated into 1-2 g cubes of egg mass and placed in each aquarium. This cube size allowed for replication across the treatments and a surface-area-to-volume ratio such that eggs at the center of the cubes experienced the treatment conditions. The cubes were taken from the periphery of the egg mass, separated by hand, quickly dried with kim wipes, and weighed. I also weighed 20 individual eggs from the full mass in order to calculate an average weight per egg and estimate the number of eggs per 1-2 g cube. Once weighed, the egg cube was placed on top of a 10x10 cm ceramic tile situated in a 500 micron mesh aquarium bag, and secured with a rubber band. The tile ensured the egg cubes rested on the bottom of the aquaria and the mesh bag made certain day-1 Lingcod larvae could not escape from the aquaria.

A total of four aquarium bags were placed in each replicate aquarium; one bag was reserved for examining metabolic rates and the other three bags were left undisturbed until hatch. Placement of the four bags was rotated every other day to ensure all bags experienced similar conditions near the aquarium pump, inflow, and outflow pipe.

2.3 Analysis of eggs and larvae

1. Does the metabolism of Lingcod embryos increase with environmental change?

I measured the oxygen consumption rate of Lingcod eggs as a proxy for standard metabolic rate using fiber optic O₂ sensors (Fibox IV, Presens). The respirometry trials took place at the same degree-day (time in days, adjusted for temperature)

development across treatments; therefore, three trials took place on successive days, starting with eggs from the year 2100 treatment and ending with eggs from the year 2020 treatment.

I ran the trials using 100ml airtight containers fitted with an oxygen sensor spot (PreSens SP-PSt4-SA) that were initially calibrated with both 100% and 0% O₂ saturated water. One egg cube from each replicate aquaria (n=6) was added to the containers and placed on top of a magnetic stir plate in a temperature-controlled water bath. Water movement was maintained inside the containers using a magnetic stir bar that was separated from the eggs by a porous plastic platform. The oxygen concentration of each container was measured at seven timepoints over ~1.5 hours and the eggs were sacrificed at the end of the trial. I used the R package LoLinR, which uses local linear regression techniques to estimate monotonic biological rates (Olito et al. 2017), to determine the rate of oxygen depletion in $\mu\text{mol}/\text{min}/\text{g}$ for each container and then corrected for the egg cube weight. I used a one-way ANOVA to test if the difference in respiration rate between treatments was statistically significant ($p < 0.05$) between treatments.

2. Is Lingcod hatch timing shifted and does percent viable hatch decrease with environmental change?

Hatch began on March 1st and was complete by March 6th for all treatments. Once a day, hatched larvae were removed from each sample bag using a pipette, counted, and

placed in a 15 ml falcon tube. The tubes were frozen in a 30% ethanol solution. Both calendar and degree days to first hatch and 50% hatch were determined for each bag (3 bags per aquarium, 6 aquaria per treatment) and the mean and standard deviation for the three treatments was calculated. Total number of hatch days was also calculated based on the number of days between the appearance of the first and last larvae. A nested mixed model ANOVA with treatment as the fixed effect and tank and bag as random effects was used to test for differences in days to first hatch and total number of hatch days among the three treatments.

Percent hatch for each bag was the number of hatched larvae counted, including deformed larvae, divided by the estimated number of eggs in the cube x 100. Percent viable hatch was also calculated using the number of larvae without deformities, viewed using a dissecting microscope. A nested mixed model ANOVA with treatment as the fixed effect and tank and bag as random effects was used to test for differences in percent hatch and percent viable hatch among the three treatments.

3. Does larval quality decrease with environmental change conditions?

To determine differences in larval quality between treatments, twelve metrics were used: 1) total length, 2) preanal length, 3) postanal length, 4) head length, 5) snout length, 6) eye diameter, 7) head depth, 8) depth at anus, 9) oil globule presence/absence and area, 10) yolk area, 11) number and type of deformity, and 12) dry weight (Figure 3). To complete the morphometric analyses, six larvae from each

falcon tube were randomly selected (a bootstrap analysis determined six larvae was a sufficient sample size) and images from the ventral and lateral side were taken using a microscope camera (AmScope 10 MP). The program ImageJ was used to record the measurements. If one or more deformities were observed, the type of deformity was cataloged. To increase confidence in our measurements of each image, I used the mean of measurements by six different individuals. After images of the larvae were taken, the larvae were freeze-dried for 48 hours and weighed to the nearest 2 μg on an analytical balance (Sartorius).

The amount of total carbon, total nitrogen, carbon-13, nitrogen-15, and the carbon to nitrogen ratio (C:N) was measured for each larva to compare body composition between treatments. To complete the analysis, samples were weighed, encapsulated in tin, and analyzed for C and N stable isotope ratios and C and N amounts by the University of California Santa Cruz Stable Isotope Laboratory using a CE Instruments NC2500 elemental analyzer coupled to a Thermo Scientific DELTAplus XP isotope ratio mass spectrometer via a Thermo-Scientific Conflo III. Measurements are corrected to VPDB (Vienna PeeDee Belemnite) for $\delta^{13}\text{C}$ and AIR for $\delta^{15}\text{N}$ against an in-house gelatin standard reference material (PUGel), which is calibrated against international standard reference materials. Measurements are corrected for size effects, blank-mixing effects, and drift effects. An externally-calibrated Acetanilide standard reference material purchased from Dr. Arndt Schimmelmann of Indiana University is measured as a sample for independent

quality control. Typical reproducibility is significantly better than 0.1 permil for $\delta^{13}\text{C}$ and significantly better than 0.2 permil for $\delta^{15}\text{N}$. Nested mixed model ANOVAs with treatment as the fixed effect and tank and bag as random effects were used to determine statistical significance of the morphometric and stable isotope data across the treatments.

III. Results

1. Metabolism of Lingcod embryos

I did not detect differences in the respiration rate of Lingcod embryos among the current, year 2050, and year 2100 environmental treatments (Supplementary Figure 2). The comparable oxygen consumption rates between the year 2020 and year 2100 treatment indicates that 10-days before hatch, the embryos in the year 2100 treatment had not yet undergone a mass mortality event (see below). It is important to note that I assumed the 1g egg masses in the respiration chambers were uniformly fertilized, which may have affected the likelihood of detecting differences in the embryos' metabolic rates.

2. Hatch timing and percent hatch

Degree days to first hatch and degree days to 50% hatch increased as temperature rose and pH and DO levels decreased across treatments, suggesting environmental change conditions retarded Lingcod embryo development (Table 2). Total hatch day

significantly decreased from 4 d in the year 2020 treatment, to 3 d in the year 2050 treatment, to less than 1 d in the year 2100 treatment (Table 2).

Percent hatch ranged from 33% to 0% across the three treatments. Percent hatch was reduced for embryos experiencing environmental change conditions; the average percent hatch was 19% for the year 2020 treatment, 9% for the year 2050 treatment, and 0.6% for the year 2100 treatment (Figure 4). The number of larvae that hatched with intact oil globules, signifying higher lipid reserves, was half of the total hatch for all three treatments (Supplementary Figure 3). Similarly, once deformities were cataloged, the number of larvae that hatched without any deformities reduced hatch success to 7% for the year 2020 and 3% for the year 2050 (Supplementary. Figure 3). All year 2100 larvae possessed deformities.

3. Larval quality

Larval quality was impacted by environmental change conditions. Larval weight was significantly lower in the year 2050 and year 2100 treatments compared to the year 2020 treatment (Figure 5). Weight decreased as hatch progressed, likely because eggs on the interior of the 1g egg masses hatched later and received less oxygen throughout development (Giorgi 1984). The total length and body depth of the Lingcod larvae declined as temperature increased and pH and DO decreased; although the year 2050 and year 2100 treatments were not statistically different (Table 3). Yolk area was unaffected by year 2050 conditions (1.54 and 1.58 mm² in

year 2020 and year 2050 conditions respectively), but yolk area dropped to an average of 0.58 mm² in the year 2100 treatment. I did not detect differences among treatments for head length, head depth, snout length, eye diameter, and oil globule area (for larvae that had oil globules).

Occurrences of spinal, anal/gut, jaw, head, eye, and c-shaped deformities were catalogued for each treatment (Table 4). For every type of deformity, the larvae from the year 2020 treatment had the lowest instances of deformities, followed by the year 2050 treatment (although the two treatments were statistically equivalent); the year 2100 treatment had the highest instances of deformities and was significantly different from the other two treatments in all deformity categories except for the number of c-shaped larvae.

Spinal deformities were the most common deformity seen in the year 2020 treatment (15.5% of larvae) and spinal and jaw deformities were the most common for the year 2050 treatment (17.5% and 18.8% respectively). Between 44% and 89% of larvae in the year 2100 treatment had a spinal, anal/gut, jaw, head, or eye deformities.

The C:N ratios for the 2020 and 2050 treatment were equivalent, while the C:N ratio was significantly higher for the year 2100 treatment (Figure 6A). Lipid content remains relatively stable throughout fish embryo development, while protein content reserves are depleted, indicating differences in C:N ratios were due to changes in

protein content (Liu et al. 2018). The weight and the total nitrogen content (amount of protein) of the year 2100 larvae were substantially lower than the other two treatments (Figure 6B). The year 2100 treatment also had a significantly higher concentration of nitrogen-15 (Figure 6C). The year 2020 and year 2050 larvae had the same concentration of nitrogen-15, indicating the larvae in the year 2050 treatment were smaller, but maintained their protein reserves (supported by the two treatments' similar average yolk areas).

IV. Discussion

My results suggest that the combined effects of multiple environmental change stressors could reduce future recruitment rates of Lingcod in a coastal upwelling system. Projected temperature, pH, and DO concentrations by the year 2050 halved the successful hatch of Lingcod embryos. Larvae reared in the year 2050 conditions were viable (abnormalities were statistically similar to normal larvae) and had sufficient protein reserves, but were significantly smaller. Even slight changes in growth can impact recruitment, as smaller size leads to reduced swimming speeds, lower encounter rates with food, and higher risk of predation (Giorgi 1981; Miller et al. 1988; Hurst et al. 2013; Hurst et al. 2010; Houde 1987). In the absence of acclimation or adaptation, my findings suggest egg and larval survival could plummet by the year 2100. In 2100 conditions, hatch was minimal (only $0.6\% \pm 2\%$ of eggs hatched); larvae were undersized; yolk reserves were exhausted; larvae were concentrating nitrogen-15, suggesting that day-1 larvae were already metabolizing

their protein reserves (Doi et al. 2017; Pimentel et al. 2014); and deformities that reduce the ability to feed were widespread. Larvae that do hatch in these conditions will require abundant prey resources immediately after hatch occurs (Laurel et al. 2018). The likelihood of meeting those favorable conditions is low because the total number of hatch days declined significantly with increasing temperature and decreasing pH and DO. A longer hatch period increases the likelihood that at least a portion of day-1 larvae would encounter favorable conditions for survival and growth (Politis et al. 2014).

These results are consistent with previous studies that found that in the northern CCS, temperatures above local natural variability reduced Lingcod larval survival and size while morphological abnormalities accumulated (Cook et al. 2005; Applebaum et al. 1995). In fact, I obtained similar results even with a temperature difference between treatments that was half that of Cook et al. 2005, indicating synergies between the three stressors could have led to the observed effects. Another early Lingcod study examined egg masses at field sites in the San Juan Islands, Washington, and found that at 85% DO saturation, mortality was 6% while at 50% DO saturation mortality increased to 48% (Giorgi 1984). DO saturations from my 2050 and 2100 treatments (80% and 70%, respectively) suggest that low DO conditions likely contributed to Lingcod embryo mortality. The majority of Lingcod eggs will be exposed to even lower DO saturations since the interior of egg masses has low interstitial oxygen levels compared to the periphery. The high mortality in the year 2100 treatment

happened after my metabolism trials concluded, 9 days before hatch. Oxygen requirements increase and resistance to hypoxia decreases as fish embryos grow larger in their egg case (Braum 1973, Hempel 1979, Alderdice et al. 1958, Giorgi 1981). It's possible that embryos in the year 2100 treatment could tolerate the low DO conditions until their oxygen requirements increased in the final stages of development.

I anticipated Lingcod embryos would develop faster in the future scenario treatments, since previous studies examining the impact of temperature on the egg stage of CCS groundfish found that time to hatch was faster at higher temperatures (Cook et al. 2005; Gadomski and Caddell 1966; Applebaum et al. 1995). But in this study, degree days to hatch was longer in the year 2050 and year 2100 treatments compared to the year 2020 treatment. This result could also be due to low DO; Giorgi (1984) found hatching of Lingcod embryos was protracted for poorly ventilated eggs. Ocean deoxygenation has received less attention in the literature, but it is one of the most drastic impacts expected with climate change (Sampaio et al. 2021; Low et al. 2021). In fact, a meta-analysis of experimental research on climate change stressors found that on average hypoxia has a stronger negative impact on marine fish performance than ocean warming (Sampaio et al. 2021). If low DO slowed Lingcod embryo development, future DO conditions may decrease growth rates of benthic egg laying species, resulting in poorer foraging ability and increased predation risk. In addition,

reduced pH has been shown to slow development in a range of species, which could have contributed to this result.

My hypothesis that metabolic rate would increase in future environmental change conditions was also rejected. Increasing or decreasing metabolic rate in response to stressors is often adaptive, improving the likelihood of embryo survival (Pörtner 2012). I predicted metabolic rate to rise because of the strong positive relationship between temperature and increased oxygen consumption (Pankhurst and Munday 2011; Collins and Nelson 1993). However, both ocean acidification and hypoxia can cause metabolic depression (Pörtner 2012; Pörtner et al., 2005; Rosa and Seibel, 2008; Baumann et al., 2012; Giorgi 1981). Dahlke et al. (2017) found that at extreme temperatures, an interactive effect between low pH and high temperature caused a reduction in oxygen consumption by Atlantic cod (*Gadus morhua*) embryos. It is also possible that Lingcod embryos' metabolic rate simply cannot adjust to stressful conditions, explaining why I did not see a difference in oxygen consumption between treatments. Future studies should re-examine how the three stressors acting in concert impact metabolic rate using embryos where fertilization success is easier to observe.

My results demonstrate that single stressor experiments likely do not capture the true impact of global environmental change on marine organisms. Experimental studies need to move toward multistressor scenarios that include temperature, pH, and DO to obtain more accurate predictions of biological responses to global change (Sampaio

et al. 2021). This is especially important in productive coastal upwelling systems that fuel the productivity of fish populations around the world. Lingcod are a potential indicator species for other benthic egg layers, including those adapted to relatively low pH and DO conditions. This study makes evident that global change conditions can diminish marine benthic egg layer recruitment rates. The size and persistence of Lingcod populations in the highly productive central CCS is dependent on acclimation or adaptation to these future conditions.

Parental acclimation to environmental change conditions could increase embryos' physiological tolerance of stressful conditions. Temperature tolerance of fish eggs often reflects the temperatures experienced by the adults during the spawning season (Gadomski and Caddell 1966). Many studies have found that acclimating mothers and fathers to conditions the offspring are exposed to helps mediate negative impacts in the embryos (Miller et al., 2012; Parker et al 2012; Pankhurst and Munday 2011; Rombough 1997). Other studies have found parental exposure does not improve tolerance; maternal exposure to stressful conditions may even reduce egg size and inhibit reproduction (Hansen and Petersen 2001; Bownds 2010; Pankhurst and Munday 2011). Although difficult for Lingcod, future experiments should attempt to capture mature adults and spawn eggs in captivity to allow for parental exposure to treatment conditions. Alternatively, future studies should compare egg and larval performance from adults that differ in their history of exposure to spatially varying upwelling conditions.

Despite my experimental finding of Lingcod egg's high sensitivity to environmental change conditions, there is considerable gene flow throughout their range, suggesting increased genetic diversity could support adaptation (Longo et al. 2020). For example, Lingcod are adapted to their local thermal environment. Cook et al. (2005) examined the effect of temperature on Lingcod embryos taken from the Seattle Aquarium and found that hatch was highest at 9°C and no hatch occurred at 15°C; the average temperature in my year 2020 treatment was 13°C and hatch occurred in the 15.7°C treatment. Lingcod age at maturity is between two to four years, indicating there may be enough generations between today and 2050 to adapt to future temperature, pH, and DO conditions (Silberberg et al. 2001). Lingcod can live up to 25 years so older mothers are less likely to be adapted to environmental change conditions. Older mothers produce more larvae that grow faster and are more resistant to starvation (Palumbi 2004; Berkeley et al. 2004). Even in the ideal scenario where all young mothers are adapted to future conditions, recruitment rates in the central CCS will likely still decline because viable hatch from the most productive mothers will decrease.

Species' vulnerability to environmental change is based on their exposure, sensitivity, and adaptive capacity to future conditions (Pacifici et al. 2015). This study is the first to experimentally demonstrate that a marine benthic egg layer in an upwelling ecosystem is highly vulnerable to environmental change conditions projected by the year 2050 in their environment. Responsive fisheries management will be needed to

maintain Lingcod's role as an important generalist predator and as an economically important fisheries species. If the pelagic egg and larval stages of other fishes from upwelling systems are as sensitive to global environmental change as benthic egg layers, we will potentially face a re-shaping of one of the most highly productive marine ecosystems. Ultimately this study can serve as an important case for coastal fisheries of the Northeast Pacific, requiring climate-ready management approaches in the face of changing ocean conditions.

Acknowledgments

Thank you to Colin Carney from UCSC's Stable Isotope Laboratory for his help with sample measurement and general mesocosm support. I am grateful to the following undergraduates for their work in the mesocosm and for collecting morphometric data:

Elizabeth Norton, Allyson Dilorenzo, Bijan Ashtiani-Eisemann, Desiree Zhuk, Raquel Lubambo Ostrovski, Erika Garig, Alize Bautista-Gallo, Taylor Merthan, Ryan Ortiz, Nora Laszlo, Elisha Villanueva, Irene Felipe, Jasmine Saucedo, Ben Wong, Justin Tran, Kristina Fleetwood, Leslie Lazo, Michelle Kwong, Sam Cormier, Vandana Teki, Zelin Yang, Haylee Bregoff, Rachel Apolinario, Josue Lopez, Clyde Dockery, Isabel Blanco, Pablo Puchol, Justin Tran, Taylor Hauenstein, Lurdez Puga, Monica Pineda, Trevor Wang, Sean Lee, Chloe Webster, and Lilia Brunsman.

Figures and Tables

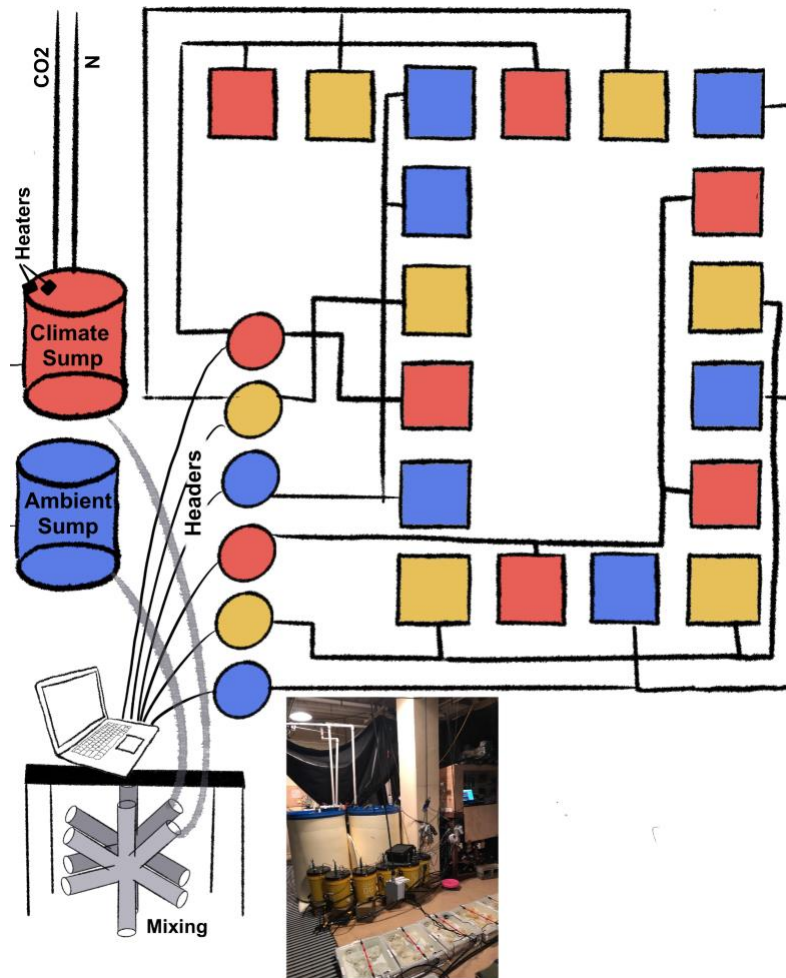


Figure 1.1: Conceptual figure illustrating the flow-through experimental mesocosm.

Blue represents the year 2020 treatment, yellow represents year 2050, and red represents year 2100. The ambient and climate change sump tank water (cylinders) is mixed as it flows to the header tanks (circles) to attain the setpoints for each treatment. There are two replicate header tanks for each treatment and each header

tank supplies water to three replicate aquaria (squares), for a total of six replicate aquaria for each treatment.

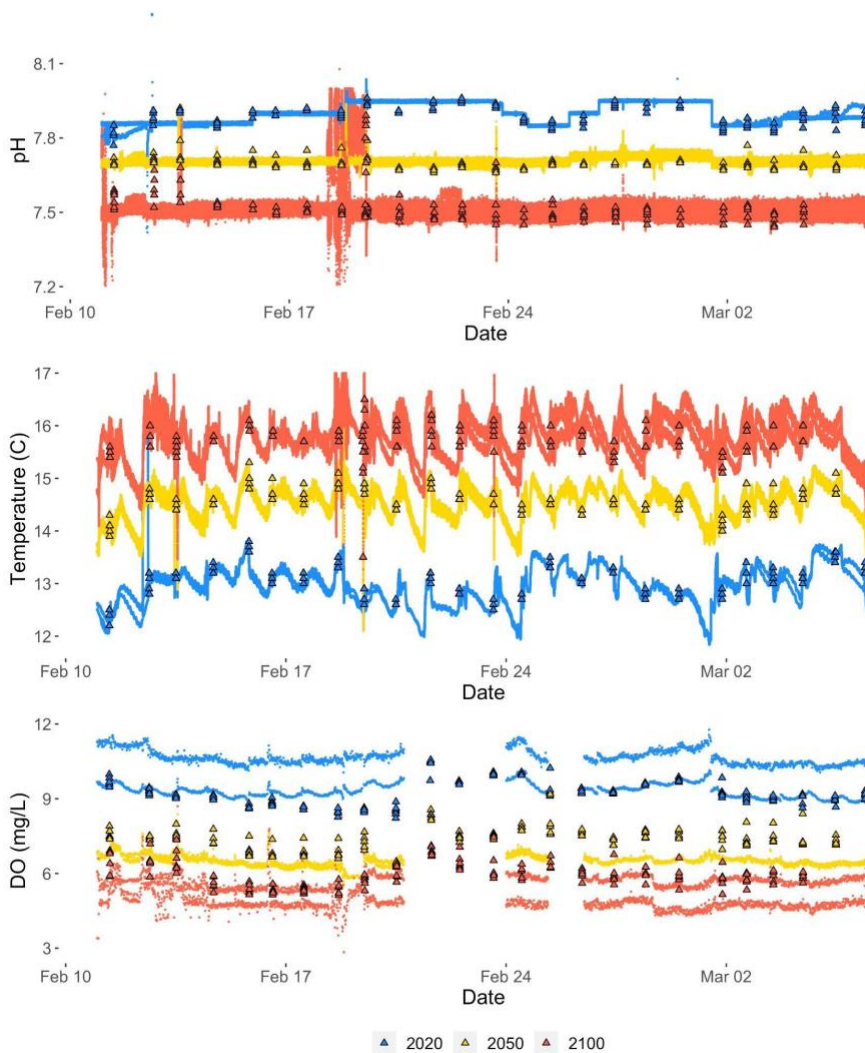


Figure 1.2: Temperature, pH, and DO values measured over the duration of the experiment for the year 2020 (blue), year 2050 (yellow), and year 2100 (red) treatments. Temperature and pH values were measured every 15 seconds by Durafet sensors in the header tanks (lines) and once daily by YSI sensors in the replicate aquaria (triangles). DO concentration was measured by Vernier sensors every 15

minutes in the header tanks (lines) and once daily by YSI sensors in the replicate aquaria (triangles).

Temperature (C)	pH	Dissolved Oxygen (mg/l)
13.0 ± 0.3	7.89 ± 0.04	9.2 ± 0.5
14.6 ± 0.2	7.70 ± 0.02	7.4 ± 0.5
15.7 ± 0.4	7.52 ± 0.07	6.0 ± 0.5

Table 1.1: Mean and standard deviation of the temperature, pH, and DO conditions measured by YSI sensors in the replicate aquaria over the duration of the experiment.

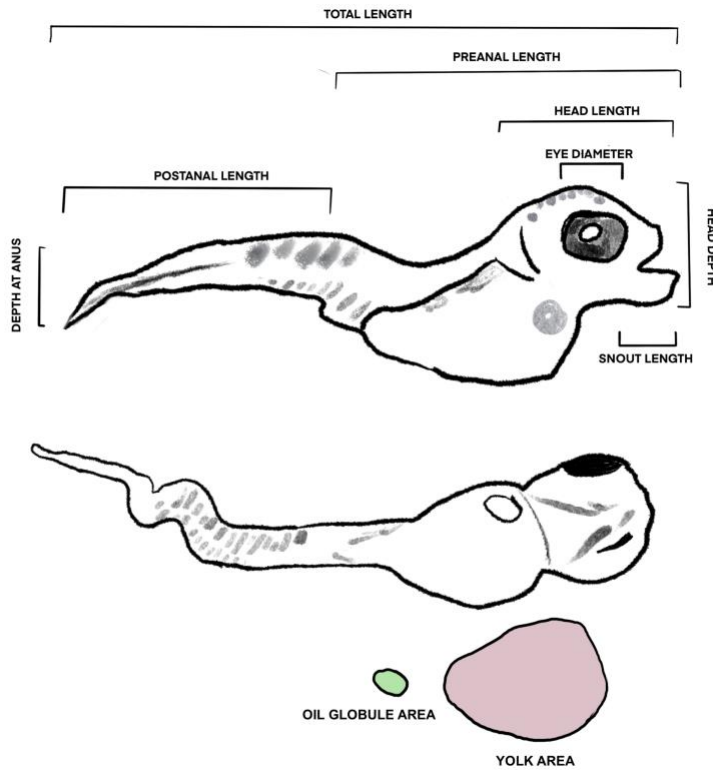


Figure 1.3: Illustration of the 10 measurements taken for each larval image using ImageJ.

	Degree Days to 1st Hatch	Calendar Days to 1st Hatch	Degree Days to 50% Hatch	Calendar Days to 50% Hatch	Total Number of Hatch Days
2020	256 ± 10	21 ± 0.8	263 ± 7	21 ± 0.6	4 ± 1
2050	281 ± 13	20 ± 0.9	287 ± 14	21 ± 0.9	3 ± 1.4
2100	320 ± 13	21 ± 0.8	320 ± 13	21 ± 0.8	.3 ± 0.6
Significant difference ANOVA (p<0.01)	Yes	No	Yes	No	Yes

Table 1.2: Mean and standard deviation of degree days and calendar days to first hatch, degree and calendar days to 50% hatch, and total number of hatch days for the year 2020, year 2050, and year 2100 treatments. Nested mixed model ANOVAs were run to determine statistical significance. Pairwise comparisons for degree days to first hatch ($p_{2020,2050} < 1 \times 10^{-4}$, $p_{2050,2100} < 1 \times 10^{-4}$, $p_{2020,2100} = 0$), degree days to 50% hatch ($p_{2020,2050} < 1 \times 10^{-4}$, $p_{2050,2100} < 1 \times 10^{-4}$, $p_{2020,2100} = 0$), and total number of hatch days ($p_{2020,2050} = 3.7 \times 10^{-3}$, $p_{2050,2100} < 1 \times 10^{-4}$, $p_{2020,2100} = 0$) were significantly different. Calendar days to first hatch ($p_{2020,2050} = 0.11$, $p_{2050,2100} = 0.02$, $p_{2020,2100} = 0.29$) and calendar days to 50% hatch ($p_{2020,2050} = 0.01$, $p_{2050,2100} = 0.15$, $p_{2020,2100} = 1$) were not significantly different.

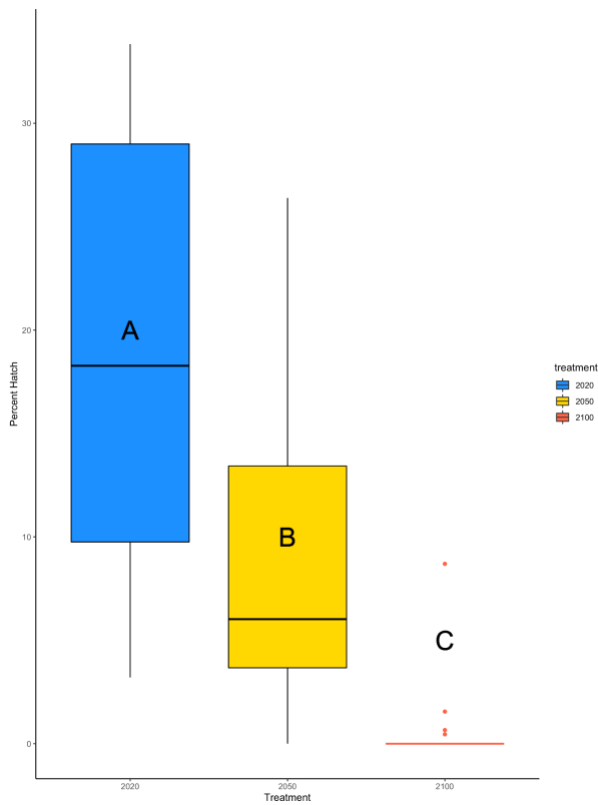


Figure 1.4: Boxplots illustrating the median, upper and lower quartile, and interquartile range of percent total hatch for the year 2020 (blue), year 2050 (yellow), and year 2100 (red) treatments. The average percent hatch was 19% for the year 2020 treatment, 9% for the year 2050 treatment, and 0.6% for the year 2100 treatment. Nested mixed model ANOVAs were run to determine statistical significance, letters indicate significant differences ($p_{2020,2050}=3 \times 10^{-4}$, $p_{2050,2100}=4 \times 10^{-3}$, $p_{2020,2100}<1 \times 10^{-4}$).

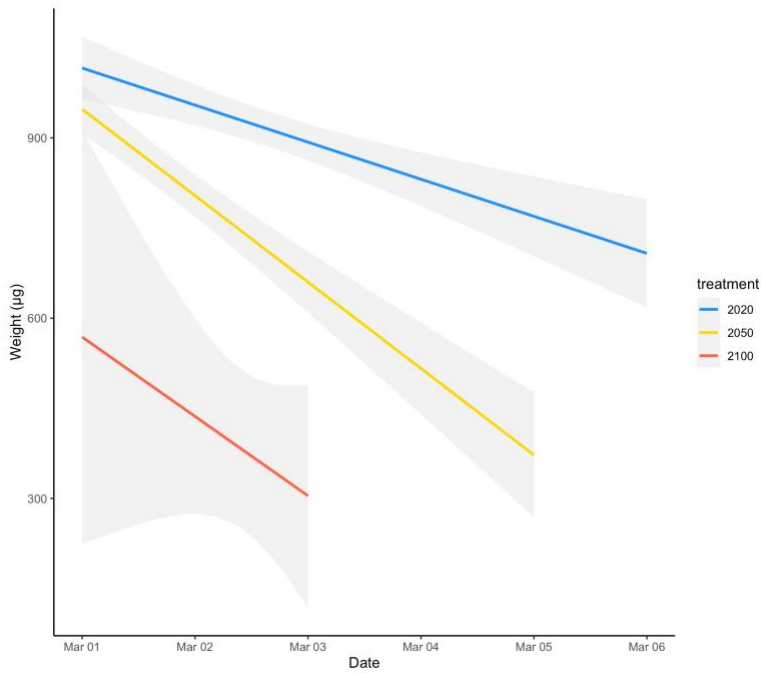


Figure 1.5: Linear regression for Lingcod larvae weight (μg) as the hatch period progresses for the year 2020 (blue), year 2050 (yellow), and year 2100 (red) treatment. A nested mixed model ANOVA was run to determine statistical significance ($p_{2020,2050}=0.21$, $p_{2050,2100}<1\times 10^{-4}$, $p_{2020,2100}<1\times 10^{-4}$).

	2020 (n=295)	2050 (n=282)	2100 (n=17)
Total Length	7.34 \pm 0.77mm ^a	6.97 \pm 0.97mm ^b	6.10 \pm 1.16mm ^b
Preanal Length	3.76 \pm 0.36mm ^a	3.63 \pm 0.55mm ^b	3.23 \pm 1.17mm ^b
Postanal Length	3.65 \pm 0.54mm ^a	3.53 \pm 0.72mm ^b	3.01 \pm 0.74mm ^b
Head Length	4.87 \pm 2.94mm ^a	4.00 \pm 2.90mm ^a	1.62 \pm 0.59mm ^a
Snout Length	0.28 \pm 0.34mm ^a	0.29 \pm 0.08mm ^a	0.25 \pm 0.09mm ^a
Head Depth	1.50 \pm 4.35mm ^a	1.24 \pm 0.16mm ^a	1.14 \pm 0.17mm ^a
Body Depth	0.79 \pm 0.11mm ^a	0.71 \pm 0.12mm ^b	0.67 \pm 0.14mm ^b
Eye Diameter	0.67 \pm 0.06mm ^a	0.64 \pm 0.08mm ^a	0.58 \pm 0.12mm ^a
Yolk Area	1.54 \pm 0.32mm ² ^a	1.58 \pm 0.35mm ² ^a	0.59 \pm 0.81mm ² ^b
Oil Globule Area	0.11 \pm 0.30mm ² ^a	0.07 \pm 0.08mm ² ^a	0.09 \pm 0.05mm ² ^a

Table 1.3: Mean and standard deviations of morphometric data for Lingcod larvae samples from year 2020, year 2050, and year 2100 treatments. Count (n=) represents the number of larvae measured using ImageJ for each treatment, not the total hatch number. Treatments with different letters for each response variable were significantly different (nested mixed model ANOVAs; $p < 0.01$).







Deformity Category	Example	% With Deformity		
		2020	2050	2100
C-shaped		4.1% ± 2% ^a	7.8% ± 3.2% ^a	11.1% ± 13.7% ^a
Spinal Deformity		15.5% ± 7.6% ^a	17.5% ± 10.5% ^a	44.4% ± 39.4% ^b
Anal/gut Deformity		2.2% ± 1.7% ^a	8.3% ± 4% ^a	58.3% ± 38% ^b
Jaw Deformity		8.2% ± 5% ^a	18.8% ± 8.6% ^a	88.9% ± 19.2% ^b
Malformed Head		4.2% ± 3.8% ^a	11.7% ± 5.4% ^a	72.2% ± 29.3% ^b
Eye Deformity		2.6% ± 2.2% ^a	6.6% ± 3.3% ^a	50% ± 43.3% ^b

Table 1.4: Mean and standard deviation for the percent of larvae from each 1g Lingcod egg mass that had a deformity in the seven deformity categories for the year 2020, year 2050, and year 2100 treatments. N represents the number of images

analyzed for each treatment. Nested mixed model ANOVAs were run to determine statistical significance, letters indicate significant differences ($p < 0.01$).

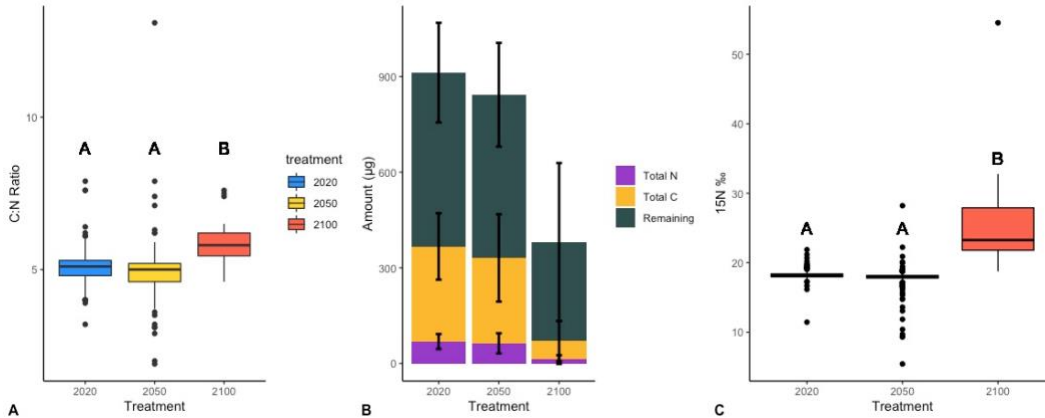
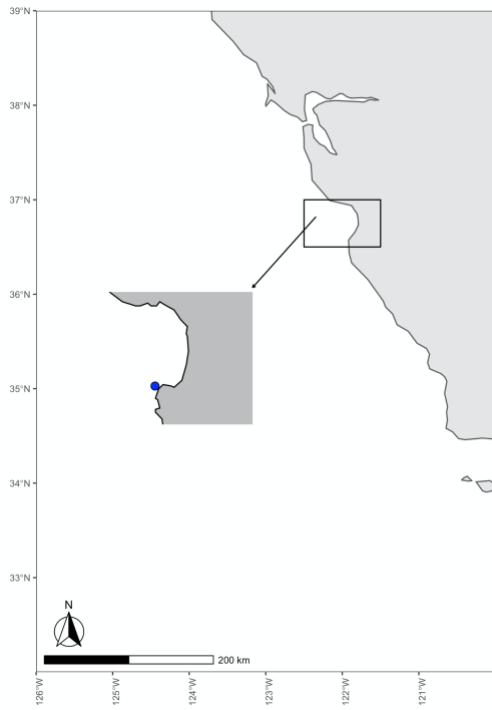


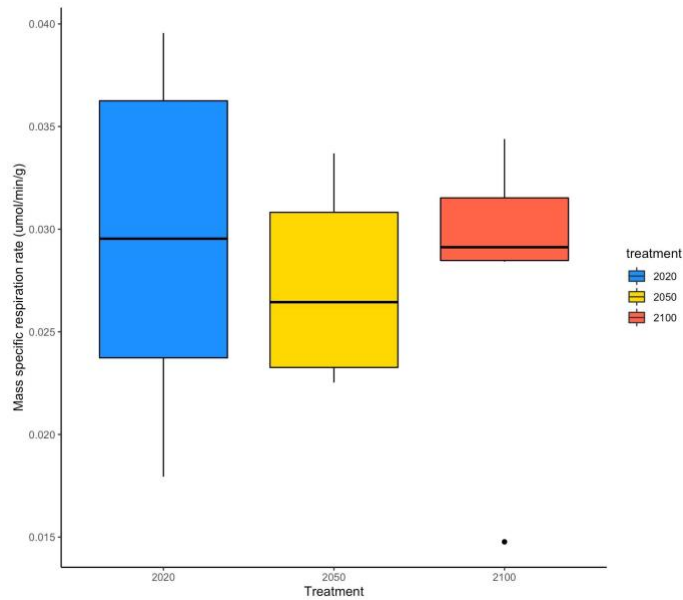
Figure 1.6: A) Boxplots illustrating the median, upper and lower quartile, and interquartile range of the C:N ratio for the year 2020 (blue), year 2050 (yellow), and year 2100 (red) treatments ($p_{2020,2050}=0.27$, $p_{2050,2100}<1 \times 10^{-4}$, $p_{2020,2100}<1 \times 10^{-4}$). B) fraction of total weight (μg) comprised of total N and total C for each treatment. C) Boxplots illustrating the median, upper and lower quartile, and interquartile range of the concentration (per mille) of nitrogen-15 in each treatment ($p_{2020,2050}=0.57$, $p_{2050,2100}<1 \times 10^{-4}$, $p_{2020,2100}<1 \times 10^{-4}$). Nested mixed model ANOVAs were run to determine statistical significance, letters indicate significant differences.



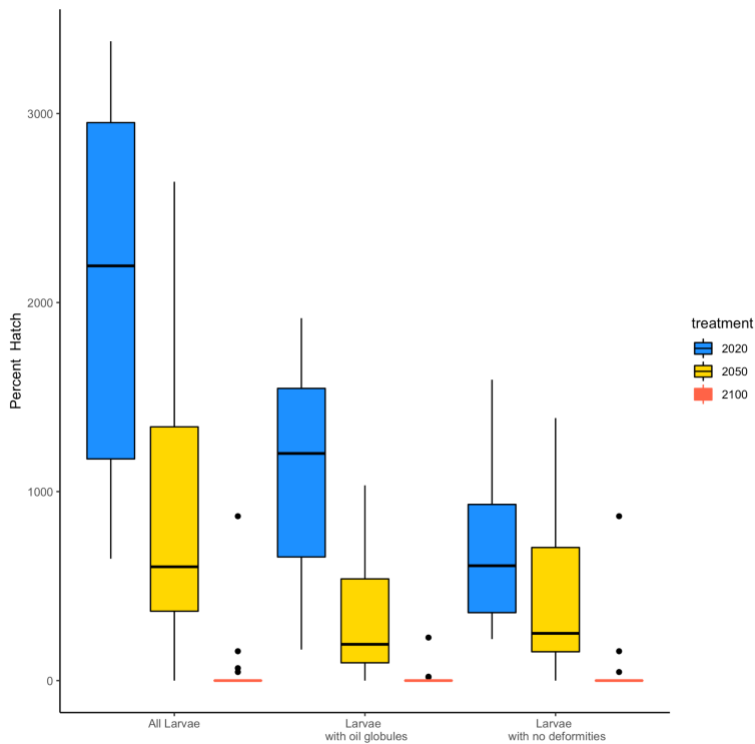
Supplementary Figure 1.1: Map of Monterey Bay, CA (black rectangle) showing location of lingcod egg mass collection (blue circle).

	2020	2050	2100
Temperature °C	13.09 ± 0.16	14.69 ± 0.21	15.82 ± 0.23
Salinity (ppt)	34.46 ± 0.05	34.45 ± 0.06	34.46 ± 0.05
Dissolved Oxygen (mgL⁻¹)	9.57 ± 0.62	7.71 ± 0.50	6.37 ± 0.56
pH	7.89 ± 0.04	7.70 ± 0.03	7.53 ± 0.06
TA (μmol kg⁻¹)	2246.9 ± 4.0	2246.51 ± 3.6	2248.81 ± 5.05
HCO₃⁻ (μmol kg⁻¹)	1961.94 ± 15.21	2058.90 ± 9.34	2108.28 ± 18.39
pCO₂ (μatm)	535.10 ± 41.94	968.79 ± 52.81	1457.18 ± 192.68
CO₂ (μmol kg⁻¹)	21.26 ± 1.65	36.47 ± 1.89	53.09 ± 6.83
CO₃²⁻ (μmol kg⁻¹)	113.78 ± 6.67	74.83 ± 3.33	55.54 ± 7.20
DIC (μmol kg⁻¹)	2096.98 ± 10.33	2170.20 ± 7.20	2216.90 ± 18.08
ΩCalcite	2.72 ± 0.16	1.79 ± 0.08	1.33 ± 0.17
ΩAragonite	1.74 ± 0.10	1.15 ± 0.05	0.85 ± 0.11

Supplementary Table 1.1: Discrete water samples were collected at three time points (2/12, 2/21, 3/2) from each replicate aquaria (n=6 per treatment) during the experiment. Tris buffer-calibrated YSI sensors measured pH, temperature, DO, and salinity at the time of discrete water sample collection. Total alkalinity from these discrete samples was measured using a Metrohm 815 Robotic USB Sample Processor XL and Titrando 905. The CO2SYS package was used to obtain the detailed state of the carbonate system.



Supplementary Figure 1.2: Boxplots illustrating the median, upper and lower quartile, and interquartile range of mass specific respiration rates ($\mu\text{mol}/\text{min}/\text{g}$) for Lingcod embryos placed in the year 2020 (blue), year 2050 (yellow), and year 2100 (red) treatments. $P > 0.01$ for all pairwise comparisons ($p_{2020,2050}=0.85$, $p_{2050,2100}=0.98$, $p_{2020,2100}=0.93$).



Supplementary Figure 1.3: Boxplots illustrating the median, upper and lower quartile, and interquartile range of percent total hatch, percent hatch of larvae with oil globules, and percent hatch of larvae without deformities for the year 2020 (blue), year 2050 (yellow), and year 2100 (red) treatments. Nested mixed model ANOVAs were run to determine statistical significance. The percent of larvae with oil globules was significantly lower in the future condition treatments compared to the year 2020 treatment ($p_{2020,2050}<0.001$, $p_{2050,2100}=0.06$, $p_{2020,2100}<0.001$). The percent of larvae with deformities was statistically similar between the year 2020 and year 2050 treatment; the percent of larvae with deformities significantly increased in year 2100 conditions ($p_{2020,2050}=0.1$, $p_{2050,2100}=0.01$, $p_{2020,2100}<1 \times 10^{-4}$).

Chapter 2: Climate-driven shifts in predator-prey interactions for commercially and ecologically important Eastern Bering Sea fishes

Abstract

Variation in species' tolerance to climate change conditions may result in changes to the strength of ecological relationships that structure and maintain the stability of ecosystems. In this study, I evaluate how historical (1982-2019) and projected (2030 through end-of-century) warming in the Eastern Bering Sea (EBS), Alaska, affects predator-prey interactions for some of the most commercially valuable fisheries in the U.S. These potential shifts in predator-prey interactions will not only impact the structure of ecological communities, but also the human communities that rely on these resources. The EBS is the largest marine ecosystem in Alaska and is already transitioning from an arctic to a subarctic system. Using a species distribution modeling approach for seven species and an ensemble of 18 statistically downscaled climate models, I project how further temperature increases will affect the geographic similarity between predator and prey populations, the proportion of locations where predator and prey co-occur, and their encounter rates. Projections suggest predator-prey encounter rates in historic prey refuges will increase, intensifying predation pressure for prey, while projections of decreasing encounter rates in the outer shelf and southern EBS indicate predators may not have sufficient prey to maintain high abundance in these regions. This study establishes that the strength of predator-prey relationships will be impacted by climate change conditions, potentially altering the relative importance of predators and prey in the system and reshaping the structure of the EBS trophic web.

I. Introduction

Physiological intolerance to a warming ocean can affect survival, reproductive capacity, growth and development rates, and the timing of ontogenetic transitions in marine species, from primary producers up to top predators (Harley et al. 2006; Doney et al. 2012). These demographic effects in conjunction with shifting species' environmental niches have caused population-level shifts in abundance and distribution (Kingsolver 2009; Perry et al. 2005; Poloczanska et al. 2013). As co-occurring species have non-uniform responses to climate change, these shifts can lead to altered species interactions, which affect community structure and may lead to the reshaping of trophic webs and the emergence of novel ecosystems (Brander 2010; Doney et al. 2012). For fished species, climate change may not only impact the structure of ecological communities, but also the human communities that rely on them (Rogers et al., 2019).

Predator-prey relationships structure and maintain the stability of ecosystems (Langbehn & Varpe 2017; Thorne & Nye 2021; Estes et al. 2013). Until recently, studies on climate change impacts have largely ignored predator-prey interactions despite the fact that co-occurring, interacting species do not necessarily react in a similar manner to global climate change (Schweiger et al. 2008; Edwards and Richardson 2004). The majority of work on how climate change will affect trophic relationships is based on temporal match-mismatches (Cushing 1990; Visser & Gienapp 2019). For example, many fish species' spawning periods are adapted to the

average date of phytoplankton blooms, with climate-driven shifts in the timing of the spring phytoplankton bloom leading to a “mismatch” between peak predator requirements and peak prey availability, resulting in poor predator recruitment (Cushing 1990).

However, spatial mismatches are likely to have just as much of an effect as temporal mismatches (Durant et al. 2007). For example, shifts in predator-prey spatial overlap can alter the location and size of prey refuges. Reduction of prey refuges could amplify range contractions and biomass reductions more than we would predict from studies modeling the responses of prey species alone. For example, as temperatures have warmed in the Eastern Bering Sea (EBS), Arrowtooth Flounder’s (*Atheresthes stomas*) range has begun expanding into the historically cooler middle-shelf region, previously a refuge for their juvenile Walleye Pollock (*Gadus chalcogrammus*) prey (Hunsicker et al. 2013; Carroll et al. 2019). Conversely, prey refuges could increase if predator range and abundance contract with climate change, allowing ecological release of the prey. Warming temperatures on the U.S. Northeastern Shelf will likely cause a contraction in Atlantic Cod’s range, potentially increasing the size of their prey species’ spatial refuges (Selden et al. 2018).

Projected shifts in a prey’s range that predators are not expected to match, or reductions in prey abundance, would lead to a larger decrease in predator abundance than expected from an individual model projecting a contraction of abiotic habitat

(Peers et al. 2014). Even if suitable habitat is projected to increase, predators will not exploit new habitat if it lacks sufficient prey resources. Climate change may also lead to a shift in the relative importance of prey species in predator diets as mismatches occur (Latham et al. 2013, Peers et al. 2014). Some species are adept at prey switching; for cod (*Gadus morhua*) and whiting (*Merlangius merlangus*) prey preference is a decreasing function of the relative density of their prey (Rindork et al. 2006). Other species are less flexible in their prey choice. The Orange Spotted Filefish, a corallivorous reef fish, continued to consume a bleached coral species over healthier, but less-preferred coral species (Brooker et al. 2014). Overall, disrupting adapted trophic relationships can amplify the impact of climate change throughout the community (Blois et al. 2013) and predicting changes in spatial overlap between predators and their prey is therefore crucial for informing climate-ready fisheries management (Kempf et al. 2013).

In this study, I examine potential changes in predator-prey relationships in the Eastern Bering Sea, Alaska, among some of the most valuable commercial fishery species in the U.S. The EBS is a subarctic ecosystem sensitive to temperature-driven changes in sea ice extent (Mueter and Litzow 2008). In ecosystems like the EBS at the boundary between arctic and boreal ecotones, climate-driven changes in predator-prey overlap can result in shifts in trophic interactions and transformations in food web architecture (Kortsch et al 2015; Goodman et al. 2022). Given the scale and value of Alaskan fisheries, the potential for shifts in fished species' distribution, abundance,

and trophic interactions in the EBS will have a substantial impact on Alaskan fishing communities' social systems and culture, the seafood industry, and statewide economics (Fissel et al. 2021; Cheung et al. 2010).

We have already observed shifts in Alaska fisheries since 2014, as anomalously warm years continue in succession. The Snow Crab fishery, a highly valuable commercial fishery in the EBS, collapsed in 2021 leading to a 88% decrease in quota (Murphy 2020; Heller-Shipley 2021). In 2020, fishing for Pacific Cod was closed in Gulf of Alaska's federal waters, likely due to a reduction in suitable thermal habitat (Laurel and Rogers 2020; Peterson et al. 2022). Rooper et al. 2021 predicted continued shifts in groundfish species' abundance and distribution in the EBS with climate change. Using a species distribution modeling (SDM) approach I projected changes in the distribution, abundance, and predator-prey overlap for four predators and four of their focal prey species as warming progresses in the Eastern Bering Sea. This study examines potential changes in predator-prey overlap to improve our predictions of how these fished species will be impacted by temperature shifts. My study questions included:

- 1) Will we see further shifts in the abundance and distribution of the study species by end-of-century compared to recent warm-year observations?
- 2) Will encounter rates between predator and prey pairs be further impacted by warming temperatures?

- 3) Will there be an overall increase or decrease in the extent of spatial overlap for each predator-prey pair by end-of-century? Where in the EBS will there be further shifts in spatial overlap?
- 4) Will there be an increase or decrease in prey refuges by end-of-century?
- 5) Will the importance of certain prey items shift as temperatures increase or will there be a simple directional change in the availability of prey?

II. Methods

2.1 Study system and species

The highly productive Eastern Bering Sea is the largest marine ecosystem in Alaska (Stevenson and Lauth 2019). The EBS is defined by a broad continental shelf (>500 km) that is divided into the inner, middle, and outer shelf separated by frontal regions (Ciannelli and Bailey 2005). The coldest temperatures are found in the middle shelf, with the outer shelf characterized by warmer basin water and the inner shelf defined by tidal mixing of warmer surface water (Ciannelli and Bailey 2005). The distribution of many species in the region is tied to changes in the extent of the “cold pool”, bottom water in the middle shelf region that is $< 2^{\circ}\text{C}$ (Mueter and Litzow 2008; Wyllie-Echeverria & Wooster 1998). In recent years, the EBS has been transitioning from an arctic to a subarctic system (Spies et al. 2020). Since 2014 anomalously warm temperatures have restricted the extent of the cold pool, with 2018 having the

smallest cold pool extent observed in history, only covering 1% of the EBS shelf bottom (Alabia et al., 2018; Spies et al. 2020; Stabeno et al., 2018).

I chose the focal predator species based on their commercial and ecological importance in the EBS. My chosen predator species were: 1) adult Walleye Pollock, 2) Pacific Cod (*Gadus macrocephalus*), 3) Pacific Halibut (*Hippoglossus stenolepis*), and 4) Arrowtooth Flounder. My chosen prey species were: 1) juvenile Walleye Pollock, 2) Tanner Crab (*Chionoecetes bairdi*), 3) Snow Crab (*Chionoecetes opilio*), and 4) Alaskan Pink Shrimp (*Pandalus eous*). Walleye Pollock are the most abundant fish species in the EBS, shaping the EBS ecosystem as both a crucial prey species and as a mid-trophic level predator (Dorn et al. 2017). The Alaskan Pollock fishery is one of the most valuable in the world and is harvested at or near the total allowable catch (Fissel et al. 2021). In 2020, commercial landings from the EBS and Gulf of Alaska were valued at approximately \$420 million (NOAA Fisheries 2022a). The Pacific Cod fishery is the second largest by volume in Alaska and is managed via multiple measures including permits and limited entry, catch quotas, closed waters, etc. (Fissel et al. 2018; NOAA Fisheries 2022b). Pacific Halibut is the largest flatfish species and one of the most valuable fisheries in the North Pacific Ocean, supporting commercial, recreational, and subsistence fisheries for over a century (Barnes et al. 2018; NOAA Fisheries 2020). Arrowtooth flounder is an ecologically significant predator in the Eastern Bering Sea because they are abundant and voracious predators of juvenile Walleye Pollock. Commercial interest in Arrowtooth Flounder has grown since 2008,

despite being a low-value fishery, and they are now typically sold in Asian markets (Spies et al. 2017; NOAA Fisheries 2022c).

The National Marine Fisheries Service's Alaska Fisheries Science Center conducts an annual bottom trawl survey during the summer in the EBS, with approximately 376 stations sampled each year since 1982 (Stauffer 2004). Species catch data and contemporaneous *in situ* environmental data were obtained from the survey, which uses a stratified systematic survey design and standardized fishing procedures. Survey methods are fully documented by Stauffer (2004) and Lauth and Conner (2017). Bottom trawl catches from survey hauls were converted to catch-per-unit-effort (CPUE) by measuring distance traveled for each tow and net width (Conner and Lauth 2017). Survey data were length-corrected to ensure that predators were large enough to capture focal prey items and to account for ontogenetic depth migration (Barbeaux and Hollowed 2018). Length classes were determined by measuring the fork length of a subsample of fish from each tow, and expanding this to the entire catch in a given tow based on the ratio of sampled weight to total towed weight for each species. Individuals were considered "predators" in the analysis at the following adult size classes: Pacific Cod >70 cm, Arrowtooth Flounder >30 cm, Pacific Halibut >40 cm, and Walleye Pollock were >40 cm. Juvenile walleye pollock were considered prey if they were <25 cm. The analysis includes annual bottom trawl survey data from 1982-2019, capturing both anomalously warm years and cold years, allowing us to analyze species' responses to temperature shifts.

Predator diets were determined using the Alaska Fisheries Science Center's North Pacific groundfish diet database (AFSC 2008). Percent weight in diet was determined by taking the mean percent weight of the prey species in the predator's diet from 2013-2017. Only prey species with sufficient sample size in the trawl survey were included in the analyses. For example, *euphausiidae* sp. and *crangonidae* sp. are a considerable portion of the focal predator diets, but the only shrimp species adequately sampled in the survey was Alaskan Pink Shrimp (*Pandalus borealis*). The four prey species of interest in this analysis for Pacific Cod were juvenile Walleye Pollock, Tanner Crab, Snow Crab, and Alaskan Pink Shrimp. The two prey species of interest for Arrowtooth Flounder were juvenile Walleye Pollock and Alaskan Pink Shrimp. The three key prey species for Pacific Halibut were juvenile Walleye Pollock, Tanner Crab and Snow Crab. The predator-prey relationships I chose to include captured approximately 40% of Pacific Cod, Arrowtooth Flounder, and Pacific Halibut's diet (Figure 1). Finally, I chose to look at the spatial overlap between adult and juvenile Walleye Pollock because cannibalism has a considerable impact on the survival and recruitment of juvenile pollock in the EBS, despite only being around 4% of adult pollock's diet (Mueter et al. 2011; Wespestad et al. 2000). The intensity of cannibalism depends on the extent of spatial overlap between adults and juveniles (Wespestad et al. 2000).

2.2 Species distribution models

I used a SDM approach to quantify changes in distribution and abundance for the four predator and four prey species. SDMs relate the geographic range and abundance of a species with information on oceanographic and habitat conditions (predictor variables). The resulting habitat models are then applied to climate projections to determine the distribution of future suitable habitat (Elith and Leathwick 2009; Pacifici et al. 2015). Predictor variables, collected *in situ* and obtained from the 1982-2019 EBS bottom trawl datasets, included: depth, rugosity, sediment grain size, sea surface temperature (SST), bottom temperature, and the difference between SST and bottom temperature (delta temperature, a proxy for stratification). Unlike the three habitat variables (depth, rugosity, and sediment grain size), the temperature variables are non-stationary climate variables. We know that temperature is the dominant driver of distributional change in marine fishes and that changes in temperature impact trophic structure (Nagelkerken et al. 2020; Hollowed et al. 2013; Sunday et al. 2012).

I used generalized additive models (GAMs) to fit SDMs for each individual species using the R package *mgcv* (v1.8-36; Wood 2011). I modeled the CPUE of a species x in an EBS trawl survey location i in year y as an additive function of the predictor variables. To accomplish this I used a traditional hurdle model approach – I first ran a presence/absence GAM, which predicted likelihood of species' occurrence, and then a haul-specific abundance model, which predicted the log of CPUE given presence. CPUE was log-transformed to reduce the skewness resulting from large catch rates at a small number of haul locations (Quinn et al. 1999). Predicted CPUE for species x in

haul location i in year y was calculated by multiplying the predictions from the presence/absence model by the exponentiated predictions from the abundance model and by a correction factor to account for retransformation bias. The GAMs were fit using 75% of the *in situ* data (training set) while 25% of the data (test set) was held back to test whether the models can replicate occurrence and abundance values in unseen portions of the data (Araújo et al. 2005).

This modeling approach was repeated for all possible combinations of the predictor variables. R's `corvif` and `acf` functions were used to test for collinearity and autocorrelation. Akaike's Information Criterion (AIC), Area Under the Curve (AUC), and deviance explained were used to choose the best model for each species. The model that included all six predictor variables and an interaction between bottom temperature (`b temp`) and depth performed best for all species (Table S1):

$$P_{x,i,y} = s(SST) + s(b\ temp) + s(delta\ temp) + s(depth) + s(grainsize^2) + s(rugosity) + s(btemp,depth)$$

$$A_{x,i,y} = s(SST) + s(b\ temp) + s(delta\ temp) + s(depth) + s(grainsize^2) + s(rugosity) + s(btemp,depth)$$

where $P_{x,i,y}$ is the probability of species x occurrence in haul i in year y and $A_{x,i,y}$ is the predicted log CPUE of species x in haul i in year y . $s()$ represents unique regression spline functions for each predictor variable. AUC was only used to evaluate the performance of the binary presence/absence models; AUC values range from 0-1,

with values closer to 1 representing models that are highly correlated with observed occupancy.

2.3 Projected shifts in species' range and distribution

To determine how climate change may affect species' range extent and CPUE I used the output of 18 statistically downscaled CMIP5 earth system models based on RCP 8.5 (a high greenhouse gas concentration trajectory) for the EBS (Morley et al. 2018). To do this, the Simple Ocean Data Assimilation ocean/ice reanalysis model (SODA3.3.1; 0.25 lat x 0.5° lon) reconstructed the historical physical history of the EBS since the beginning of the 20th century. Then each climate model was regridded to match the finer spatial resolution of the Simple Ice Data Assimilation (SODA) 3.3.1 data and the depth strata for projecting bottom temperatures was refined according to this finer spatial resolution of bathymetry. I calculated the difference between future temperatures and the modeled baseline period (1995-2014) for each of the 18 earth system models; the delta values were then added to a mean temperature climatology developed from SODA 3.3.1 data (Hare et al. 2012). The data were aggregated into five twenty-year bins (2007-2020, 2021-2040, 2041-2060, 2061-2080, 2081-2100) and averaged across the 18 earth system models. For the SODA grid cells outside the domain of a climate model, I used data from the nearest climate model grid cell. The fitted SDMs were used to project likelihood of occupancy and future CPUE for species x in each grid cell (0.25 lat x 0.5° lon) for each twenty-year time bin.

2.4 Abundance and Range Shifts

Projected range extent for each twenty-year time bin was calculated as the mean of the likelihood of occupancy for grid cells within the EBS survey region. Projected CPUE for each grid cell was summed across the entire EBS survey region to obtain projected CPUE sums for each twenty-year time bin.

2.5 Predator/prey overlap metrics

To understand historic and future patterns of spatial interactions between predator and prey pairs, I calculated three spatial predator-prey overlap metrics for both the observed period (1982-2019) and the climate projections (SODA's five twenty-year bins): area overlap, the global index of collocation, and Hurlbert's index (Carroll et al., 2019).

Area overlap is the only presence/absence based metric I chose, which is important because I have the most confidence in the presence/absence model outputs. Area overlap measures the proportion of sampled locations where species co-occur on a scale of 0-1 (0 indicates no co-occurrence and 1 indicates complete co-occurrence). This metric can be used to infer the presence or absence of prey refuges. The global index of collocation is also on a 0-1 scale and measures how distinct a predator and prey's centre of gravity are (0 is completely distinct and 1 is coincident). I used an encounter metric, Hurlbert's index, to visualize where in space overlap will change

between the 2007-2020 and 2081-2100 time bins. Hurlbert's index assesses whether two species use space in proportion to its availability (0 indicates species do not share space, 1 indicates species share proportion to its availability, and >1 indicates the two species prefer certain areas and that their preferences coincide). The formula for each metric can be found in Table S2.

III. Results

The mean bottom temperature from the ensemble of 18 downscaled models revealed that warming of 3.25°C is likely in the EBS (Figure 2). Species distribution models were well fit to data, with on average 33% explained deviance (Table S1), and performed well during cross-validation (average AUC of 0.86; Table S1). SDM response curves to environmental covariates revealed specific non-linear environmental preferences that varied among species (Figures S1-S12). By end-of-century I project an increase in both the range and abundance of Arrowtooth Flounder and Pacific Halibut (33% and 30% range increase, respectively and a 30% and 234% increase in abundance, respectively), while the abundance of adult Walleye Pollock and Pacific Cod is projected to decrease (63% and 43%, respectively; Figure S13). With warming, I project abundance will decrease for all four prey species by end-of-century (15% for juvenile Walleye Pollock, 58% for Alaskan Pink Shrimp, 56% for Tanner Crab, and 76% for Snow Crab; Figure S14). The specific dynamics and impact of these projected shifts on predator-prey overlap is detailed below.

3.1 Pacific Cod

Area overlap between Pacific Cod and three of its prey species – juvenile pollock, tanner crab, and snow crab – has been increasing since the last cool period in 2010 (Figure 3A). Area overlap between cod and juvenile pollock reached a maximum in 2019 (0.74) and will remain at that maximum through end-of-century (Figure 3A). I project a 19% increase in encounter rates between cod and juvenile pollock between the 2007-2020 and 2081-2100 projections for the EBS (Figure 4A). By 2081-2100, I project both cod and juvenile pollock CPUE will decrease on the outer shelf and the majority of their biomass may be found on the middle and inner northern shelf region (Figure S13C & Figure S14A). Accordingly, encounter rates are projected to decline on the outer shelf, but increase considerably on the middle and inner northern shelf (Figure 4A).

Similar to juvenile pollock, area overlap between cod and tanner crab reached its observed maximum in 2019. I project that area overlap will increase through the 2021-2040 time period and then remain at that new maximum until end-of-century (0.7; Figure 3A). However, encounter rates between cod and tanner crab are projected to decrease 24% by 2081-2100 as abundance of both species decreases in the southern EBS (Figure 4C; Figure S13C; Figure S14A). The projected increase in interspecific encounter rates in the northern EBS, as cod biomass aggregates in the north, does not fully compensate for the decreased overlap in the south (Figure 4C).

Area overlap between cod and snow crab also reached the observed maximum in 2019 (Figure 3A). Unlike juvenile pollock and tanner crab, I project cod and snow crab area overlap will decrease under future warming. Snow crab's range is projected to contract 44% by 2081-2100; I project area overlap with cod by end-of-century will be the mean overlap observed from 1982-2019 (0.45; Figure 3A & Figure S14D). With increased cod abundance on the middle shelf of the northern EBS, I project a 35% rise in encounter rates with snow crab (Figure 4D & Figure S13C).

Area overlap between cod and pink shrimp is projected to decrease with future warming as pink shrimp moves out of the southern inner shelf and cod moves in (Figure 3A; Figure S13C; Figure S14B). By end-of-century I project an area overlap similar to the minimum overlap in the 1982-2019 time series (0.16; Figure 3A). Encounter rates between cod and pink shrimp are also projected to decrease 21% in the northern outer shelf of the EBS by 2081-2100 (Figure 4B).

The global index of collocation, a calculation of similarity in cod and its prey populations' centres of gravity, shows considerable swings from year-to-year (Figure 8A). As temperatures increase, distinctness between cod and all of its prey populations' centre of gravity is projected to remain in between the first and third quartile of 1982-2019 observations.

3.2 Arrowtooth Flounder

Comparable to recent warm-year observations, I project Arrowtooth Flounder's range will expand into the middle shelf as the extent of the cold pool decreases (Figure S13B). Area overlap between flounder and juvenile pollock has been increasing since the last cool period (2010) with the highest overlap observed in 2018/2019 (0.69; Figure 3B). In fact, area overlap in 2018/2019 is higher than my twenty-year projections until the 2081-2100 time period (Figure 3B). Projected 2081-2100 area overlap matches what we observed in 2018/2019. I project an overall increase in interspecific encounter rate between flounder and juvenile pollock in the EBS because of the expansion of flounder in the middle shelf and northern trawl region (Figure 5A & Figure S13B). There will likely be a moderate decrease in encounter rate between the predator-prey pair on the outer shelf as juvenile pollock CPUE decreases in the outer shelf region (Figure 5A & Figure S14A).

Unlike flounder and juvenile pollock, area overlap between flounder and Alaskan Pink Shrimp is projected to decrease with increasing temperatures (Figure 3B). Similar to cod and pink shrimp, I project that pink shrimp's range will contract marginally in the southern inner shelf region, while flounder is expected to expand into that region and into the middle shelf, reducing area overlap (Figure S13B & Figure S14B). By end-of-century, area overlap between flounder and pink shrimp is projected to be similar to 1994-1996 observations (0.16; Figure 3B). On the other hand, interspecific encounter rate between this predator-prey pair is projected to increase with warming temperatures (Figure 5B). Interspecific encounter rates will

likely increase in the outer shelf region as flounder abundance increases (Figure 5B & Figure S13B).

Finally, my calculation of the geographic index of collocation between flounder and both of its prey species indicates that both predator-prey pairs' future centres of gravity will be similar to multiple years in the observed period (1982-2019) when the distinctness between the two populations' centre of gravity was at its minimum (Figure 8B).

3.3 Pacific Halibut

I project an 44% increase in Pacific Halibut's range in the EBS trawl survey region as temperatures rise (Figure S13D). This range expansion results in a high area overlap between halibut and all three of its prey species (Figure 3C). Area overlap with juvenile pollock by 2021-2040 is higher than all historical values and continues to increase until end-of-century; the mean area overlap during the observed period was 0.48, by end-of-century area overlap increases to 0.84 (Figure 3C). Encounter rates with juvenile pollock will also likely increase. I project a 30% increase in encounter rates from 2007-2020 to 2081-2100 (Figure 6A). Similar to cod and flounder, halibut's overlap with juvenile pollock will likely decrease on the outer shelf, but a stronger increase in encounter rate is projected for the middle and inner shelf (Figure 6A).

Observed area overlap between halibut and tanner crab decreased after the 2014-2016 heatwave, despite similarly high temperatures in 2018 and 2019 (Figure 3C). With projected range expansion of halibut, my models project future area overlap will be similar to the peak I observed during the 2014-2016 heatwave (0.69, Figure 3C). However, encounter rates between halibut and tanner crab are projected to decline by end-of-century, due to the strong decrease in encounter rate in the southern EBS where I project a substantial decrease in tanner crab CPUE (Figure 6B & Figure S14C).

Halibut's area overlap with snow crab is typically higher during cool periods, when snow crab range expands southward (Figure 3C & Figure S15). However, I project an area overlap during the 2021-2040 time period that is similar to the values seen during the last cool period (0.57; Figure 3C). But by end-of-century, snow crab's projected range has decreased by 44% and area overlap is equivalent to the mean observed from 1982-2019 (0.38; Figure 3C & Figure S14D). Encounter rates between halibut and snow crab are projected to increase in the northern EBS and decrease in the southern EBS by end-of-century as halibut range expands northward and snow crab biomass contracts northward (Figure 6C; Figure S13D; Figure S14D). Therefore, Hulbert's index for the entire EBS does not change between 2007-2020 and 2081-2100 projections.

The global index of collocation shows that throughout the observed time series, the distinctness between halibut and juvenile pollock centre of gravity has changed markedly from year-to-year. In two warm years, 2016 and 2019, the global index of collocation shifted from 0.38 to 0.85 respectively (Figure 8C). I project that the two populations' centres of gravity will remain similar until end-of-century (0.83, Figure 8C). Halibut and tanner crab populations' centre of gravity have been close together in space throughout the observed period and the global index of collocation indicates they will remain coincident in the future (Figure 8C). Finally, the global index of collocation indicates that the distinctness between halibut and snow crab populations' projected centres of gravity will remain around the mean of the observed period (Figure 8C).

3.4 Adult Walleye Pollock

The range extent of adult and juvenile pollock is not projected to increase past 2007-2020 projections of range extent (Figure S13A & S14A). Accordingly, area overlap was at its peak in 2019 and is projected to remain at that peak through end-of-century (0.85; Figure 3D). However, encounter rate is projected to increase beyond historical observations (Figure 7). Hurlbert's index increases by 32% between 2007-2020 and 2081-2100 projections (Figure 7). Adult pollock CPUE is projected to decrease throughout the EBS by 2081-2100, with the sharpest CPUE declines on the outer shelf (Figure S13). Future adult pollock biomass is projected to be concentrated on the northern middle shelf, where the 2081-2100 projected juvenile pollock CPUE is

highest (Figure S13 & S14). Predator-prey encounter rates are projected to decrease on the outer shelf, but there will be a stronger increase in encounter rates along the middle shelf (Figure 7). Despite increasing encounter rates, the distinctness between adult and juvenile pollock populations' centre of gravity will be similar to the average distinctness observed during the historical period (Figure 8D).

IV. Discussion

My results suggest that continued warming in the EBS will affect interspecific interactions for four key piscivores and their prey. Further shifts in the range and abundance of the predator and prey species are projected, and the overlap metric projections indicate these shifts will not be congruous. Changes in these adapted trophic relationships have the potential to affect EBS prey refuges and biomass; control the abundance of predator species; and impact competition for prey resources.

The EBS middle and inner shelf historically served as a prey refuge for juvenile pollock and $>59^\circ$ latitude served as a prey refuge for snow crab from the predator species explored. As temperatures continue to rise, I project an increase in juvenile pollock and snow crab encounter rates with their primary predators in both regions, essentially eliminating two important prey refuges by end-of-century. This increase in encounter rate would likely result in a decrease in juvenile pollock and snow crab biomass that is greater than we would predict from an individual SDM for either of these prey species. The snow crab fishery already collapsed in 2021; my projections

of a 44% range contraction (reflected in the decrease in area overlap with cod and halibut by end-of-century) will be exacerbated by increasing encounter rates within their historic prey refuge.

The projected loss of juvenile pollock's prey refuge in the middle shelf will likely increase the occurrence of cannibalism on juvenile pollock by adults. Cannibalism intensifies as overlap between adult and juvenile pollock populations increases (Boldt et al. 2012). I predict a rise in pollock cannibalism as the encounter rate between adult and juvenile pollock increases 32% in the middle shelf by end-of-century. My predictions are supported by Boldt et al. 2012, who observed that cannibalism increases during warm years. Multiple other studies have also predicted decreases in pollock abundance due to the negative effects of increasing temperature (Rogers et al. 2021; Spencer et al. 2016; Hunt 2011); Holsman et al. 2020 predicted >70% decrease in the pollock fishery by 2071-2100 under RCP8.5. My prediction of increased cannibalism while both adult and juvenile pollock CPUE decreases will further reduce pollock recruitment. However, the role of cannibalism here might provide prey for pollock in poor years and may provide an upper limit for pollock populations in good years (Boldt 2012).

Projected predator biomass may be similarly impacted by shifts in prey range and abundance. The individual SDMs for flounder and halibut projected increased CPUE throughout the EBS by end-of-century. I project encounter rates with their prey will

decline on the outer shelf and southern EBS as prey biomass drops. Encounter rates with juvenile pollock abundance are decreasing substantially on the outer shelf and marginally in the southern EBS, while tanner crab and snow crab encounter rates are decreasing in the southern EBS. I hypothesize that this decline in predator-prey encounters may prevent increases in flounder and halibut abundance in these two regions. However, the four prey species included in the analysis only captured approximately 40% of cod, flounder, and halibut diet and cannibalism only comprises 4% of pollock's current diet. Increased consumption of a more abundant prey item or prey switching is possible.

It is also possible that flounder and halibut abundance will remain similar to the individual SDM projections, since I project decreases in both adult pollock and cod abundance on the outer shelf and southern EBS, reducing competition for prey. The net impact from a projected decrease in prey alongside a decrease in competition is difficult to predict. To disentangle the effect of a decrease in prey and competition, future studies should use a joint species distribution model approach, which simultaneously models distributions of multiple species (Wilkinson et al. 2020). Overall, as projected flounder and halibut abundance and range increase, the projected abundance of cod and adult pollock decreases.

Adult pollock abundance will remain an order of magnitude higher than the other three predators with future warming. But, the relative importance of flounder and

halibut as predators will likely grow, and have a greater role regulating the biomass of the four prey species. Arrowtooth flounder currently plays a key role in regulating the abundance of pollock in the Gulf of Alaska (Ciannelli et al. 2012). The same will likely occur in the EBS since flounder abundance has already increased eight-fold over the last 30 years in the EBS, and we project further increases by end-of-century (Wilderbuer et al. 2010). In fact, in 2018/2019 area overlap for flounder and juvenile pollock was what I projected by end-of-century, indicating flounder range has expanded faster than expected from my model projections. Future area overlap between Pacific Halibut and juvenile pollock/tanner crab is projected to be higher than all observed values, which matches the projected 44% increase in halibut range by end-of-century. Halibut biomass has been decreasing in the Gulf of Alaska, which was attributed to bottom temperatures $>9^{\circ}\text{C}$ (Barnes et al 2018). The majority of bottom temperatures in the EBS will remain $<9^{\circ}\text{C}$ by end-of-century, likely improving habitat suitability outside of the outer shelf and southern EBS where their prey abundance is decreasing.

The three overlap metrics I used in my analysis showed distinct trends that were not always in agreement. The proportion of locations where cod and tanner crab co-occurred (area overlap metric) hit a new projected maximum in 2021-2040 as both species' range slightly increased from their 2019 peak. But, the abundance of both cod and tanner crab is projected to drop in the southern EBS, despite still being present in the area at low CPUE, so encounter rates (Hurlbert's index) are projected

to decrease. The global index of collocation in 2081-2100 was a bit higher (0.86) than the mean value from the historical period (0.82). I found that the global index of collocation was the least predictive as an indicator of how future warming will impact predator-prey overlap. Examining shifts in centres of gravity is a common approach to understand how global change conditions will impact the range, abundance, and ecological relationships of species. Future studies should ensure that centre of gravity is not the only metric used to assess how species are going to be impacted by climate change.

My models only include changes in SST, bottom temperature, and stratification expected from one climate scenario, RCP8.5. Additionally, models were fit using data from the summer trawl survey, and population dynamics during other seasons are not captured. Rooper et al. 2021 assessed shifts in EBS trawl survey species' range and CPUE using GAMs and Regional Ocean Modeling System (ROMS) climate projections, a dynamically downscaled climate model which includes tidal and bottom current. Although depth and bottom temperature were the most significant variables in their GAMs, the magnitude of shifts for cod, flounder, pollock, snow crab, and tanner crab were considerably less than my projections that used an ensemble of statistically downscaled climate models. However, Holsman et al. (2020) assessed changes in the Pacific Cod and Walleye Pollock fishery using the ROMSNPZ model, which included changes in the plankton community, and projected significant declines in both populations which is in contrast to my results.

This study strongly suggests that predator-prey relationships in the EBS will be impacted by climate change conditions. Ecosystem models are more advanced in quantifying trophic relationships, but the overlap metrics I used allow an examination of shifts in spatial relationships between predator-prey pairs that ecosystem models do not capture (Christensen and Walters 2004). My projections of increasing encounter rates in historic prey refuges suggest CPUE declines for prey will intensify, while my projections of decreasing encounter rates in the outer shelf and southern EBS indicate predators may not have sufficient prey to maintain high abundance here. Predators may be able to increase consumption of another prey item, or add new prey species to their diet. These novel interactions could reduce fitness as the predators lack a co-evolutionary history with a new prey species (Gilman et al. 2010). For the predator and prey species with projected declines in range and abundance, their biomass may begin increasing in the northern Bering Sea (Spies et al. 2020; Stevenson & Lauth 2019). If this occurs, community structure of the northern Bering Sea may similarly be impacted by changes in adapted trophic relationships as warming continues.

Figures















Predators	Prey	% Weight in Diet
Pacific Cod 	Juvenile Pollock 	12%
	Alaskan Pink Shrimp 	2%
	Tanner Crab 	29%
	Snow Crab 	
Arrowtooth Flounder 	Juvenile Pollock 	38%
	Alaskan Pink Shrimp 	4%
Pacific Halibut 	Juvenile Pollock 	22%
	Tanner Crab 	19%
	Snow Crab 	
Adult Walleye Pollock 	Juvenile Pollock 	4%

Figure 2.1: The four predator species of interest and their focal prey species in the EBS (percent weight in predator diet listed on right-hand side).

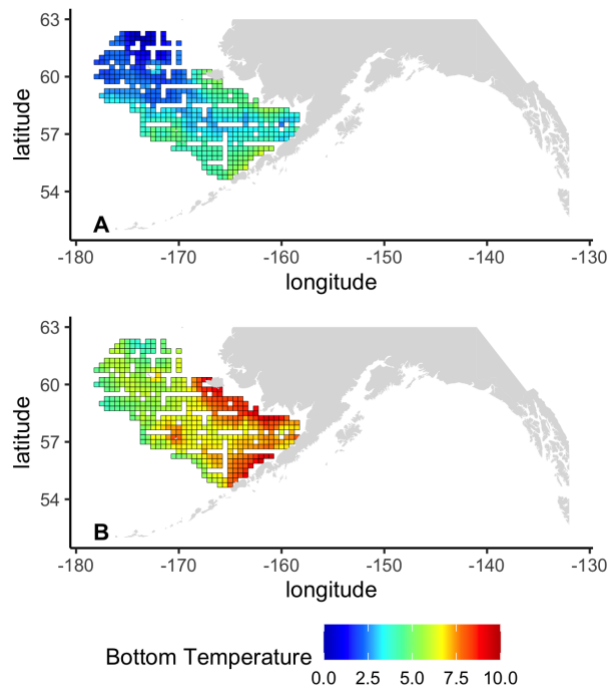


Figure 2: Bottom temperature projections from SODA’s ocean reanalysis that were statistically downscaled for the Eastern Bering Sea. A) Projections from the modeled baseline period (1982-2014). B) RCP 8.5 projections for 2081-2100. Projections are the average across 18 earth system models from CMIP5, missing grid cells are locations not adequately sampled by the Eastern Bering Sea trawl survey.

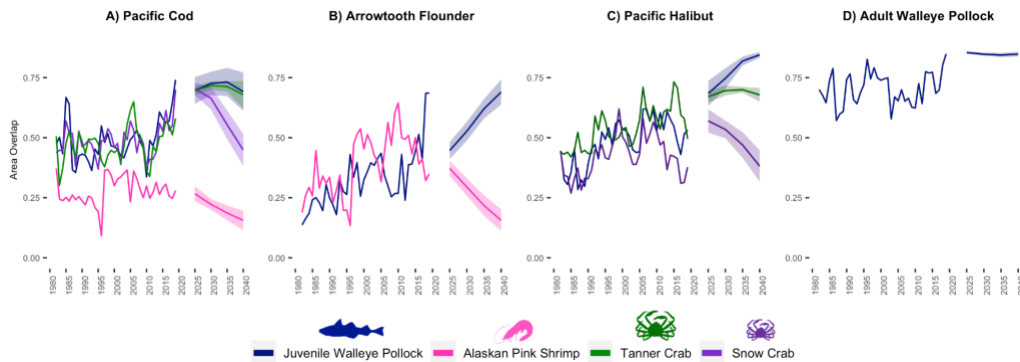


Figure 2.3: Area overlap between predator-prey pairs during the historical period (1982-2019) and for the projected period (2021-2040 through 2081-2100). Each panel

shows the proportion of the study area where the predator co-occurs with its prey (0-1 scale) within the Eastern Bering Sea trawl survey region for predators: A) Pacific Cod, B) Arrowtooth Flounder, C) Pacific Halibut, and D) Adult Walleye Pollock. Each line in the figures represents the predator's overlap with a single prey species: Juvenile Walleye Pollock (blue), Alaskan Pink Shrimp (pink), Tanner Crab (green), and Snow Crab (purple). Shaded regions in the projections represent the 95% confidence interval from the ensemble of 18 earth system models.

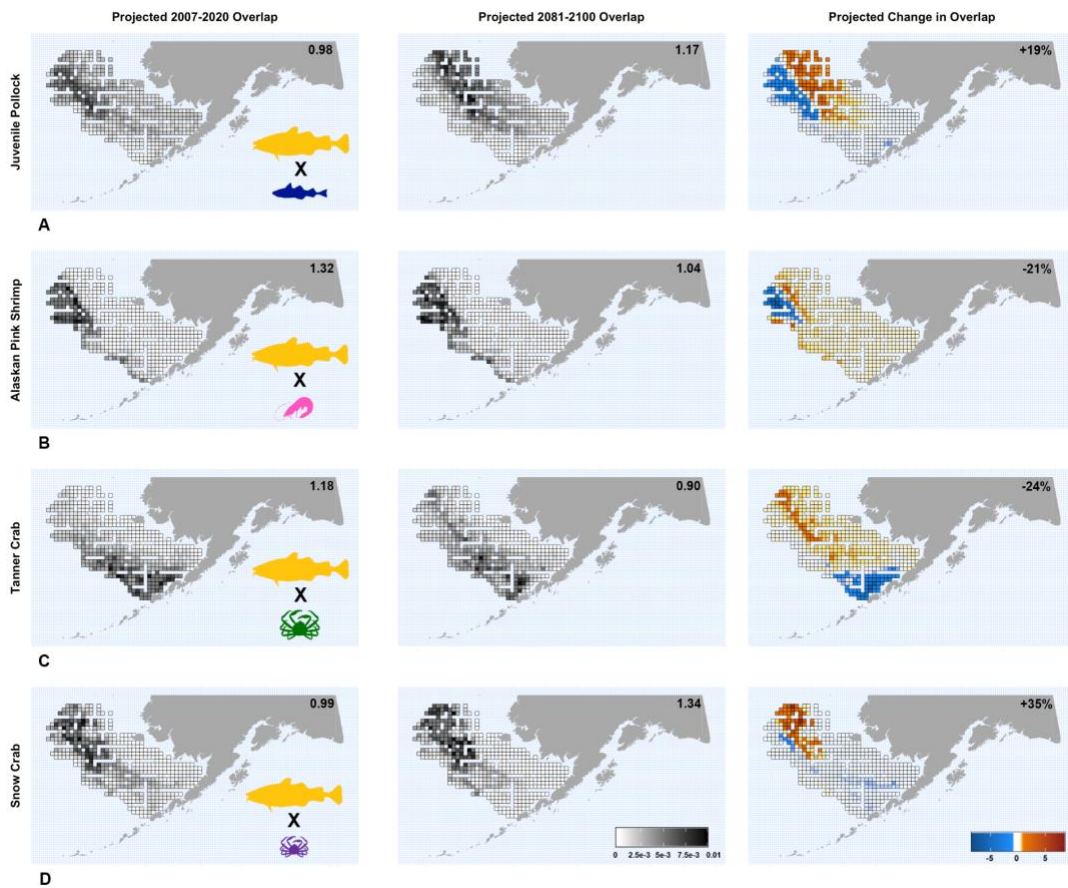


Figure 2.4: Pacific Cod's spatial overlap, calculated using Hurlbert's Index, with A) juvenile Walleye Pollock, B) Alaskan Pink Shrimp, C) Tanner Crab, and D) Snow

Crab for 2007-2020 projections (left), 2081-2100 projections (center), and the change in overlap between the current and future projections (right). Hurlbert’s Index was used to illustrate the spatial overlap projections because it is the only encounter metric that explicitly accounts for the size of the area occupied by each species (shared legend in bottom center panel; Carroll et al. 2019). Change in overlap was calculated by subtracting the 2081-2100 from the 2007-2020 overlap projections for each grid cell and then calculating the z-score for each grid cell. Blue represents a likely decrease in future predator-prey overlap, red represents a likely increase in predator-prey overlap (shared legend in bottom right panel).

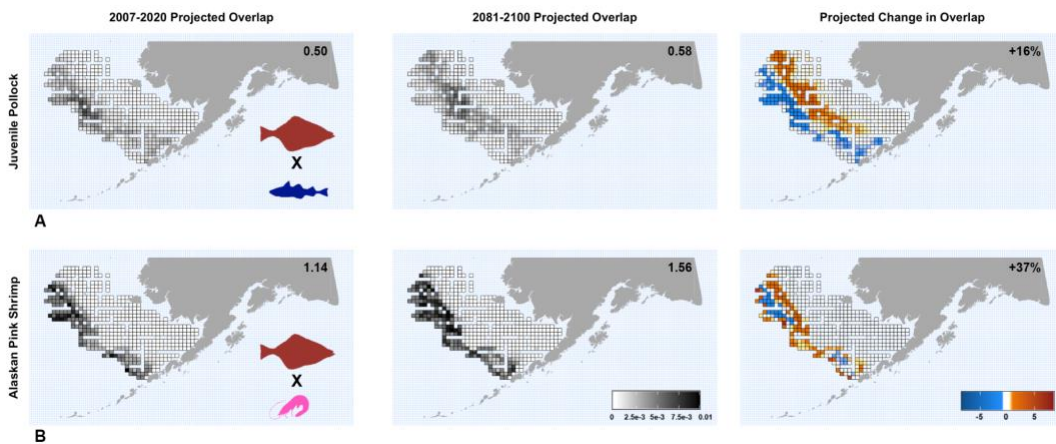


Figure 2.5: Arrowtooth Flounder’s projected spatial overlap, calculated using Hurlbert’s Index, with A) juvenile Walleye Pollock and B) Alaskan Pink Shrimp for SODA’s 2007-2020 projections (left), 2081-2100 projections (center), and the change in overlap between the current and future projections (right).

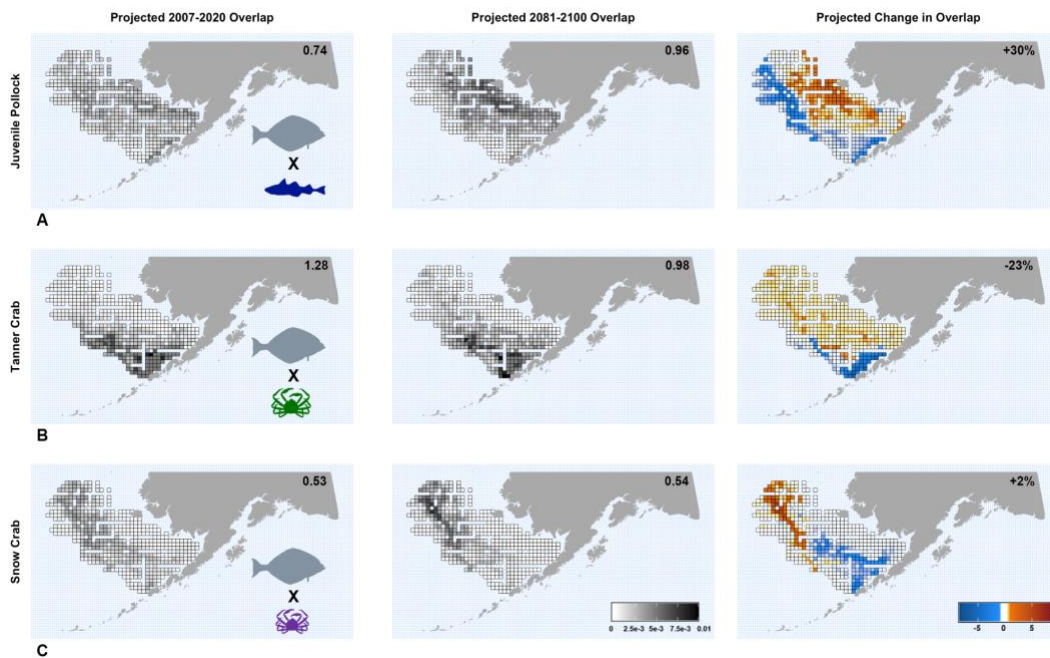


Figure 2.6: Pacific Halibut’s projected spatial overlap, calculated using Hurlbert’s Index, with A) juvenile Walleye Pollock, B) Tanner Crab, and C) Snow Crab for SODA’s 2007-2020 projections (left), 2081-2100 projections (center), and the change in overlap between the current and future projections (right).

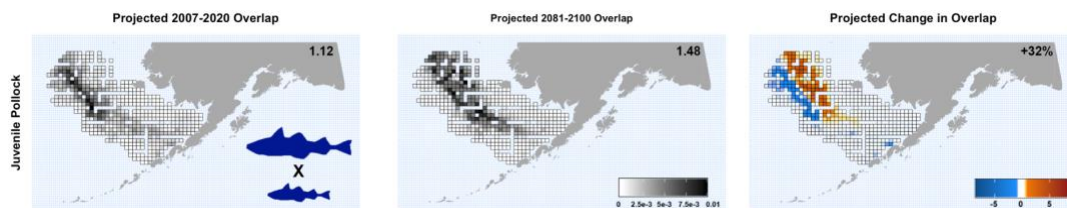


Figure 2.7: Adult Walleye Pollock’s projected spatial overlap, calculated using Hurlbert’s Index, with juvenile Walleye Pollock for SODA’s 2007-2020 projections (left), 2081-2100 projections (center), and the change in overlap between the current and future projections (right).

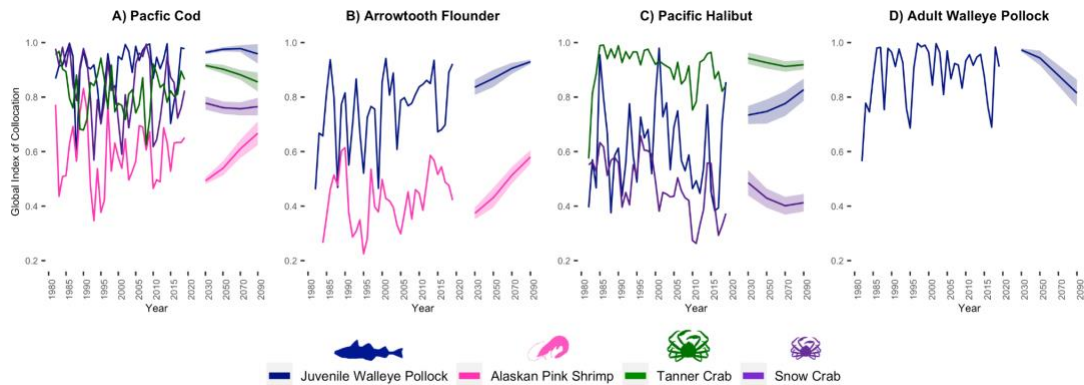


Figure 2.8: Shifts in the global index of collocation between predator-prey pairs during the historical period (1982-2019) and for the projected period (2030 through 2100). Each panel shows the geographical distinctness between a predator and their prey's centres of gravity within the Eastern Bering Sea trawl survey region (0 is completely distinct and 1 is coincident) for predators: A) Pacific Cod, B) Arrowtooth Flounder, C) Pacific Halibut, and D) Adult Walleye Pollock. Each line in the figures represents the predator's overlap with a single prey species: Juvenile Walleye Pollock (blue), Alaskan Pink Shrimp (pink), Tanner Crab (green), and Snow Crab (purple).

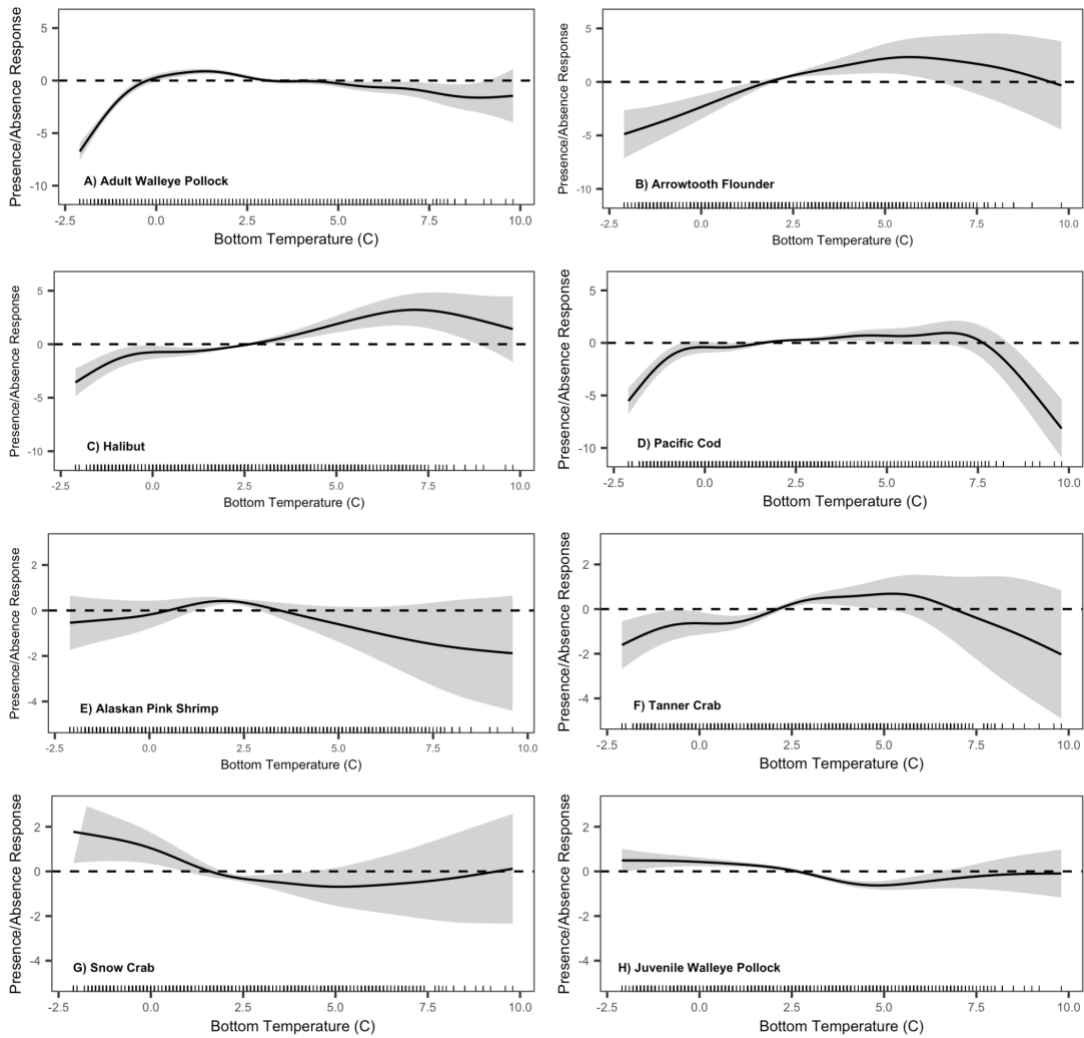
Supplementary Figures

	Presence/Absence GAMs			Abundance GAMs	
	Deviance Explained	AUC	AIC	Deviance Explained	AIC
Adult Walleye Pollock	0.29	0.86	4277.94	0.42	29278.28
Juvenile Walleye Pollock	0.16	0.77	8348.47	0.14	24829.78
Pacific Halibut	0.20	0.80	8969.46	0.26	14361.61
Pacific Cod	0.11	0.70	10497.28	0.09	12884.76
Arrowtooth Flounder	0.61	0.96	4643.52	0.50	10373.74
Alaskan Pink Shrimp	0.43	0.91	5642.05	0.37	8264.32
Snow Crab	0.53	0.94	4710.50	0.40	24980.78
Tanner Crab	0.46	0.92	5834.61	0.26	20815.99

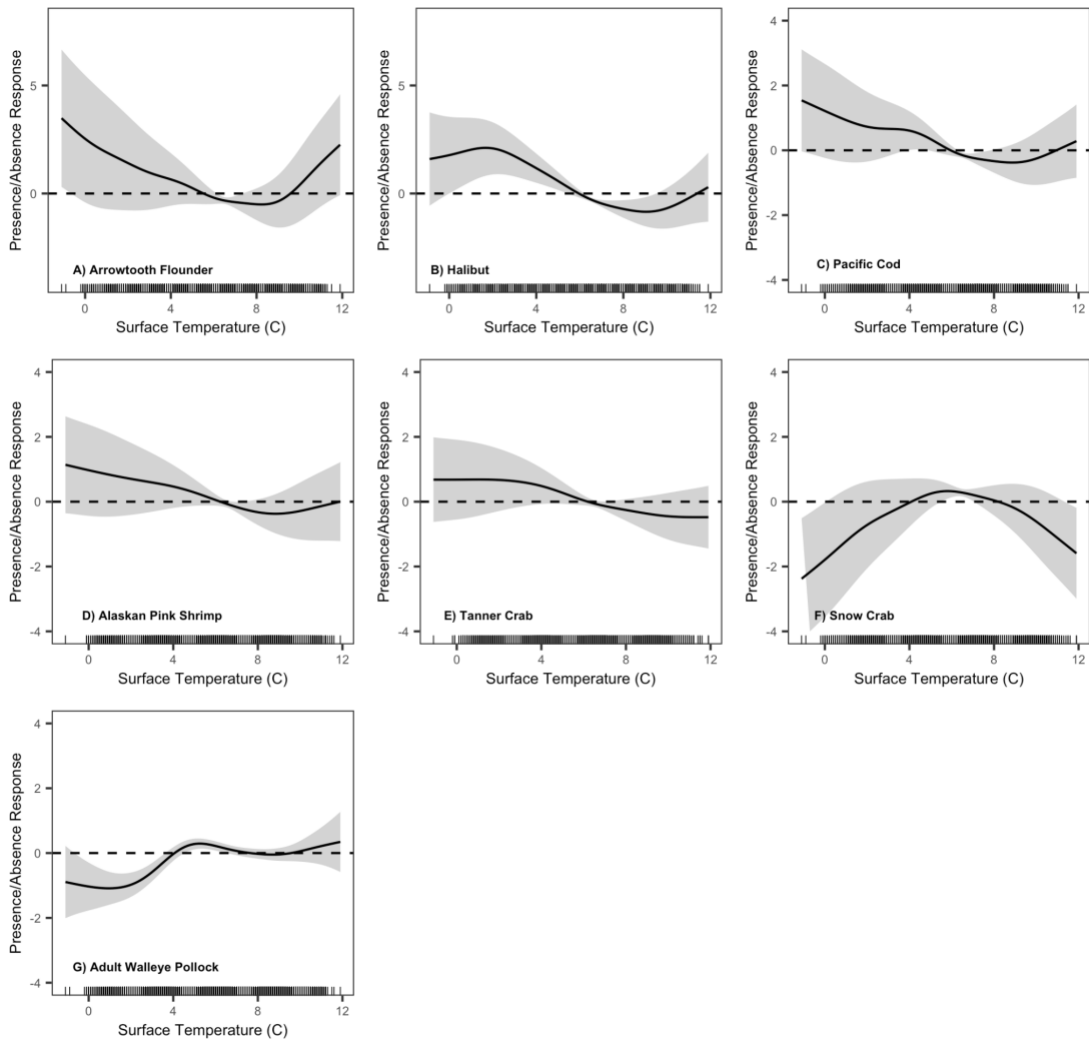
Supplementary Table 2.1: Deviance explained, AUC, and AIC of the selected presence/absence and abundance GAM for the predator and prey species.

Metric	What they measure	Formula
Presence/Absence Based:		
Area overlap	Measures the proportion of all sampled locations across a predefined area where species co-occur (Saraux et al. 2014)	$A_{pred,prey}/A_{total}$
Abundance Based:		
Global Index of Colocation	Measures geographical distinctness by comparing <u>centres</u> of gravity of populations with the dispersion of sampled individuals (Bez and Rivoirard 2000)	$1 - \frac{\Delta CG_{pred,prey}^2}{\Delta CG_{pred,prey}^2 + I_{pred} + I_{prey}}$ <p>where:</p> $CG_{pred,i} = \frac{\sum_i l * pred_i}{\sum_i pred_i}$ <p>and:</p> $I_{pred} = \frac{\sum_i (i - CG_{pred,i})^2}{\sum_i pred_i}$
Hurlbert's index	Measures interspecific encounter rate between predator and prey (Hurlbert 1978)	$\sum_i^n \left(\frac{p_{pred_i} * p_{prey_i}}{Ai/A_{occupied}} \right)$

Supplementary Table 2.2: Table adapted from Carroll et al. 2019 showing the three spatial predator-prey overlap metrics used for our historical and future projections of changes in species overlap in the Eastern Bering Sea. $A_{pred, prey}$ is the area occupied by both species, A_{total} is the total size of the study area, $A_{occupied}$ is the total area occupied by at least one of the species. p_{pred_i} and p_{prey_i} are the proportions of the total number of predator and prey in grid cell i . $CG_{pred,i}$ is the latitude or longitude (l) centre of gravity for the predator (same formula for prey). I is Inertia.

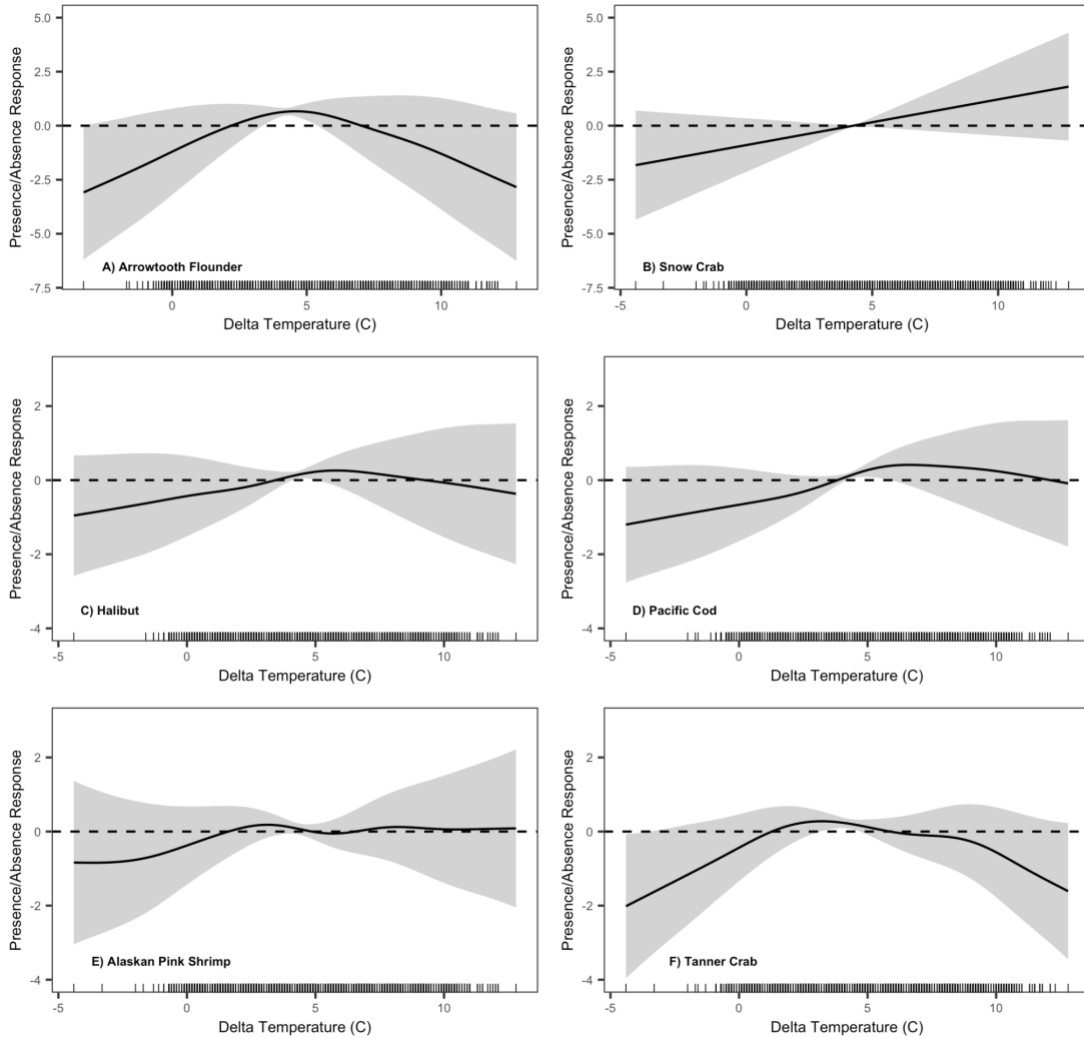


Supplementary Figure 2.1: Generalized additive model response curves for sea bottom temperature from binary presence/absence models for species A-H. Solid black lines are the fitted relationships between sea bottom temperatures and the partial responses, with the gray shaded area representing the 95% confidence interval. The predicted probability of occurrence is <0 below the dashed horizontal line and >0 above the dashed horizontal line. Black dashes along the x axis show the density of sea bottom temperature values observed in the survey. The vertical scale is the same for species A-D (-10 to 5) and the same for species E-H (-4 to 2).



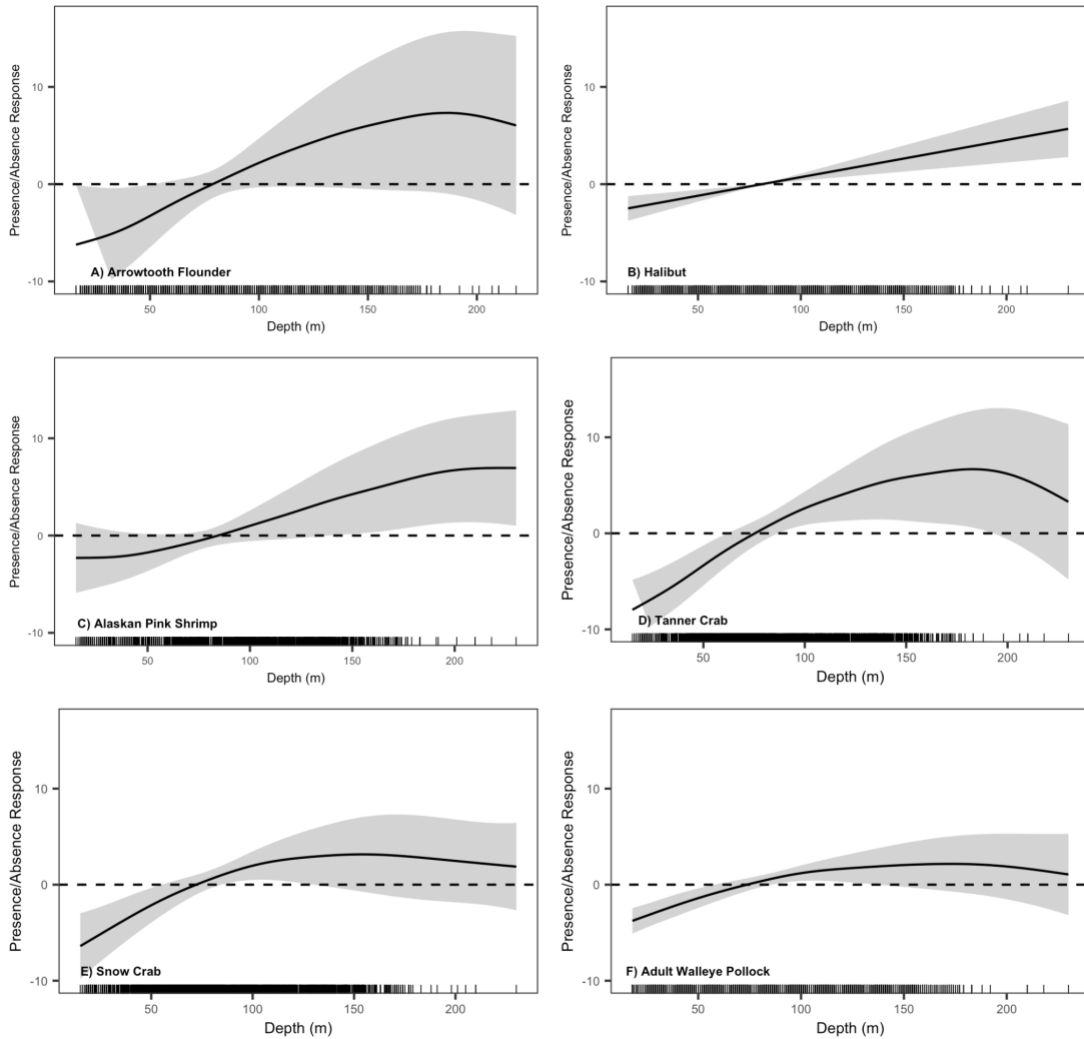
Supplementary Figure 2.2: Generalized additive model response curves for sea surface temperature from binary presence/absence models for species A-G. Sea surface temperature was not significant for the juvenile Walleye Pollock GAM. Solid black lines are the fitted relationships between sea surface temperatures and the partial responses, with the gray shaded area representing the 95% confidence interval. The predicted probability of occurrence is <0 below the dashed horizontal line and >0 above the dashed horizontal line. Black dashes along the x axis show the density of

sea surface temperature values observed in the survey. The vertical scale is the same for species A-B (-4 to 8) and the same for species C-G (-4 to 4).



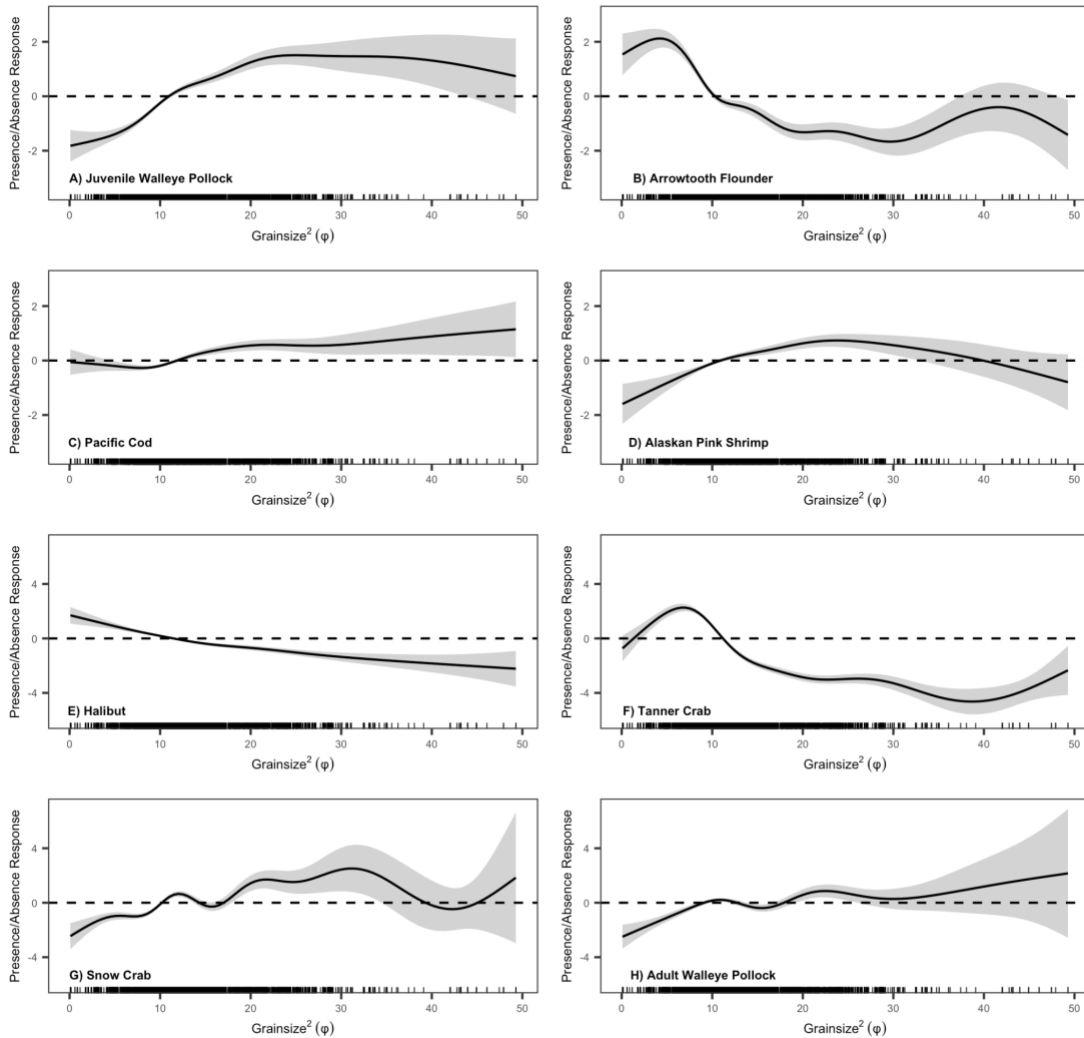
Supplementary Figure 2.3: Generalized additive model response curves for delta temperature (the difference between sea surface temperature and sea bottom temperature) from binary presence/absence models for species A-F. Delta temperature was not significant for the adult and juvenile Walleye Pollock GAMs. Solid black lines are the fitted relationships between delta temperatures and the partial responses, with the gray shaded area representing the 95% confidence interval. The

predicted probability of occurrence is <0 below the dashed horizontal line and >0 above the dashed horizontal line. Black dashes along the x axis show the density of delta temperature values observed in the survey. The vertical scale is the same for species A-B (-7.5 to 5) and the same for species C-G (-4 to 2).



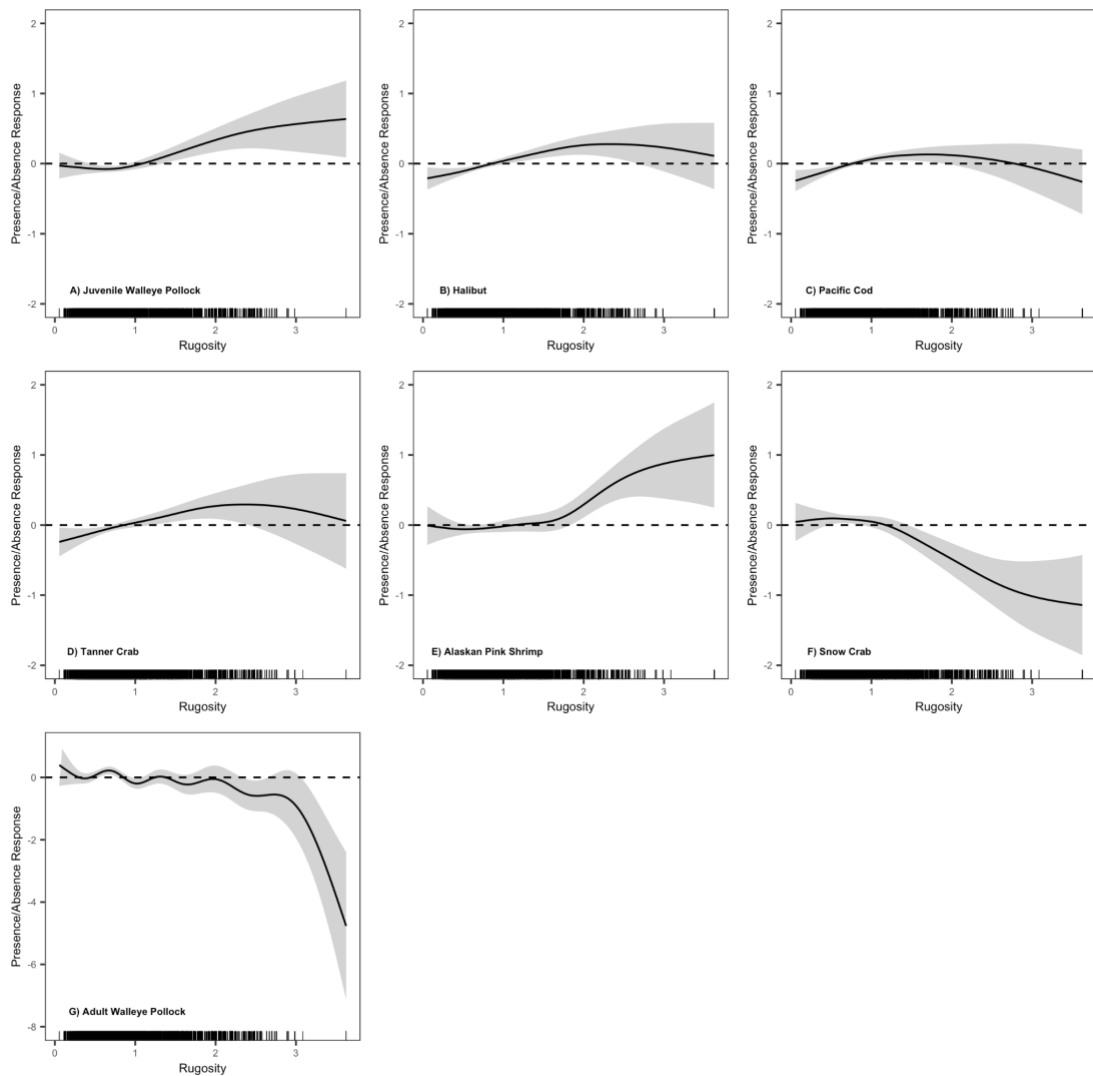
Supplementary Figure 2.4: Generalized additive model response curves for depth from binary presence/absence models for species A-F. Depth was not significant for the Pacific Cod and juvenile Walleye Pollock GAMs. Solid black lines are the fitted relationships between depth and the partial responses, with the gray shaded area

representing the 95% confidence interval. The predicted probability of occurrence is <0 below the dashed horizontal line and >0 above the dashed horizontal line. Black dashes along the x axis show the density of depths observed in the survey.



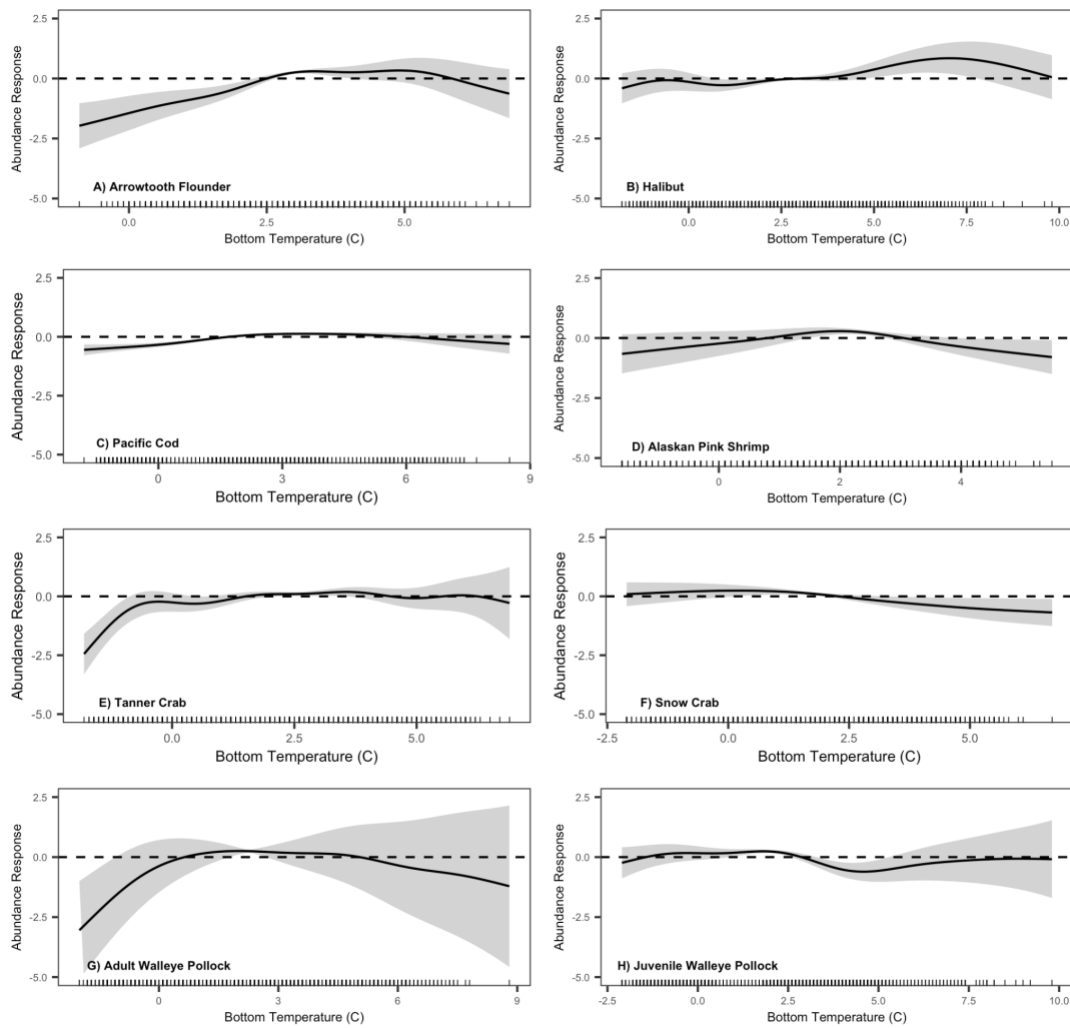
Supplementary Figure 2.5: Generalized additive model response curves for grain size from binary presence/absence models for species A-H. Solid black lines are the fitted relationships between depth and the partial responses, with the gray shaded area representing the 95% confidence interval. The predicted probability of occurrence is

<0 below the dashed horizontal line and >0 above the dashed horizontal line. Black dashes along the x axis show the density of squared grain sizes observed in the survey. The vertical scale is the same for species A-D (-2 to 2) and same for species C-G (-4 to 2).



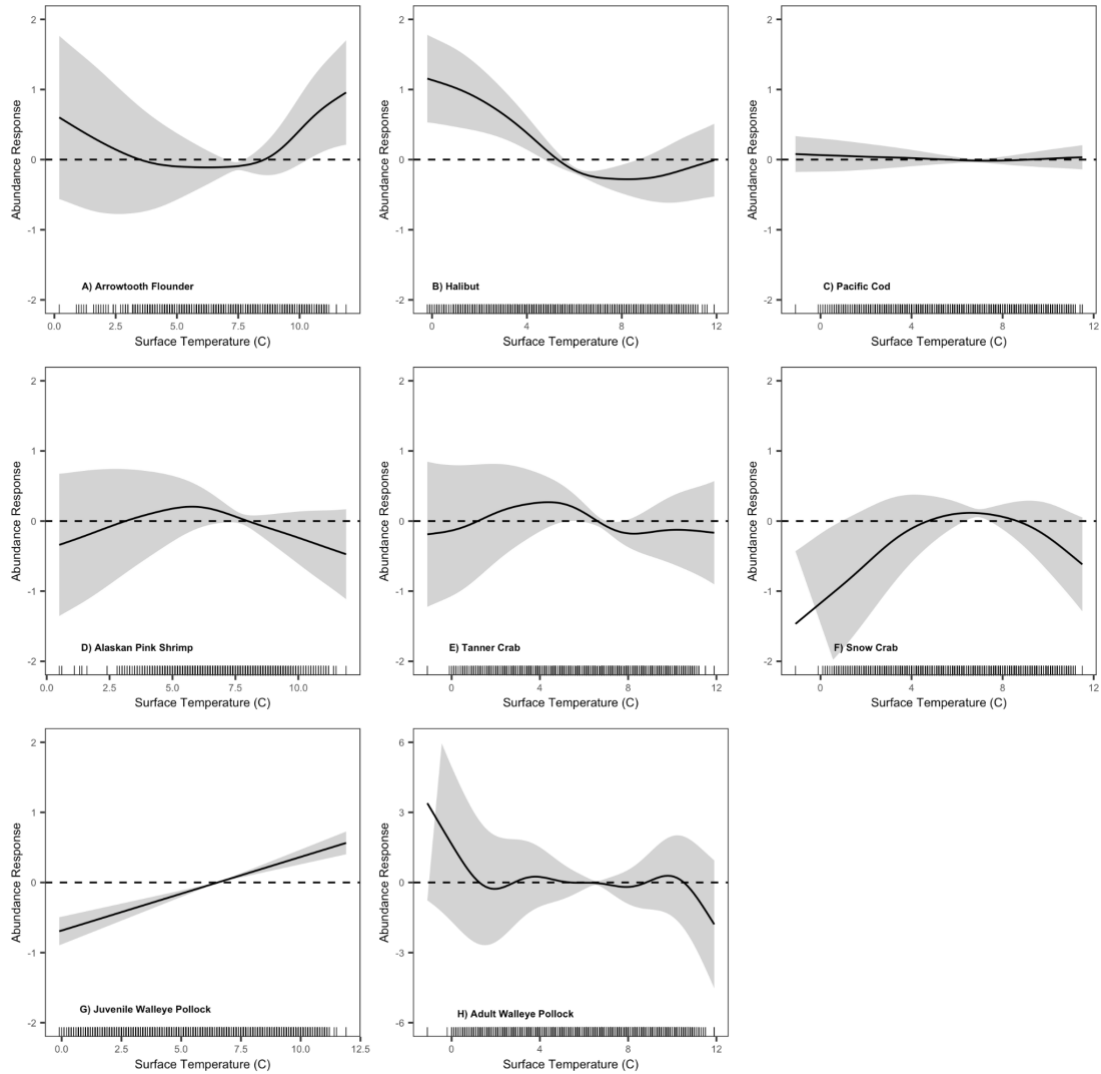
Supplementary Figure 2.6: Generalized additive model response curves for rugosity from binary presence/absence models for species A-G. Rugosity was not significant for the Arrowtooth Flounder abundance GAM. Solid black lines are the fitted

relationships between depth and the partial responses, with the gray shaded area representing the 95% confidence interval. The predicted probability of occurrence is <0 below the dashed horizontal line and >0 above the dashed horizontal line. Black dashes along the x axis show the density of rugosities observed in the survey.



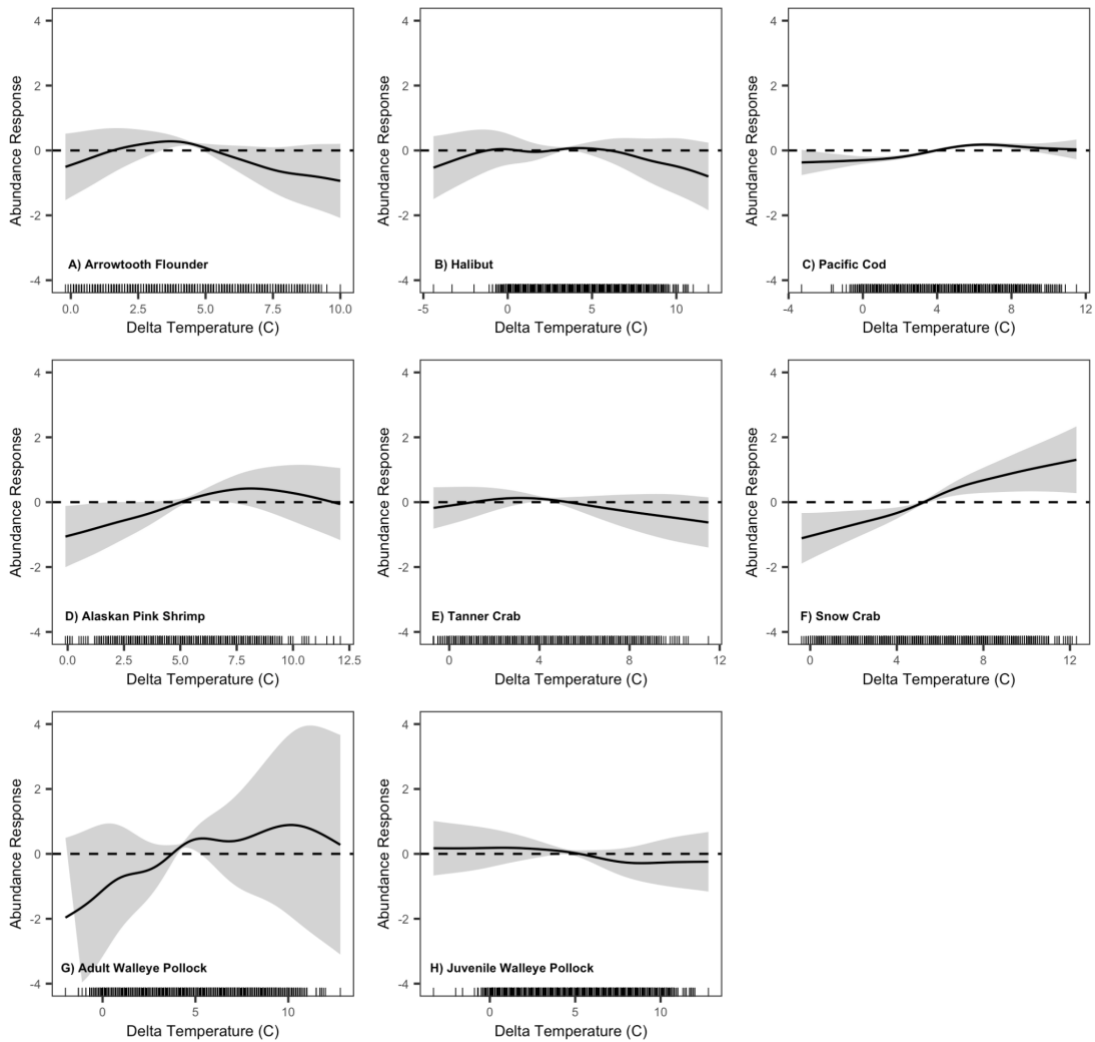
Supplementary Figure 2.7: Generalized additive model response curves for sea bottom temperature from log catch per unit effort models assuming presence for species A-H. Solid black lines are the fitted relationships between sea bottom

temperature and the partial abundance responses, with the gray shaded area representing the 95% confidence interval. Black dashes along the x axis show the density of sea bottom temperatures observed in the survey.



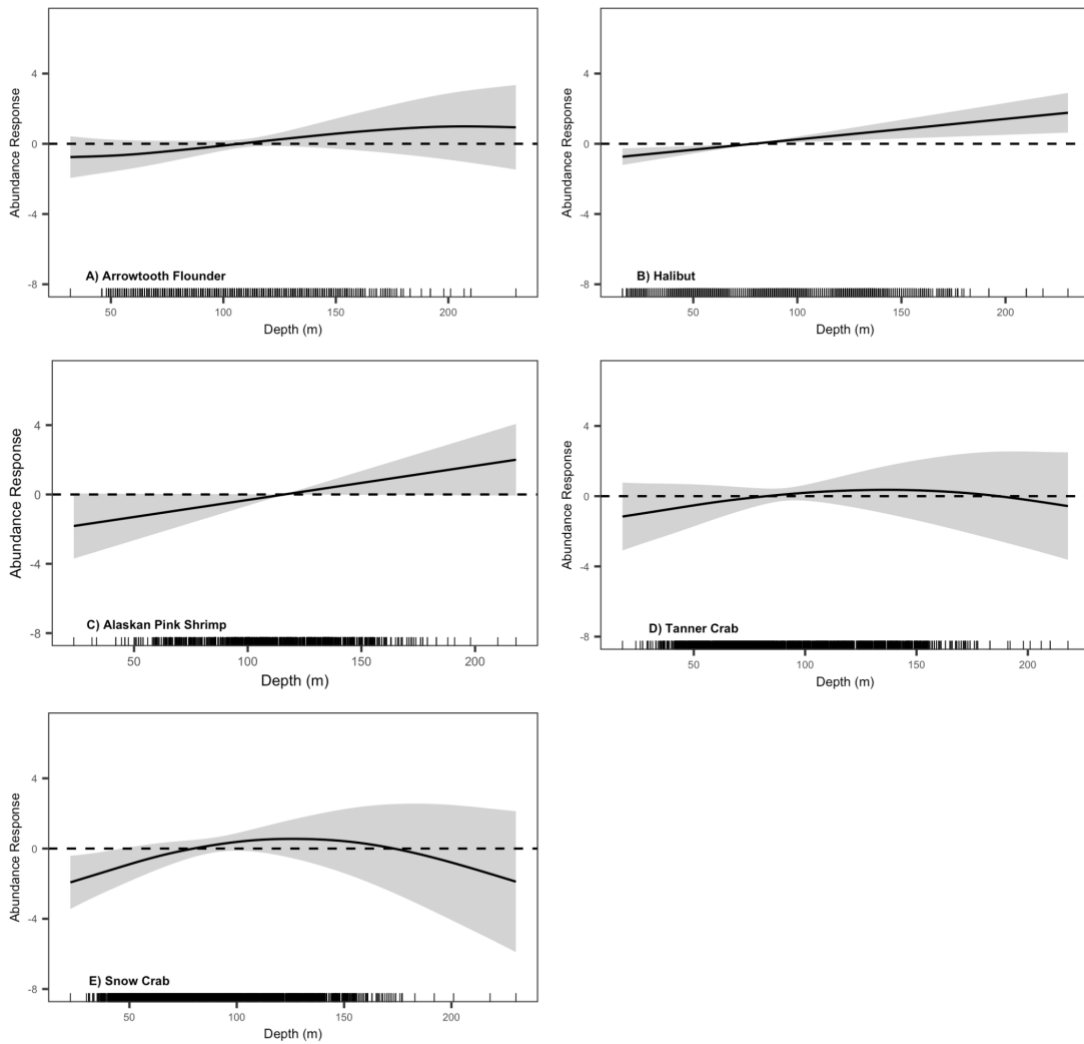
Supplementary Figure 2.8: Generalized additive model response curves for sea surface temperature from log catch per unit effort models assuming presence for species A-H. Solid black lines are the fitted relationships between sea bottom

temperature and the partial abundance responses, with the gray shaded area representing the 95% confidence interval. Black dashes along the x axis show the density of sea surface temperatures observed in the survey. The vertical scale is the same for species A-G (-2 to 2) and changes for species H (-6 to 6).



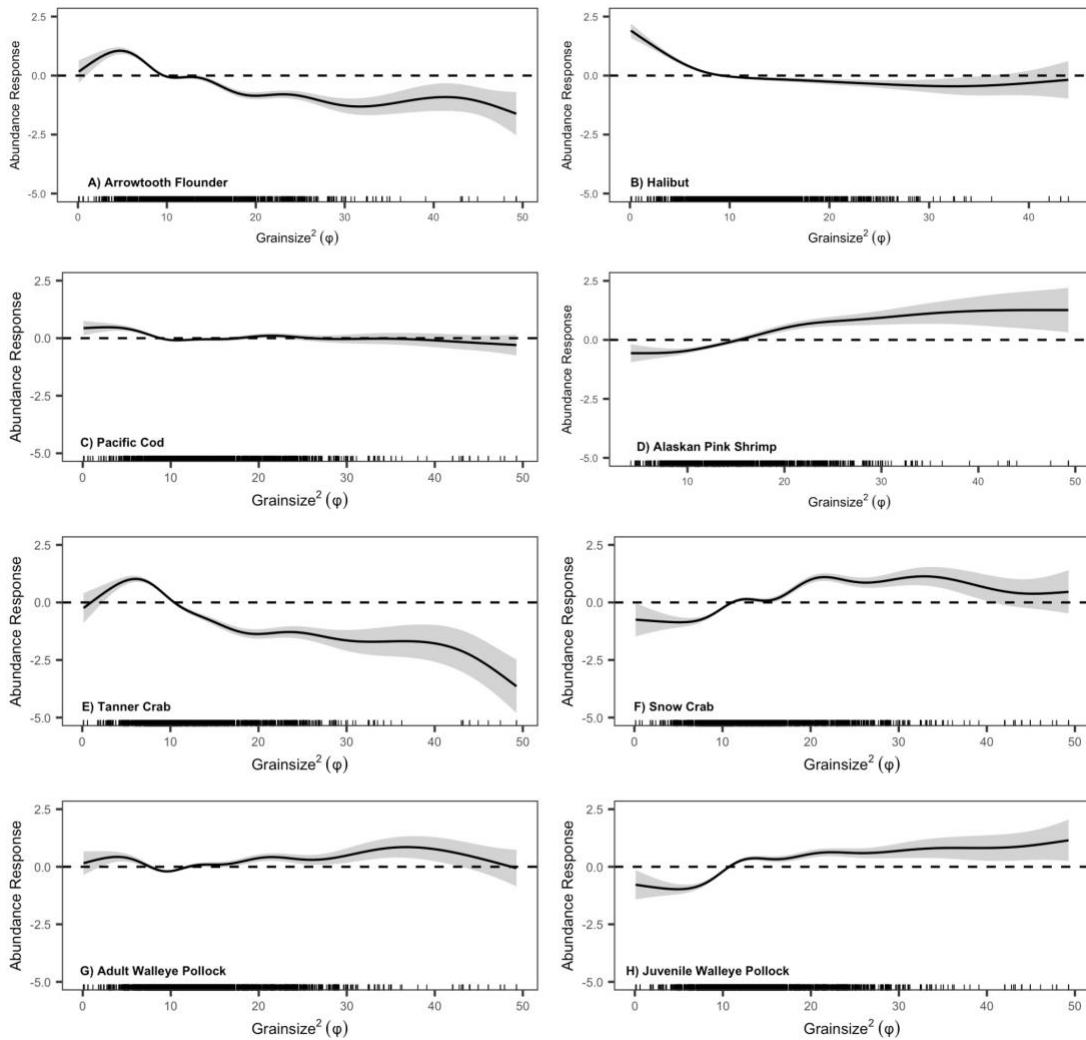
Supplementary Figure 2.9: Generalized additive model response curves for delta temperature (the difference between sea surface temperature and sea bottom temperature) from log catch per unit effort models assuming presence for species A-

H. Solid black lines are the fitted relationships between delta temperature and the partial abundance responses, with the gray shaded area representing the 95% confidence interval. Black dashes along the x axis show the density of delta temperatures observed in the survey.



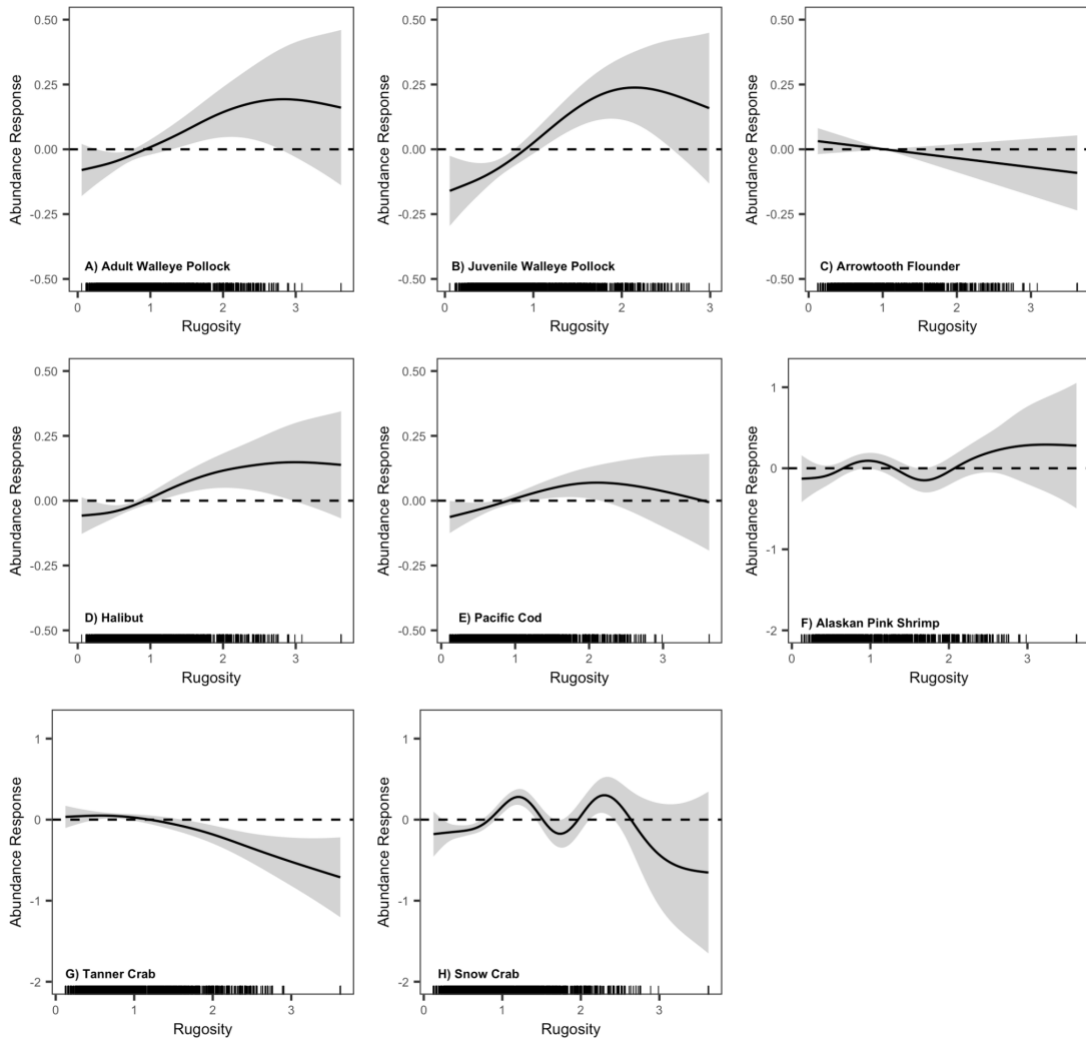
Supplementary Figure 2.10: Generalized additive model response curves for depth from log catch per unit effort models assuming presence for species A-E. Depth was not significant for the Pacific Cod, adult Walleye Pollock, and juvenile Walleye

Pollock abundance GAMs. Solid black lines are the fitted relationships between depth and the partial abundance responses, with the gray shaded area representing the 95% confidence interval. Black dashes along the x axis show the density of depths observed in the survey.



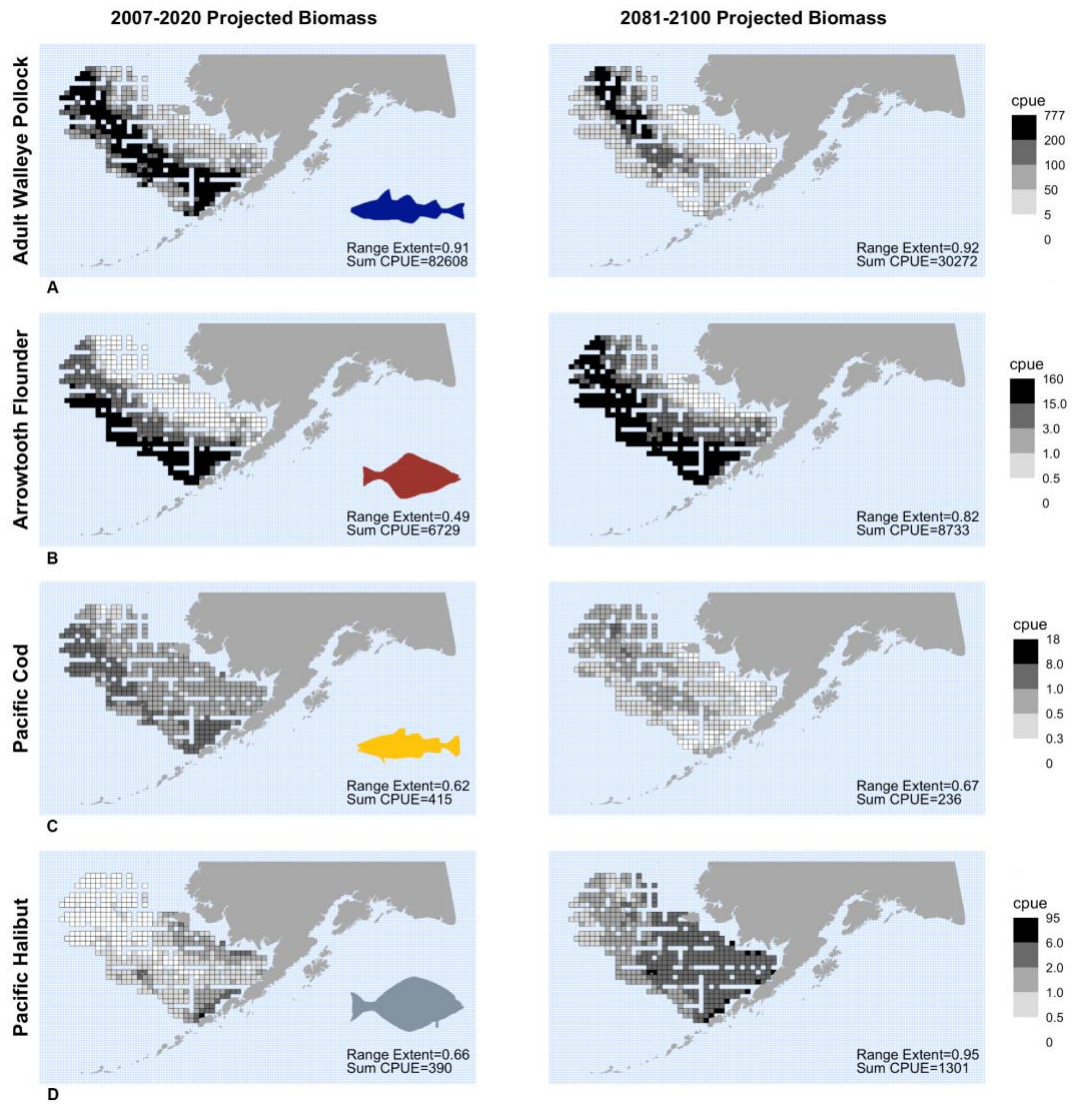
Supplementary Figure 2.11: Generalized additive model response curves for grain size from log catch per unit effort models assuming presence for species A-H. Solid black lines are the fitted relationships between depth and the partial abundance

responses, with the gray shaded area representing the 95% confidence interval. Black dashes along the x axis show the density of squared grain sizes observed in the survey.



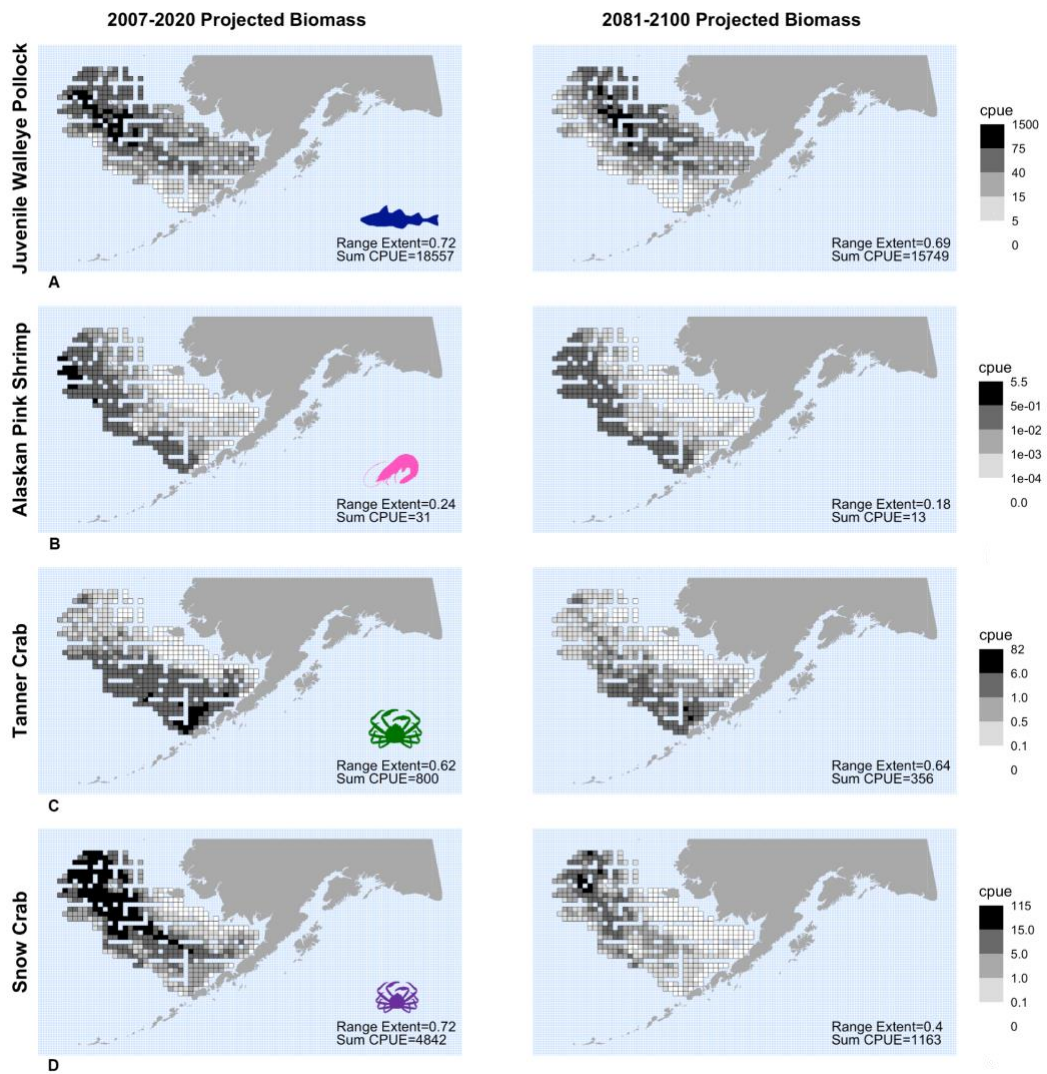
Supplementary Figure 2.12: Generalized additive model response curves for rugosity from log catch per unit effort models assuming presence for species A-H. Solid black lines are the fitted relationships between depth and the partial abundance responses, with the gray shaded area representing the 95% confidence interval. Black

dashes along the x axis show the density of rugosities observed in the survey. The vertical scale is the same for species A-E (-0.50 to 0.50) and the same for species F-H (-2 to 1).



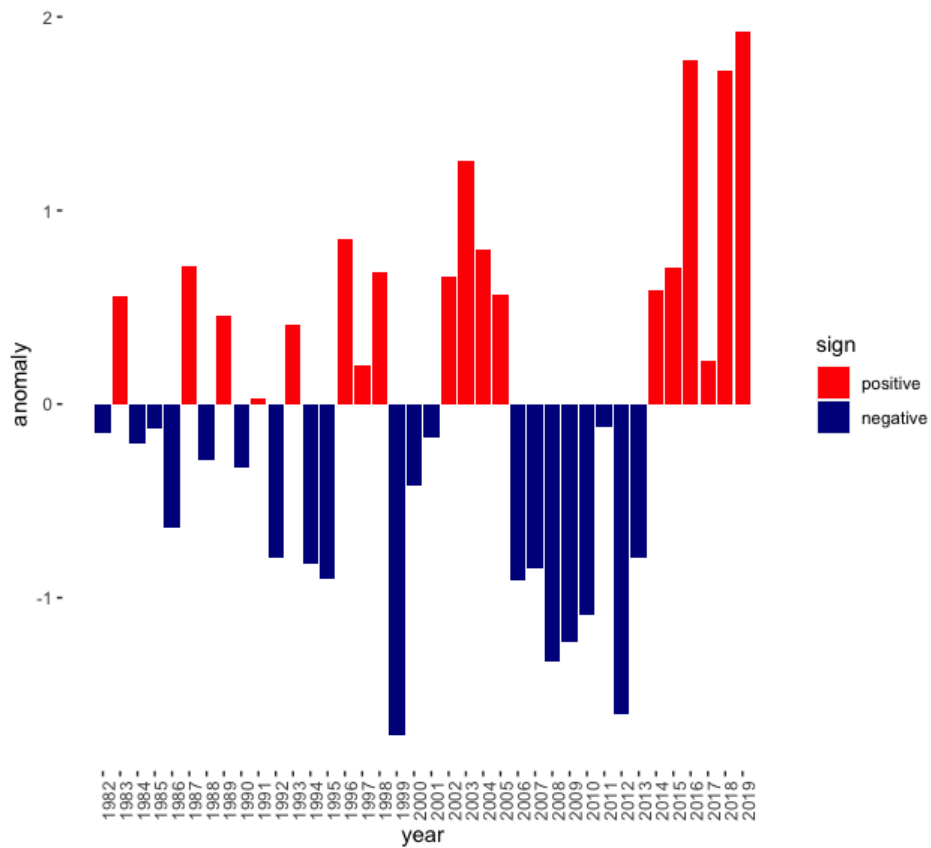
Supplementary Figure 2.13: Maps of historical (2007-2020) and future (2081-2100) biomass for each grid cell of the Eastern Bering Sea trawl survey region for the four predator species: A) adult Walleye Pollock, B) Arrowtooth Flounder, C) Pacific Cod,

and D) Pacific Halibut. Projections are the average across 18 earth system models (CMIP5; RCP8.5). Range extent was defined as the mean presence/absence probability for the entire trawl area. The projected CPUE for each grid cell was summed throughout the trawl region to obtain the total biomass estimate.



Supplementary Figure 2.14: Maps of current (2007-2020) and future (2081-2100) projected biomass for each grid cell of the Eastern Bering Sea trawl survey region for the four prey species: A) juvenile Walleye Pollock, B) Alaskan Pink Shrimp, C)

Tanner Crab, and D) Snow Crab. Range extent was defined as the mean presence/absence probability for the entire trawl area. The projected CPUE for each grid cell was summed throughout the trawl region to obtain the total biomass estimate.



Supplementary Figure 2.15: Yearly temperature anomaly for the Eastern Bering Sea based on the average observed temperature from 1982-2019.

Chapter 3: Market squid fishery participant responses to past climate perturbations: Implications for a socio-ecological fishery network as climate change progresses

Abstract:

Fisheries are complex social-ecological systems driven by marine resource availability, socioeconomic conditions, and culture. California Market Squid (*Doryteuthis opalescens*) is often ranked as the top fishery in the state for both pounds landed and ex-vessel value, but the short-lived species' abundance and distribution is tightly tied to environmental conditions. To prepare for the impacts of climate change, we need to understand the vulnerability of both Market Squid and squid fishery participants to future conditions in the California Current System. I use a network analysis approach to examine how relationships among squid permitted vessels, squid buyers, and ports adapted to past climate perturbations (El Niño and La Niña years). I then use a dynamically downscaled climate model to project changes in Market Squid's habitat suitability and center of gravity by the year 2100. The sharp decline in total pounds landed at California ports during the 2015-2016 El Niño indicates the Market Squid fishery is vulnerable to future warming. However, larger vessels with greater spatial mobility and buyers with receiving capacity and processing facilities in multiple locations may be more resilient to projected decreases in habitat suitability in Southern California and increases in habitat suitability in Northern California. The majority of relationships between vessels and buyers carried through multiple years, with only 32% of vessels sold to new buyers in different thermal conditions. This fidelity is likely adaptive, ensuring access to processing facilities and markets while allowing for flexibility when necessary. Most squid fishery participants have long personal and family ties to the fishing community.

Improving understanding of the Market Squid fishery's resilience and adaptability to changing conditions can inform management to support climate-ready fisheries.

I. Introduction:

Food-producing communities exist at the intersection of environment and society (Fisher et al. 2021; Tsenkova & Youssef 2014). These communities are particularly vulnerable to environmental changes that alter resource availability, with consequences for individual livelihoods, local economics, and the culture of the region (Dubik et al. 2019; Cheung et al. 2010; Bindoff et al. 2019). To help prepare for and buffer the negative impacts of climate change, understanding the vulnerability of food-producing communities to likely changes in resource availability is critical.

Fisheries are one of these communities. They are complex social-ecological systems driven by both marine resource availability and socioeconomic conditions (Pikitch et al. 2004). Fishing communities can cope with environmental change in each of three ways: 1) by enduring without changing behavior, 2) by shifting location and reorganizing their social networks, or 3) by exiting a fishery and switching to another or exiting fishing altogether (Mason et al. 2022; Aguilera et al. 2018; Powell et al. 2022). Understanding past responses to climate perturbations can inform efforts to predict how fishery participants and communities may respond to climate change.

California fisheries have a long-history of coping with oceanographic regime cycles that impact the availability of commercially fished species. California's Market Squid (*Doryteuthis opalescens*) fishery is often the top fishery in the state in terms of ex-vessel (dockside) value and volume landed per year (Ralston et al. 2018; Heine 2017; CDFW 2005). It also is a species with a short life-span, making its abundance and distribution tightly tied to concurrent environmental conditions (Heine 2017). Along the coast of California, El Niño years (warm, low productivity) result in significant declines in squid abundance, while La Niña years (cool, high productivity) are associated with high squid abundance (Zeidberg et al. 2006; Van Noord & Dorval 2017; Reiss et al. 2004). California Market Squid fishermen have noted that during the low productivity, El Niño years, squid are scarce on traditional fishing grounds and are found spawning further north (Powell et al. 2022)

The impact of these climate events on the Market Squid fishing community is not known because participation in the fishery is not simply based on the availability of the resource (Aguilera et al 2015; Powell et al. 2022). Fisheries include the participating fishermen; vessel capacity; the labor and facilities at the landing port, including ice, fuel, pumps, forklifts, etc.; and the first receivers, buyers, and transportation to processing facilities. This creates a complex social network of fishery participants, with relationships built on loyalty and reciprocity that form a community (Dubik et al. 2019; Holland et al. 2020). Most squid fishermen have strong and long-standing personal and family ties to their fishing community, which

may encourage continued participation in the squid fishery even when resource availability is low (Holland et al. 2020; Johnson et al. 2014; Pomeroy et al. 2002). For example, even if squid abundance is higher in northern California, squid fishermen may decide to remain in southern California if they have buyers they are loyal to who won't travel north or families they don't want to separate from for the season (Johnson et al. 2014; Papaioannou et al. 2021).

This study examines how California's Market Squid fishery participants and networks changed in response to past climate perturbations to help determine how this fishery may respond to climate change. Recent projections indicate sea surface temperature in the California Current System will rise by 2.5-5°C by 2090 (Pozo Buil et al. 2021). El Niño conditions in the California Current System are a good proxy for thermal conditions we expect to see as climate change progresses. I use a network analysis approach to examine how the relationships among squid permitted vessels, squid buyers, and ports changed between the most recent strong El Niño (2015-2016), the most recent strong La Niña (2010-2011), and a neutral season (2012-2013). My study questions included:

1. Does the number of fishery participants (squid permitted vessels and squid buyers) change depending on the environmental context? If so, are there certain participants who are more likely to exit the fishery (e.g. buyers with

plants in southern locations, smaller vessels using brail gear versus purse seiners)?

2. Do squid-permitted vessels show home port fidelity, landing port fidelity, and buyer fidelity when they land squid or do these relationships change depending on the environmental context? Does this fidelity depend on the type of gear and vessel or permit?

I then use a species distribution model approach to project changes in suitable Market Squid habitat along the U.S. West Coast by 2070-2100.

Strong community networks can confer resilience to climate change (Bodin and Crona 2009; Ramirez-Sanchez and Pinkerton 2009); on the other hand, if squid habitat changes substantially, inflexibility in participant relationships can increase vulnerability to climate change (Fisher et al. 2021). By examining both the connectivity between fishery participants, their networks on shore, and potential habitat shifts with climate change, we will be better able to anticipate and mediate the impacts of climate change on the California Market Squid fishery.

II. Study System

2.1 Study Species (Doryteuthis opalescens)

Market squid are a small coleoid cephalopod that range from British Columbia, Canada to Baja California, Mexico (Wing and Mercer 1990; Vojkovich 1998). Squid

form mating-spawning aggregations on sandy seafloor habitats in nearshore areas or in deeper waters close to offshore banks and islands (Recksiek & Frey 1978; Zeidberg et al. 2012; Navarro et al. 2018). These spawning aggregations occur in the winter in the southern part of their range, and in the spring-summer in the northern part of their range (Recksiek & Frey 1978). Market squid have a very fast growth rate and a short lifespan (6-9 months); therefore, the species is very responsive to changes in oceanographic conditions resulting in extensive interannual variability in population size (Butler et al. 1999; Ralston et al. 2018; Koslow & Allen 2011; Pecl & Jackson 2008; Zeidberg et al. 2004). Commercial landings of squid are highest when caught in waters between 10-12°C at depths of 20-70m (Zeidberg et al. 2012). Currently, the highest abundance of squid is found off of southern and central California (Wing and Mercer 1990; Vojkovich 1998).

2.2 Market squid fishery

California's Market Squid fishery has a long history. The species was first fished by Chinese vessels in the 1860s in Monterey; in 1985 landings south of Point Conception overtook those in Monterey; and in the mid-1990s Market Squid became the largest fishery in California (Koslow & Allen 2011; Recksiek & Frey 1978; Yaremko 2002; Ralston et al. 2018). The fishery peaks when market squid spawning aggregations occur; accordingly, landings primarily occur during the fall and winter in southern California and in the spring and summer in northern California (Ralston et al. 2018). There are three centers of activity: 1) Monterey Bay, 2) Ventura/Port

Hueneme, and 3) San Pedro/Terminal Island (Pomeroy et al. 2002). The southern California fishery is spread over a vast area, including the Channel Islands, while fishing in northern California occurs nearshore (Recksiek & Frey 1978).

Most vessels are between 9 and 27 meters in length and use round-haul gear (e.g., purse seines, drum seines), with a smaller portion of the fleet using scoop or brail gear (Pomeroy et al. 2002; Aguilera et al. 2018). The squid fishery acts as a day-trip fishery. Vessels fish at night and return to port the following morning (Recksiek & Frey 1978; Pomeroy et al. 2002; Aguilera et al. 2015). Light boats often assist catcher vessels, using high intensity lights to attract and concentrate the squid. Once at the landing port, squid are transferred to a weighing bin using a shore-based pump. Once the catch is weighed it is transferred to totes packed with ice, the totes are transferred to trucks using a forklift, and the truck transports the catch to a processing plant (Pomeroy et al. 2002).

The Market Squid fishery is managed by the California Department of Fish and Wildlife (CDFW) and is monitored by the federal Coastal Pelagic Species Fisheries Management Plan (Pomeroy et al. 2002). Fishery control rules include: 1) a seasonal catch limit of 118,000 tons, 2) weekend closures, 3) 30,000 watt maximum and required shields for attracting lights, and 4) squid monitoring through fish ticket landing receipts and logbook records (CDFW 2005). There are five types of squid vessel permits: transferable and non-transferable vessel permits, transferable and non-

transferable brail permits, and transferable light boat permits (CDFW 2005). Many squid-permitted vessels also have the federal Coastal Pelagic Species finfish permit, making them members of the California wetfish fishery (Pomeroy et al. 2002; Aguilera et al. 2015; Aguilera et al. 2018). The California wetfish fishery (Northern Anchovy, Jack and Pacific Mackerel, Pacific Sardine, and Market Squid) has changed in recent years with the decline and closure of the Pacific Sardine fishery in 2015 and the low market value of anchovies and mackerel in comparison to squid (Aguilera et al. 2015; Powell et al. 2022). The wetfish fishery is now primarily a single-species fishery focused on Market Squid (Aguilera et al. 2015).

III. Methods:

3.1 Data Acquisition and Cleaning

I obtained commercial landing receipts, commercial fishing vessel registration and permit, and commercial fish business data through a CDFW-UCSC data-sharing agreement and associated non-disclosure agreement to ensure the confidentiality of individuals' data. The data were reviewed, cleaned, and Market Squid-relevant entries were extracted from each dataset for the period 2005, when the Market Squid Fishery Management Plan (MSFMP) was adopted and implemented.

The landing receipts, which are completed by the first receiver when the catch is landed at port, include pounds landed, 10x10 nm CDFW block location fished, gear used, and first receiver/buyer of the catch for each fishing trip by squid-permitted

vessels. Landings receipts with vessel identifiers or business identifiers not listed in the commercial vessel registration and permits data or the commercial fish business data were excluded from the analyses. I also excluded all landing receipts that didn't use the three most common gear types (purse seine, drum seine, and brail). Vessel home port was obtained from the commercial vessel registrations and permits data. Fish business processing facility locations were obtained from the commercial fish business data. Home ports and plant locations were categorized as being in Northern or Southern California if they were above or below 35° latitude, respectively. Vessel length was extracted from the commercial fishing vessel registration data. To adhere to confidentiality requirements, data representing fewer than three fishermen or buyers was removed. All data fields used in the analysis are listed in Table S1 and Table S2.

3.2 Annual Landings and Fishery Participant Analysis

I calculated total lbs landed per calendar year (2005-2021) for four groups differentiated by whether vessel home ports were in Northern or Southern California and whether vessels used brail or purse/drum seine gear. I similarly summed the number of vessels participating in the squid fishery each year for the four groups. I calculated total lbs received by buyers each year for three groups: businesses with processing facilities in Northern California, Southern California, or businesses with processing facilities in both parts of the state. The number of buyers participating in the squid fishery each year was summed for the three groups.

For each landing receipt, the distance between the centroid of the reported fishing block and the port of landing was calculated using the geosphere package in R (Hijmans et al. 2017). The average distance between fishing location and port of landing was calculated each year for Southern California and Northern California. Finally, I determined the proportion of lbs landed in Northern versus Southern California each year.

3.3 Network Analysis

I used a network analysis approach to depict relationships between 1) squid-permitted vessels and ports and 2) squid-permitted vessels and buyers during an El Niño, La Niña, and a neutral period. Network nodes were vessels, buyers, and ports; edges (i.e. lines between the nodes) were the interactions between vessels and buyers or vessels and ports. To create the networks, I first extracted landing receipt data for three time periods: 2015-2016 (most recent strong El Niño), 2010-2011 (most recent strong La Niña), and 2012-2013 (a neutral period).

3.3.1 Vessel-Port Network

For each environmental time period, I created a two-node, valued network between vessels using purse/drum seines and landing ports using the xUCINET and sna package in R (Borgatti et al. 2022; Butts 2008). Brail vessels are on average 5 meters shorter than seiner vessels and have a different pattern of fishing activity, so I created

a separate network for interactions between vessels using brail gear and landing ports. The number of times a vessel landed at a port determined the edge-weight between the two nodes. The average tie strength (edge-weight) and the degree of centrality (number of connections each node has) was calculated for both networks and compared across the three time periods.

3.3.2 Vessel-Buyer Network

I then created a two-node, valued network between vessels and buyers for the three time periods. The number of times a buyer purchased catch from a vessel determined the edge-weight between the two nodes. Tie strength and degree of centrality were calculated and compared across time periods. Finally, I used the Louvain method to identify communities of vessels and buyers using the R package xUCINET (Borgatti et al. 2022). This method was used to determine if vessel-buyer communities are flexible during different climate conditions or if they remain unchanged.

3.4 Future Market Squid Habitat Suitability in the California Current System

I used a Species Distribution Modeling (SDM) approach to quantify changes in habitat suitability for Market Squid by 2070-2100 in the California Current System (CCS). SDMs relate the presence/absence of a species (response variable) with environmental (oceanographic, geomorphological) conditions (predictor variables) to determine preferred habitat. The resulting habitat models are then applied to climate

projections to determine the distribution of future suitable habitat (Elith and Leathwick 2009).

Squid presence/absence was identified using NOAA Fisheries' Rockfish Recruitment and Ecosystem Assessment Survey (RREAS) and environmental data were obtained from the Regional Ocean Modeling System (ROMS) built for the CCS. The RREAS is an annual midwater trawl survey that starting in 1983 sampled fixed station locations from Monterey Bay to just north of Point Reyes and then in 2004 expanded to include the majority of California coastal waters (32.5 to 41.5°N; Ralston et al. 2018). The details of the sampling design are described in Sakuma et al. 2016, but the modified-Cobb trawl is effective at retaining squid with 20-50mm mantle length (Ralston et al. 2018). The ROMS built for the CCS provided daily environmental predictors from 30°N to 48°N at a 0.1° by 0.1° spatial scale that were matched to squid presence/absence data (Veneziani et al. 2009; Pozo Buil et al. 2021; Succa et al. 2022; Moore et al., 2011; Neveu et al., 2016).

I used a generalized additive model (GAM) to fit a SDM for Market Squid using the R package mgcv (v1.8-36; Wood 2011). The model included four environmental predictor variables: sea surface temperature (SST), wind stress curl (a proxy for upwelling-influenced water), depth, and rugosity:

$$P_{x,y} = s(SST) + s(Curl) + s(Depth) + s(Rugosity)$$

where $P_{x,y}$ is the probability of squid occurrence at survey station x in year y .

This model was selected because it performed well on two validation datasets: 1) a diet database for California sea lions (*Zalophus californianus*) and 2) the southern California fishery landings dataset. This is in accordance with our understanding of squid's preference for water temperatures between 10° and 14°C, depths of 20-70m, and upwelling-influenced water (Zeidberg et al. 2012). Adding sea surface height and chlorophyll-a to the model improved model fit, but were excluded because of the propagation of uncertainty for those two variables in my climate projections.

The GAM output was used to get daily projections of squid habitat suitability from 1980 to 2100 for three dynamically downscaled general circulation models: the Geophysical Fluid Dynamics Laboratory (ROMs-GFDL) ESM2M, Institut Pierre Simon Laplace (ROMs-IPSL) CM5A-MR, and the Hadley Center HadGEM2-ES (ROMs-HAD) (Pozo Buil et al. 2021). These models are able to represent regional-scale features that are often missing from global climate models. The average habitat suitability (probability of occurrence from 0-1) was calculated for the historical projections (1985-2015) and for future projections (2070-2100) for the three downscaled climate models. Finally, the center of gravity by latitude was calculated for each year (1980-2100) using the ClassStat and COGravity function in R.

IV. Results

4.1 Annual Landings and Fishery Participant Analysis

Total pounds of Market Squid landed and purchased in California was at a maximum during the 2010-2011 La Niña and dropped by an order of magnitude during the 2015-2016 El Niño and dropped even further in 2019, which was a comparatively weak El Niño (Figure 3.1 & Figure 3.2). The majority of brail permitted vessels with home ports in Southern CA did not participate in the fishery during the 2015-2016 El Niño and in 2021 participation was still below pre-2015 levels (Figure 3.1). Seiner-permitted vessels did not experience a similar drop in participation; while there was some decrease in the number of participating seiner vessels with Southern CA home ports over time, there has been a steady increase in participation for seiner vessels with Northern CA home ports (Figure 3.1). This is in accordance with the steady increase in the proportion of squid landed at Northern CA ports and a decrease in landings at Southern CA Ports (Figure 3.3). In fact, the proportion of catch landed in Northern CA ports in 2020 was higher than observed during the 2015-2016 El Niño (Figure 3.3).

Total pounds of Market Squid purchased declined markedly during the 2015-2016 El Niño, for both buyers with facilities in Southern CA and with facilities in both Northern and Southern California (Figure 3.2). Buyer participation also declined markedly at the onset of the 2015-2016 El Niño in Southern California, but primarily for buyers with plant facilities in Southern CA (Figure 3.2). Participation remained

comparatively stable from 2005-2021 for squid buyers with facilities in both Northern and Southern CA (Figure 3.2).

In Northern California, distance from fishing grounds (CDFW fishing block location) to landing port peaked for seiner vessels during the 2015-2016 El Niño and trends were almost identical for vessels from Northern and Southern California (Figure 3.4). In Southern California, Southern seiner vessels traveled greater distances from port than Northern seiner vessels, both of which were at a high during the 2015-2016 El Niño, but there were similar peaks during previous years (Figure 3.4). It is clear that brail vessels travel shorter distances than seiner vessels and their distance to fishing grounds remained stable from 2005-2021 (Figure 3.4).

4.2 Vessel-Port Network

4.2.1 Brail vessel-port network

During the 2015-2016 El Niño, there were fewer brail-permitted vessels participating in the fishery compared to the 2010-2011 La Niña and the 2012-2013 neutral period (Figure 3.1 & Figure 3.5C). For brail vessels that remained in the fishery, the tie strength between the vessels and landing ports (i.e., the number of times a vessel landed at a port) was also substantially lower during the El Niño period (Figure 3.5C). The average tie strength between brail vessels and landing port was 1.37 during the El Niño period, compared to 4.38 during the La Niña period and 3.19 during the neutral period.

Brail vessels only landed in Southern CA ports, even during the 2015-2016 El Niño (Figure 5C). In all three periods, San Pedro was the primary port brail vessels landed at and was the most central node in the brail vessel-landing port network, contributing most to the structure of the network (Figure 5C). San Pedro had 74 ties in the El Niño period, 1557 ties during the La Niña period, and 1650 ties during the neutral period.

4.2.2 Seiner vessel-port network

Unlike the brail vessel-landing port network, seiner-permitted vessels landed at more Northern CA ports during the 2015-2016 El Niño compared to the 2010-2011 La Niña (Figure 5B). Many seiner vessels were fishing farther north during the El Niño period.

In the seiner vessel-landing port network there was a greater tie strength and more centrality in the nodes during the La Niña period compared to the El Niño period, ports had an average of 314 ties during El Niño and 554 ties La Niña (Figure 3.5C). Six ports had a high degree of centrality (i.e. the number and strength of vessel connections) during the 2010-2011 La Niña: Ventura, Terminal Island, Port Hueneme, San Pedro, Moss Landing, and Monterey. However, the other six ports where landings occurred during the La Niña were on the periphery with three or less ties (Figure 3.5C). The opposite was the case during the El Niño period, only two ports had less than three ties in a network with 12 landing ports. This may be because

most vessels had connections to more than one landing port. During the El Niño period, 87% of vessels had interactions with more than one port; during the La Niña period, 72% of vessels had interactions with more than one port. Overall, the La Niña period had greater tie strength and more centrality, while during the El Niño period vessels had more connections to multiple ports, but comparatively lower tie strength. The neutral period had a level of centrality and tie strength in between that of the El Niño and La Niña period.

4.3 Vessel-Buyer Network

Fewer vessel-buyer interactions occurred during the 2015-2016 El Niño compared to the 2010-2011 La Niña (average tie strength of 2.32 and 4.23 respectively; Figure 3.5A). For all three environmental periods, buyers with plant facilities in Northern CA had few interactions with vessels in comparison to buyers with plant facilities in Southern CA and buyers with plants in both Southern and Northern CA (Figure 5A). The primary buyers (strongest tie strengths) were the same across the three periods, the number of major buyers just increased during the La Niña and neutral period compared to the El Niño period (Figure 6).

During the El Niño period, there was a clear separation among the buyers between those with ties with vessels with Northern CA home ports and those with Southern CA home ports. Vessels with Southern CA home ports were primarily selling to buyers with plant locations in Southern CA while vessels with Northern home ports

were primarily selling to buyers with plants both in Southern and Northern CA (Figure 3.5A). Vessels with Northern CA home ports had double the amount of strong interactions with buyers than vessels with Southern CA home ports (Figure 3.5A). This separation did not exist during the 2010-2011 La Niña, there were many more vessels with home ports in Southern CA that had strong ties to buyers with plant locations in both Northern and Southern CA (Figure 3.5A).

In all three time periods, most vessels sold catch to between one and two buyers (Figure 3.5A & Figure 3.6). Many relationships between vessels and buyers carried through all three environmental time periods. For the top five buyers, an average of 68% of vessels they purchased catch from in one period, they had purchased from that same vessel another period. For the 32% of vessels that didn't sell to the same buyer, they often did not exit the fishery, they sold catch to another buyer (Figure 3.6).

4.4 Climate Change Projections

All three dynamically-downscaled climate models project the center of gravity for squid habitat will shift northward as climate change progresses and by 2100 will be between San Francisco and Eureka, CA (Figure 3.7). Although a range contraction is not projected, habitat suitability may increase north of Point Conception and decline south of Point Conception by 2100 (Figure 3.8). ROMs-HAD projects the largest increase in habitat suitability in Northern CA (Figure 3.8B), followed by ROMs-IPSL

(Figure 3.8C), and ROMs-GFDL only projects a modest increase in the North with habitat suitability largely remaining unchanged around the Channel Islands (Figure 3.8A). It is important to note that my SDM did not consider the impact of global change conditions on squid recruitment, which is a key component of predicting suitable habitat for adult squid.

V. Discussion:

The decline in total pounds landed and purchased in California during the 2015-2016 El Niño and the further decrease in 2019 indicates the Market Squid fishery is vulnerable to future warming in the California Current System. However, my network analyses depict flexibility in numerous relationships between fishery participants, suggesting the fishery may be moderately adaptable to shifting conditions.

Brail-permitted vessels are likely more vulnerable to climate change than seiner-permitted vessels. I project habitat suitability may decrease in Southern CA and increase north of Point Conception, similar to 2015-2016 El Niño conditions. But, brail vessels didn't shift distance to fishing grounds or land in any Northern CA ports under El Niño conditions. In fact, the majority of Southern CA brail vessels exited the fishery for the 2015-2016 season. Seiner vessels likely have greater adaptive capacity, in 2015-2016 the number of connections to ports and the number of landings in Northern CA ports increased. A network analysis examining the impact of the 2014-2016 marine heatwave on California's Dungeness Crab fishery similarly found that

larger vessels displayed more spatial mobility (Fisher et al. 2021). Small vessel communities are more likely to shift target species than shift fishing grounds (Papaioannou et al. 2021). However, squid fishermen who depend on squid for the majority of their income (>60%) are more likely to exit the fishing industry altogether than switch to another fishery (Powell et al. 2022). The small vessels that remained in the fishery during the 2015-2016 El Niño may not have relied on squid as their primary income or benefited from a reduced fleet size. As climate change progresses, small vessel owners and operators in the Market Squid fishing fleet may be replaced by larger vessels (Powell et al. 2022).

The increase in seiner vessels with Northern CA home ports and the decrease in seiner vessels with Southern CA home ports from 2005-2021 may be an adaptive response to increasing squid catch in Northern CA ports. These vessels could be shifting home port, or Southern CA vessel permit holders may be transferring their permits to Northern CA vessels. Many Albacore fishermen that used to reside in Southern CA have either retired from the fishery or established permanent residence in Oregon or Washington as Albacore catches increase in the Pacific Northwest (2000-2016; Frawley et al. 2021). Those that retain their Southern CA home port relocate to northern fishing grounds seasonally (Frawley et al. 2021). We may be witnessing a similar phenomenon for seiner-permitted vessels, a trend that could continue as climate change progresses, which is likely not a first choice for fishermen

(Papaioannou et al. 2021). A shift in home port could break family ties and undermine Southern CA fishing community cohesion (Papaioannou et al. 2021).

Squid buyers with plant facilities in both Northern and Southern CA likely have lower vulnerability to climate change than buyers with plants only located in Southern CA, since participation in the fishery was more stable over time for the former. However, I expected buyers with plants in Northern CA to have higher centrality in the vessel-buyer network during the 2015-2016 El Niño, but this was not the case. This may be because of strong loyalty in vessels and buyer relationships, which is supported by my finding that relationships between vessels and buyers often carried through all three environmental time periods. This cohesion can be adaptive, ensuring access to processing facilities and markets (Papaioannou et al. 2021).

However, it is difficult to predict how the strength of these vessel-buyer relationships will change with a longer term shift in oceanographic conditions instead of a two-year climate shock. Loyalty between vessel and buyer may decrease as climate change progresses; there may be an increase in the percent of vessels selling to different buyers, especially if Oregon buyers enter as participants in the fishery. If vessel-buyer relationships remain intact, like they did during the 2015-2016 El Niño, trucking from Northern CA regions may increase as long as road transportation is possible.

Model outputs from fishery-independent survey data show there has been a fivefold increase in squid abundance from central California to northern Washington from 1998 to 2019 (Chasco et al. 2022). During the 2015-2016 El Niño, there were fishermen reports of Market Squid in the Gulf of Alaska (Cavole et al. 2016; Burford et al. 2022). This provides support for our model projections that squid will shift their center of gravity north to between San Francisco and Eureka, CA by 2100.

The fishing community's response to this long-term northward shift in habitat suitability may differ from historical short-term responses. This study suggests that many seiner-permitted vessels can "follow the fish" northward. However, fishing is often more dangerous in Northern CA (e.g. weather conditions, harbor access) and most squid fishermen haven't yet built the local environmental knowledge needed to successfully fish these new locations (Pfeiffer & Grats 2016; Papaioannou et al. 2021). In addition, consistent access to portable pumps, totes, ice, fuel docks will be necessary at Northern CA ports (e.g. Bodega Bay, Fort Bragg, Eureka) to support a long-term squid fishing community (Pomeroy et al. 2002). Buyers will require safe road access to processing facilities. Finally, I did not assess the impact of this northward shift on other fishery participants, support services and labor (e.g, light boat operators, which work in tandem with seiner vessels). Seiner vessels and buyers with processing facilities in multiple regions may be resilient to the projected northward shift in squid habitat suitability, but further work is necessary to fully assess California's Market Squid fishery vulnerability to climate change.

Figures and Tables

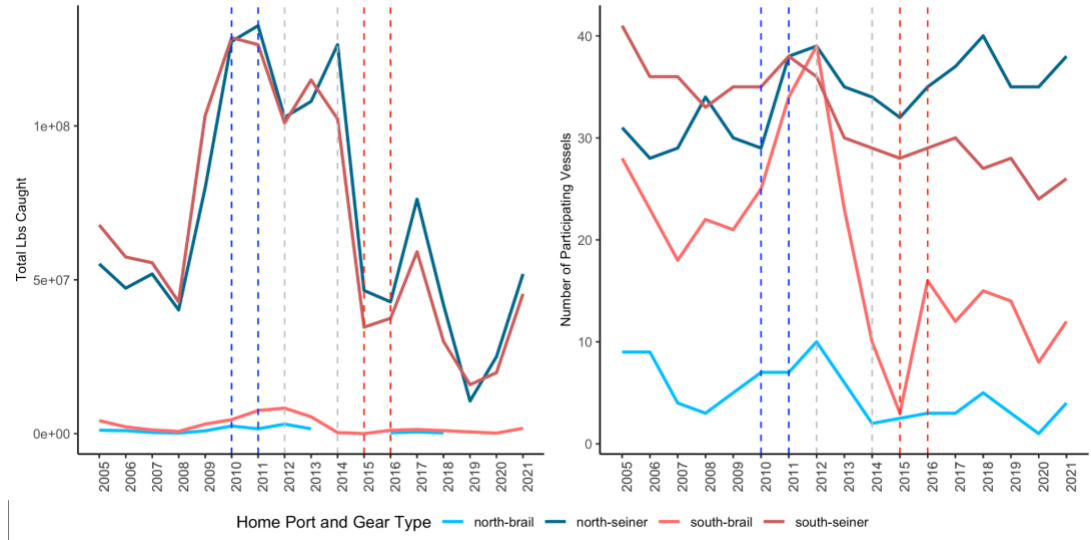


Figure 3.1: Total pounds caught (left) and number of participating vessels (right) per year (2005-2021) for vessels that use brail and purse/drum seine gear with home ports north of 35° lat (blue) and south of 35° lat (red). Dashed vertical lines indicate the strongest La Niña (2010-2011; blue), strongest El Niño (2015-2016; red), and the neutral period in-between (gray).

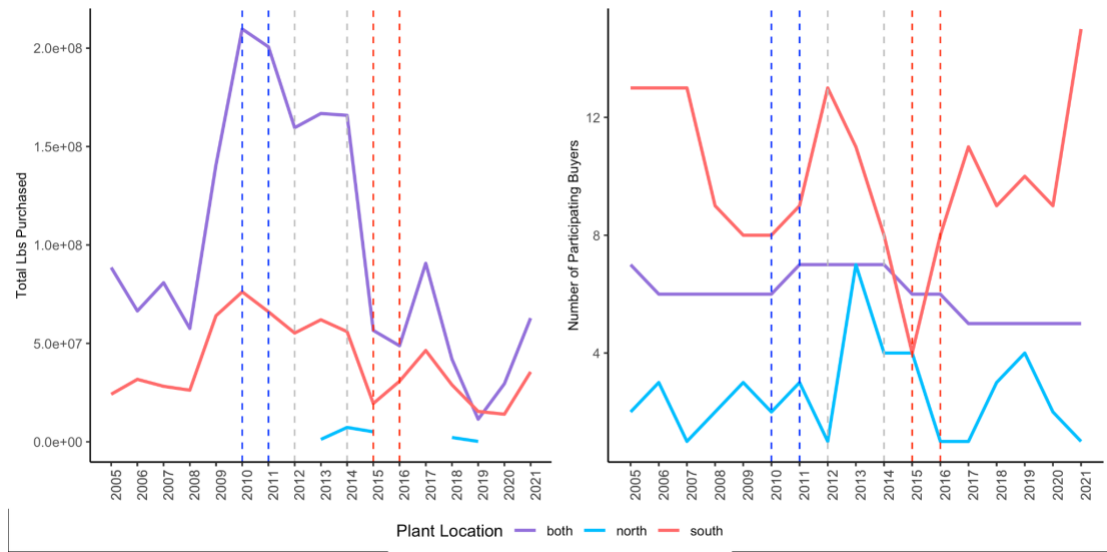


Figure 3.2: Total pounds purchased (left) and number of participating buyers (right) per year (2005-2021) for buyers with plant locations north of 35° lat (blue), south of 35° lat (red), and in both the north and south of California (purple). Dashed vertical lines indicate the strongest La Niña (2010-2011; blue), strongest El Niño (2015-2016; red), and the neutral period in-between (gray).

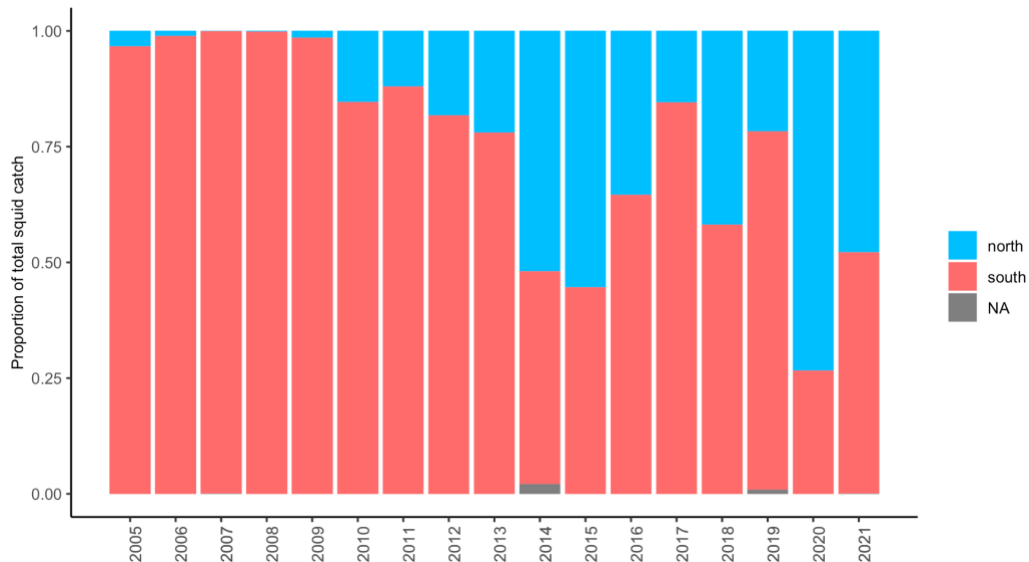


Figure 3.3: Proportion of squid landed in northern ports (>35° lat; blue) versus southern ports (>35° lat; red).

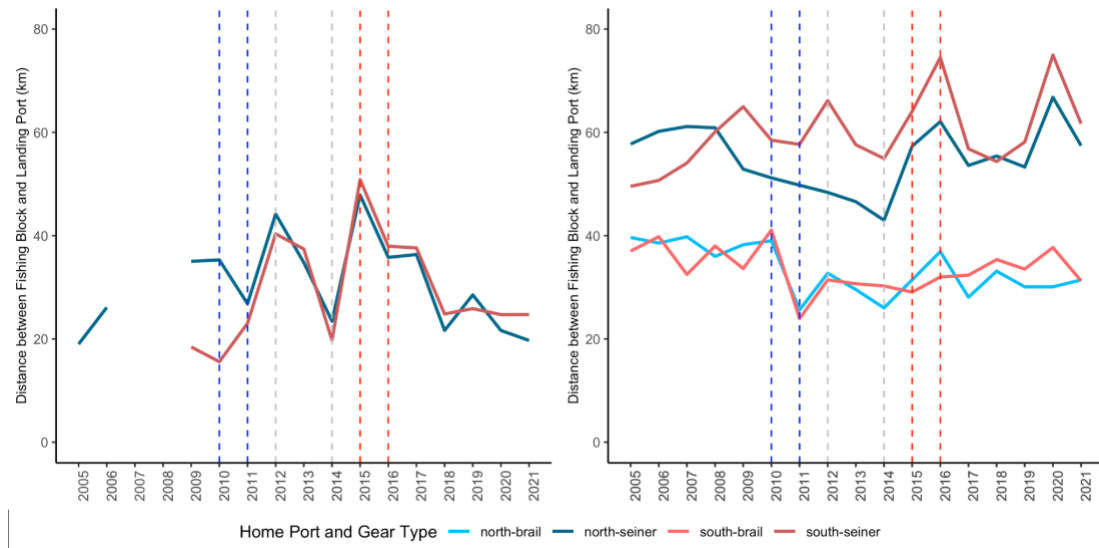


Figure 3.4: Average distance traveled between fishing location (centroid of reported fishing block) and A) Northern California landings ports and B) Southern California landing ports. Vessels were separated based on gear type and home port location, north of 35° lat (blue) and south of 35° lat (red). Brail vessels were not included for Northern California landing ports to adhere to confidentiality requirements. Dashed vertical lines indicate the strongest La Niña (2010-2011; blue), strongest El Niño (2015-2016; red), and the neutral period in-between (gray).

Figure 3.5: A) Network between squid vessels (circles) and buyers (triangles) during the strongest El Niño (2015-2016), La Niña (2010-2011), and a neutral period (2012-2013). Blue (red) represents vessels or buyers with home ports or plant facilities in Northern California (Southern California). Purple represents buyers with plant facilities in both Northern and Southern California. B) Network between vessels (squares) using purse/drum seines and landing port (circles) during the strongest El Niño (2015-2016), La Niña (2010-2011), and a neutral period (2012-2013). Blue (red) represents ports in Northern California (Southern California). C) The same network as Figure 3.5B, but for vessels using brail gear.

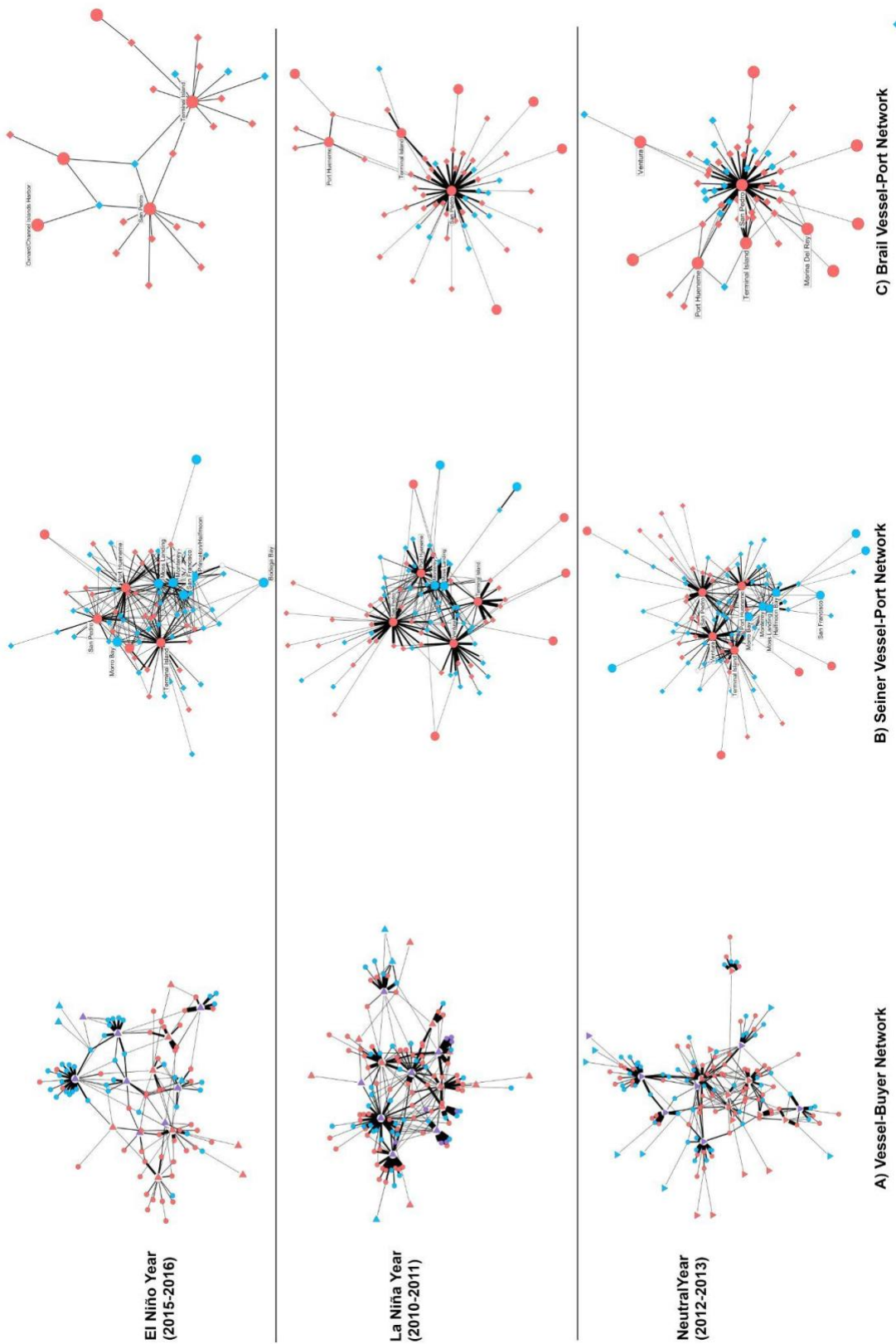


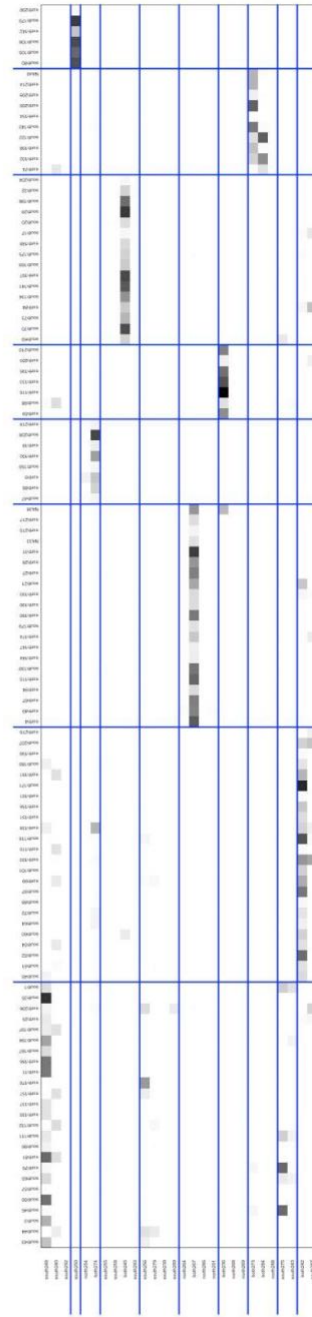
Figure 3.6: Matrix showing vessel-buyer interactions for 2015-2016 El Niño, 2010-2011 La Niña, and 2012-2013 (a neutral year). Row names are buyers and column names are vessels (renamed to protect confidentiality). Darker colors represent a greater number of interactions. Boxes created with blue lines represent vessel-buyer communities identified using the Louvain method.



**El Niño Year
(2015-2016)**



**La Niña Year
(2010-2011)**



**Neutral Year
(2012-2013)**

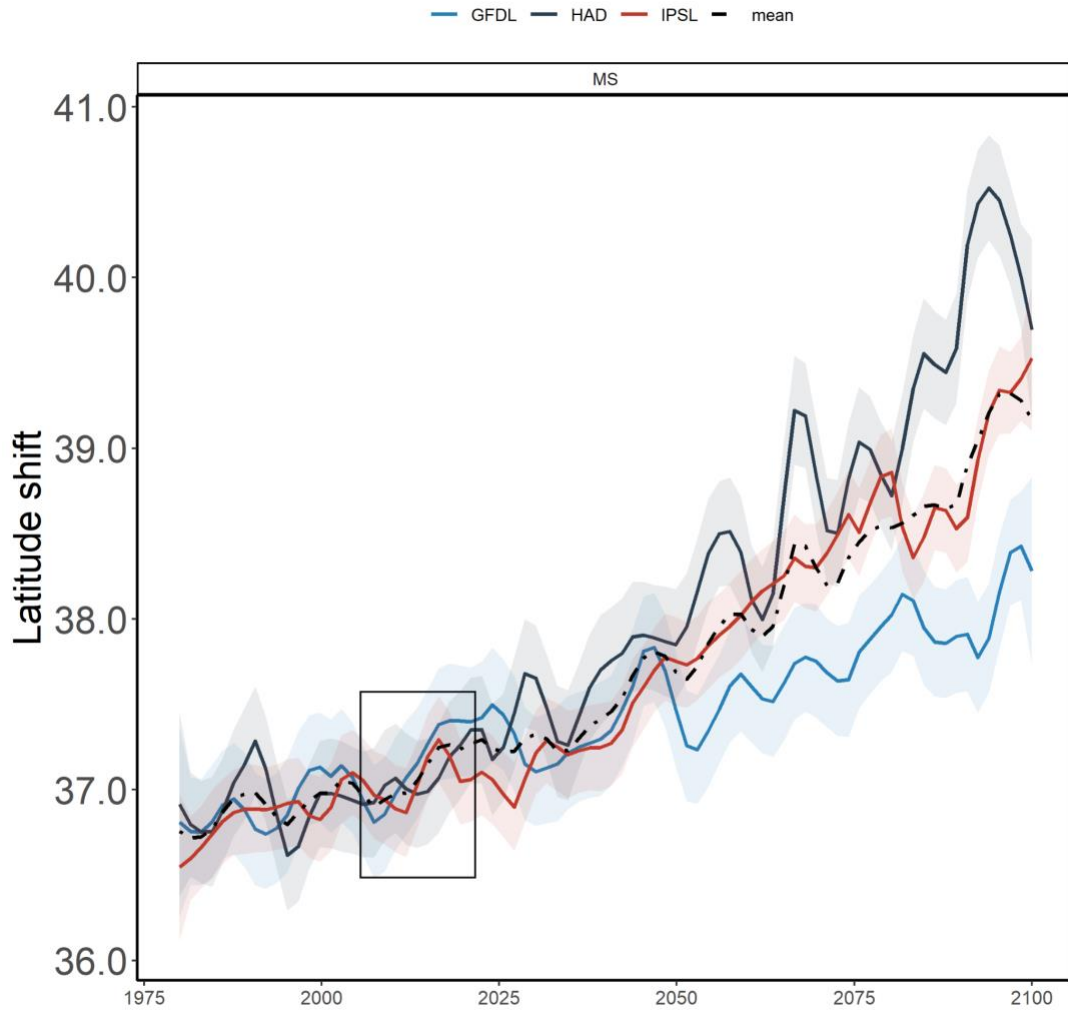


Figure 3.7: Projected center of gravity by latitude from 1980-2100 for the three GCMs (ROMs-GFDL; ROMs-HAD and ROMs-IPSL). Gray bounding box shows the 2005-2021 time period (the start of the Market Squid fishery management plan).

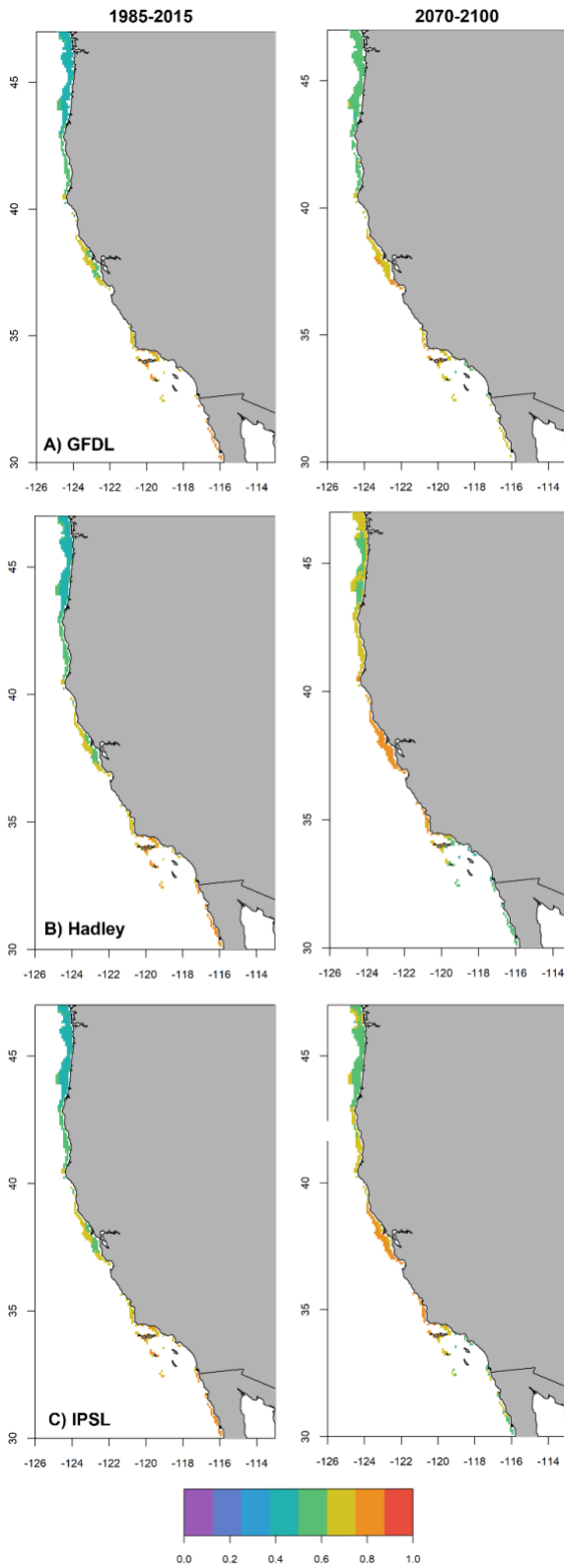


Figure 3.8: Projected habitat suitability (probability of occurrence between 0-1) for 1985-2015 (left) and 2070-2100 (right) for the three GCMs: A) ROMs-GFDL, B) ROMs-HAD, and C) ROMs-IPSL.

Supplementary Tables

Data Set	Fields Used
Landings Receipts	PortID, VesselID, Business ID, Pounds, GearName, LandingYear, CDFWBlockID
Commercial Vessel Registrations and Permits	VesselID, HomePort, PortCounty
Commercial Fish Business	FishBusinessID, PlantStreetCity,
Commercial Fishing Vessel Registration	VesselID, length

Supplementary Table 3.1: Fields used to run my analyses for each CDFW acquired data set.

2005-2021	El Niño (2015-2016)	La Niña (2010-2011)	Neutral (2012-2013)
49,929	3,910	8,920	7,618

Supplementary Table 3.2: Number of landings receipts for the entire study period (2005-2021), the El Niño period (2015-2016), the La Niña period (2010-2011), and the neutral period (2012-2013).

Conclusions and Future Directions

In this dissertation, I assessed the vulnerability of both fished species and a fishing community to global environmental change conditions in the Northeast Pacific Ocean. I chose to study some of the top ranked fisheries in both pounds landed and ex-vessel value along the US West Coast to help inform climate-ready fisheries management. I used a diverse array of climate vulnerability assessment techniques to answer my study questions including a laboratory mesocosm experiment, species distribution modeling, and social network analyses.

In chapter one, I exposed Lingcod eggs to temperature, pH, and DO conditions projected for the year 2050 and 2100. I found that by the year 2050, recruitment of this ecologically and commercially important species will likely decline along the highly-productive central coast of California. This study is the first to expose a benthic egg layer to multistressor climate change scenarios, and my results suggest that single stressor experiments may not capture the true impact of global change on marine organisms.

In chapter two, I first projected the effect of increasing temperatures on the distribution and abundance of four commercially important predators and their prey species. I then used predator-prey overlap metrics to examine if future warming in the Eastern Bering Sea, Alaska will cause spatial mismatches between these predator and

prey species. Predator-prey relationships in the Eastern Bering Sea will likely change with continued warming. Prey refuges are projected to decrease in the north and middle shelf; predator encounter rates with prey species may decline on the outer shelf and southern Eastern Bering Sea; and the relative importance of predators in the ecosystem will likely shift (Pacific Halibut and Arrowtooth Flounder are projected to increase in importance as Pacific Cod and Walleye Pollock decrease).

In chapter three, I used a network analysis approach to examine how California Market Squid fishery participants responded to past climate shocks to help assess their vulnerability to projected shifts in squid habitat by 2100. I found that the fishery is vulnerable to shifts in oceanographic conditions and will likely be negatively impacted by a projected decrease in Market Squid habitat suitability in Southern CA and an increase in habitat suitability in Northern CA. However, certain fishery participants were more resilient to climate perturbations. Larger vessels and squid buyers that have processing facilities in multiple regions are more likely to remain in the fishery, suggesting many fishery participants may be moderately adaptable to a northward shift in squid habitat.

My main objective throughout this dissertation was to understand how fished species' physiological intolerance to global change conditions could affect their abundance and distribution along the US West Coast. And subsequently, how these changes could impact both trophic structure and the livelihood and culture of the human

communities that rely on these species. My work demonstrates it is difficult to predict the vulnerability of fisheries to global change. Even in my attempt to fill our knowledge gaps for how these commercially and ecologically important species would be impacted by global change, I was not able to assess every aspect of vulnerability. In my mesocosm experiment, I didn't examine how parental acclimation to stressful conditions would affect their embryos' tolerance. In my predator-prey modeling study I wasn't able to incorporate my spatial understanding of predator-prey overlap shifts into an ecosystem-based model that predicts the response of the entire trophic web to climate change. In my study of fishery participant responses to shifts in target species' distribution, I did not assess if port communities further North were prepared for an influx of fisheries landings.

A comprehensive assessment of vulnerability includes 1) understanding the impact of climate change on the most vulnerable life stage; 2) determining how trophic webs will respond to global change; and 3) anticipating the response of fishery participants, support services, infrastructure, and markets to shifts in fished species' abundance and distribution. The species we assume are most in need of climate-ready fisheries management should be prioritized for climate vulnerability research. My dissertation adds to this body of research for US West Coast Fisheries.

Bibliography:

- Aguilera, S. E., Broad, K., & Pomeroy, C. (2018). Adaptive capacity of the monterey Bay wetfish fisheries: Proactive responses to the 2015–16 El Niño event. *Society & natural resources*, 31(12), 1338-1357.
- Aguilera, S.E., J. Cole, E.M. Finkbeiner, E. Le Cornu, N.C. Ban, M.H. Carr, J.E. Cinner, L.B. Crowder, S. Gelcich, C.C. Hicks, J.N. Kittinger, R. Martone, D. Malone, C. Pomeroy, R.M. Starr, S. Seram, R. Zuercher, K. Broad. 2015. Managing small-scale commercial fisheries for adaptive capacity: Insights from dynamic social-ecological drivers of change in Monterey Bay. PLoS ONE 10(3): e0118992.
- Alabia, I. D., García Molinos, J., Saitoh, S. I., Hirawake, T., Hirata, T., & Mueter, F. J. (2018). Distribution shifts of marine taxa in the Pacific Arctic under contemporary climate changes. *Diversity and Distributions*, 24(11), 1583-1597.
- Alaska Fisheries Science Center (AFSC). (2008, September 10). *Resource Ecology and ecosystem modeling home diet table*. Resource Ecology and Ecosystem Modeling Groundfish Diet Data. Retrieved from <https://apps-afsc.fisheries.noaa.gov/refm/reem/webdietdata/dietdataintro.php>
- Alderdice, D. F., & Forrester, C. R. (1971). Effects of salinity and temperature on embryonic development of the petrale sole (*Eopsetta jordani*). *Journal of the Fisheries Board of Canada*, 28(5), 727-744.
- Alderdice, D. F., Wickett, W. P., & Brett, J. R. (1958). Some effects of temporary exposure to low dissolved oxygen levels on Pacific salmon eggs. *Journal of the Fisheries Board of Canada*, 15(2), 229-250.
- Alin, S. R., Feely, R. A., Dickson, A. G., Hernández-Ayón, J. M., Juraneck, L. W., Ohman, M. D., & Goericke, R. (2012). Robust empirical relationships for estimating the carbonate system in the southern California Current System and application to CalCOFI hydrographic cruise data (2005–2011). *Journal of Geophysical Research: Oceans*, 117(C5).
- Appelbaum, S., Clarke, W. C., Shelbourn, J. E., Jensen, J. O., Whyte, J. N., & Iwama, G. K. (1995). Studies on rearing of lingcod *Ophiodon elongatus*. *Aquaculture*, 135(1-3), 219-227.
- Araújo, M. B., Pearson, R. G., Thuiller, W., & Erhard, M. (2005). Validation of species–climate impact models under climate change. *Global change biology*, 11(9), 1504-1513.

- Barbeaux, S. J., & Hollowed, A. B. (2018). Ontogeny matters: Climate variability and effects on fish distribution in the eastern Bering Sea. *Fisheries Oceanography*, 27(1), 1-15.
- Barnes, C. L., Beaudreau, A. H., Hunsicker, M. E., & Ciannelli, L. (2018). Assessing the potential for competition between Pacific Halibut (*Hippoglossus stenolepis*) and Arrowtooth Flounder (*Atheresthes stomias*) in the Gulf of Alaska. *PloS one*, 13(12), e0209402.
- Baumann, H., & Smith, E. M. (2018). Quantifying metabolically driven pH and oxygen fluctuations in US nearshore habitats at diel to interannual time scales. *Estuaries and Coasts*, 41(4), 1102-1117.
- Baumann, H., Talmage, S. C., & Gobler, C. J. (2012). Reduced early life growth and survival in a fish in direct response to increased carbon dioxide. *Nature Climate Change*, 2(1), 38-41.
- Beaudreau, A. H. (2009). *The predatory role of lingcod (Ophiodon elongatus) in the San Juan Archipelago, Washington*. [Doctoral dissertation, University of Washington].
- Bell, R. J., Odell, J., Kirchner, G., & Lomonico, S. (2020). Actions to promote and achieve climate-ready fisheries: summary of current practice. *Marine and Coastal Fisheries*, 12(3), 166-190.
- Berkeley, S. A., Chapman, C., & Sogard, S. M. (2004). Maternal age as a determinant of larval growth and survival in a marine fish, *Sebastes melanops*. *Ecology*, 85(5), 1258-1264.
- Bindoff NL, Cheung WWL, Kairo JG, Arístegui J, Guinder VA, Hallberg R, et al. Changing ocean, marine ecosystems, and dependent communities. IPCC Spec Rep Ocean Cryosph a Chang Clim. 2019; 477–587.
- Blaxter, J. H. S. (1988). 1 Pattern and Variety in Development. In *Fish physiology* (Vol. 11, pp. 1-58). Academic Press.
- Blois, J. L., Zarnetske, P. L., Fitzpatrick, M. C., & Finnegan, S. (2013). Climate change and the past, present, and future of biotic interactions. *Science*, 341(6145), 499-504.
- Bodin, O., and B.I. Crona. 2009. The role of social networks in natural resource governance: What relational patterns make a difference? *Global Environmental Change* 19: 366–374.

Boldt, J. L., Buckley, T. W., Rooper, C. N., & Aydin, K. (2012). Factors influencing cannibalism and abundance of walleye pollock (*Theragra chalcogramma*) on the eastern Bering Sea shelf, 1982–20.

Borgatti, S. P., Everett, M. G., Johnson, J. C., & Agneessens, F. (2022). *Analyzing Social Networks Using R*. SAGE Publications Ltd.

Bownds, C., Wilson, R., & Marshall, D. J. (2010). Why do colder mothers produce larger eggs? An optimality approach. *Journal of Experimental Biology*, 213(22), 3796-3801.

Boyd, P. W., Collins, S., Dupont, S., Fabricius, K., Gattuso, J. P., Havenhand, J., ... & Pörtner, H. O. (2018). Experimental strategies to assess the biological ramifications of multiple drivers of global ocean change—a review. *Global change biology*, 24(6), 2239-2261.

Brander, K. (2010). Impacts of climate change on fisheries. *Journal of Marine Systems*, 79(3), 389-402.

Braum, E. (1973). Einflüsse chronischen exogenen Sauerstoffmangels auf die Embryogenese des Herings (*Clupea harengus*). *Netherlands Journal of Sea Research*, 7, 363-375.

Brauner, C. J. (2008). Acid-base balance. In *Fish Larval physiology*, pp. 185–198. Ed. by R. N. Finn, and B. G. Kapoor. Science Publishers, Enfield. 724 pp.

Breitburg, D. (2002). Effects of hypoxia, and the balance between hypoxia and enrichment, on coastal fishes and fisheries. *Estuaries*, 25(4), 767-781.

Bromhead, D., Scholey, V., Nicol, S., Margulies, D., Wexler, J., Stein, M., ... & Lehodey, P. (2015). The potential impact of ocean acidification upon eggs and larvae of yellowfin tuna (*Thunnus albacares*). *Deep Sea Research Part II: Topical Studies in Oceanography*, 113, 268-279.

Brooker, R. M., Munday, P. L., Brandl, S. J., & Jones, G. P. (2014). Local extinction of a coral reef fish explained by inflexible prey choice. *Coral Reefs*, 33(4), 891-896.

Burford, B. P., Wild, L. A., Schwarz, R., Chenoweth, E. M., Sreenivasan, A., Elahi, R., ... & Denny, M. W. (2022). Rapid range expansion of a marine ectotherm reveals the demographic and ecological consequences of short-term variability in seawater temperature and dissolved oxygen. *The American Naturalist*, 199(4), 523-550.

Butler, J. L., D. Fuller, and M. Yaremko. 1999. Age and growth of Market Squid (*Loligo opalescens*) off California during 1998. Calif. Coop. Oceanic Fish. Invest. Rep. 40: 191–195.

Butts, C. T. (2008). network: a Package for Managing Relational Data in R. *Journal of statistical software*, 24, 1-36.

California coastal ocean modeling study: 1. Forward model and the influence of
Cavole, L. M., Demko, A. M., Diner, R. E., Giddings, A., Koester, I., Pagniello, C. M., ... & Franks, P. J. (2016). Biological impacts of the 2013–2015 warm-water anomaly in the Northeast Pacific: winners, losers, and the future. *Oceanography*, 29(2), 273-285.

CDFW [California Department of Fish and Wildlife] (2005) Market squid fishery management plan. California Department of Fish and Game Marine Region. <https://www.wildlife.ca.gov/Conservation/Marine/MSFMP>. Accessed 3 April 2022.

Chavez FP, Costello C, Aseltine-Neilson D, et al (2017) Readying California fisheries for climate change. California Ocean Science Trust, Oakland, CA.

Cheresh, J., & Fiechter, J. (2020). Physical and biogeochemical drivers of alongshore pH and oxygen variability in the California Current System. *Geophysical Research Letters*, 47(19), e2020GL089553.

Cheung, W.W.L., V. W., Sarmiento, J. L., Kearney, K., Watson, R. E. G., Zeller, D., & Pauly, D. (2010). Large-scale redistribution of maximum fisheries catch potential in the global ocean under climate change. *Global Change Biology*, 16(1), 24-35.

Christensen, V., & Walters, C. J. (2004). Ecopath with Ecosim: methods, capabilities and limitations. *Ecological modelling*, 172(2-4), 109-139.

Ciannelli, L., and K. Bailey. 2005. Landscape dynamics and resulting species interactions: the cod-capelin system in the southeastern Bering Sea. *Marine Ecology Progress Series* 291:227–236.

Ciannelli, L., Bartolino, V., & Chan, K. S. (2012). Non-additive and non-stationary properties in the spatial distribution of a large marine fish population. *Proceedings of the Royal Society B: Biological Sciences*, 279(1743), 3635-3642.

Collins, L. A., & Nelson, S. G. (1993). Effects of temperature on oxygen consumption, growth, and development of embryos and yolk-sac larvae of *Siganus randalli* (Pisces: Siganidae). *Marine Biology*, 117(2), 195-204.

Conner, J., and R. R. Lauth. 2017. Results of the 2016 eastern Bering sea continental shelf bottom trawl survey of groundfish and invertebrate resources. U.S. Dep. Commer., NOAA Tech. Memo. NMFS-AFSC352,159 p.

Cook, M. A., Guthrie, K. M., Rust, M. B., & Plesha, P. D. (2005). Effects of salinity and temperature during incubation on hatching and development of lingcod *Ophiodon elongatus* Girard, embryos. *Aquaculture Research*, 36(13), 1298-1303.

Crain, C. M., Kroeker, K., & Halpern, B. S. (2008). Interactive and cumulative effects of multiple human stressors in marine systems. *Ecology letters*, 11(12), 1304-1315.

Cushing, D. H. (1990). Plankton production and year-class strength in fish populations: an update of the match/mismatch hypothesis. In *Advances in marine biology* (Vol. 26, pp. 249-293). Academic Press.

Dahlke, F. T., Leo, E., Mark, F. C., Pörtner, H. O., Bickmeyer, U., Frickenhaus, S., & Storch, D. (2017). Effects of ocean acidification increase embryonic sensitivity to thermal extremes in Atlantic cod, *Gadus morhua*. *Global change biology*, 23(4), 1499-1510.

Dahlke, F. T., Wohlrab, S., Butzin, M., & Pörtner, H. O. (2020). Thermal bottlenecks in the life cycle define climate vulnerability of fish. *Science*, 369(6499), 65-70.

Doi, H., Akamatsu, F., & González, A. L. (2017). Starvation effects on nitrogen and carbon stable isotopes of animals: an insight from meta-analysis of fasting experiments. *Royal Society open science*, 4(8), 170633.

Doney, S. C., Ruckelshaus, M., Emmett Duffy, J., Barry, J. P., Chan, F., English, C. A., ... & Talley, L. D. (2012). Climate change impacts on marine ecosystems. *Annual review of marine science*, 4, 11-37.

Dorn, M., Aydin, K., Fissel, B., Jones, D., McCarthy, A., Palsson, W., & Spalinger, K. (2017). Assessment of the walleye pollock stock in the Gulf of Alaska.

Dudley, P. N., Rogers, T. L., Morales, M. M., Stoltz, A. D., Sheridan, C. J., Beulke, A. K., ... & Carr, M. H. (2021). A more comprehensive climate vulnerability assessment framework for fisheries social-ecological systems. *Frontiers in Marine Science*, 8, 674.

Durant, J. M., Hjermann, D. Ø., Ottersen, G., & Stenseth, N. C. (2007). Climate and the match or mismatch between predator requirements and resource availability. *Climate Research (CR)*, 33(3), 271-283.

Earth Systems Research Laboratory (ESRL). NOAA's Ocean Climate Change Web Portal. 2019. Available: <http://www.esrl.noaa.gov/psd/ipcc/ocn/>

Edwards, M., & Richardson, A. J. (2004). Impact of climate change on marine pelagic phenology and trophic mismatch. *Nature*, 430(7002), 881-884.

Elith, J., & Leathwick, J. R. (2009). Species distribution models: ecological explanation and prediction across space and time. *Annual Review of Ecology, Evolution, and Systematics*, 40(1), 677.

Estes, J. A., Steneck, R. S., & Lindberg, D. R. (2013). Exploring the consequences of species interactions through the assembly and disassembly of food webs: a Pacific-Atlantic comparison. *Bulletin of Marine Science*, 89(1), 11-29.

Faria, A. M., Filipe, S., Lopes, A. F., Oliveira, A. P., Gonçalves, E. J., & Ribeiro, L. (2017). Effects of high pCO₂ on early life development of pelagic spawning marine fish. *Marine and Freshwater Research*, 68(11), 2106-2114.

Feely, R. A., Doney, S., Cooley, S., & Greeley, D. (2010). Oceans acidification: present status and future conditions in a high-CO₂ world. *Oceanography*, 22(4), 36-47.

Fisher, M. C., Moore, S. K., Jardine, S. L., Watson, J. R., & Samhuri, J. F. (2021). Climate shock effects and mediation in fisheries. *Proceedings of the National Academy of Sciences*, 118(2), e2014379117.

Fissel, B., Dalton, M., Garber-Yonts, B., Haynie, A., Kasperski, S., Lee, J., Lew, D., Seung, C., Sparks, K., Szymkowiak, M., Wise, S.. Stock Assessment and Fishery Evaluation Report for the Groundfish Fisheries of the Gulf of Alaska and Bering Sea/Aleutian Islands Area: Economic Status of the Groundfish Fisheries off Alaska, 2019. (2021). Economic and Social Sciences Research Program, Alaska Fisheries Science Center, National Marine Fisheries Service, NOAA.

Forsgren, E., Dupont, S., Jutfelt, F., & Amundsen, T. (2013). Elevated CO₂ affects embryonic development and larval phototaxis in a temperate marine fish. *Ecology and evolution*, 3(11), 3637-3646.

Franke, A., & Clemmesen, C. (2011). Effect of ocean acidification on early life stages of Atlantic herring (*Clupea harengus* L.). *Biogeosciences*, 8(12), 3697-3707.

Free, C. M., Thorson, J. T., Pinsky, M. L., Oken, K. L., Wiedenmann, J., & Jensen, O. P. (2019). Impacts of historical warming on marine fisheries production. *Science*, 363(6430), 979-983.

- Frieder, C. A., Nam, S. H., Martz, T. R., & Levin, L. A. (2012). High temporal and spatial variability of dissolved oxygen and pH in a nearshore California kelp forest. *Biogeosciences*, 9(10), 3917-3930.
- Frommel, A. Y., Maneja, R., Lowe, D., Malzahn, A. M., Geffen, A. J., Folkvord, A., ... & Clemmesen, C. (2012). Severe tissue damage in Atlantic cod larvae under increasing ocean acidification. *Nature Climate Change*, 2(1), 42-46.
- Gadomski, D. M., & Caddell, S. M. (1996). Effects of temperature on the development and survival of eggs of four coastal California fishes. *Oceanographic Literature Review*, 12(43), 1246.
- Gilman, S. E., Urban, M. C., Tewksbury, J., Gilchrist, G. W., & Holt, R. D. (2010). A framework for community interactions under climate change. *Trends in Ecology & Evolution*, 25(6), 325-331.
- Giorgi, A. E., & Congleton, J. L. (1984). Effects of current velocity on development and survival of lingcod, *Ophiodon elongatus*, embryos. *Environmental Biology of Fishes*, 10(1), 15-27.
- Giorgi, A. E. (1981). *The environmental biology of the embryos, egg masses and nesting sites of the lingcod, Ophiodon elongatus* [Doctoral dissertation, University of Washington].
- Goodman, M. C., Carroll, G., Brodie, S., Grüss, A., Thorson, J. T., Kotwicki, S., ... & De Leo, G. A. (2022). Shifting fish distributions impact predation intensity in a sub-Arctic ecosystem. *Ecography*, e06084.
- Gruber, N., Hauri, C., Lachkar, Z., Loher, D., Frölicher, T. L., & Plattner, G. K. (2012). Rapid progression of ocean acidification in the California Current System. *science*, 337(6091), 220-223.
- Guevara-Fletcher, C., Alvarez, P., Sanchez, J., & Iglesias, J. (2016). Effect of temperature on the development and mortality of European hake (*Merluccius merluccius* L.) eggs from southern stock under laboratory conditions. *Journal of Experimental Marine Biology and Ecology*, 476, 50-57.
- Hansen, T. K., & Falk-Petersen, I. B. (2001). The influence of rearing temperature on early development and growth of spotted wolffish *Anarhichas minor* (Olafsen). *Aquaculture research*, 32(5), 369-378.
- Hare JA, Wuenschel MJ, Kimball ME (2012) Projecting Range Limits with Coupled Thermal Tolerance - Climate Change Models: An Example Based on Gray Snapper (*Lutjanus griseus*) along the U.S. East Coast. PLoS ONE 7(12): e52294. <https://doi.org/10.1371/journal.pone.0052294>

- Harley, C. D., Randall Hughes, A., Hultgren, K. M., Miner, B. G., Sorte, C. J., Thornber, C. S., ... & Williams, S. L. (2006). The impacts of climate change in coastal marine systems. *Ecology letters*, 9(2), 228-241.
- Hart, J.L. (1973). Pacific fishes of Canada. Fish. Res. Board. Can. Bull. No. 180. 740 pp.
- Hassell, K. L., Coutin, P. C., & Nugegoda, D. (2008). Hypoxia impairs embryo development and survival in black bream (*Acanthopagrus butcheri*). *Marine Pollution Bulletin*, 57(6-12), 302-306.
- Hauri, C., Gruber, N., Vogt, M., Doney, S. C., Feely, R. A., Lachkar, Z., ... & Plattner, G. K. (2013). Spatiotemporal variability and long-term trends of ocean acidification in the California Current System. *Biogeosciences*, 10(1), 193-216.
- Heine, J. N. 2017. California Cooperative Oceanic Fisheries Investigation (Report No.55). California Department of Fish and Wildlife; University of California, Scripps Institute of Oceanography; National Oceanographic and Atmospheric Association, National Marine Fisheries Service. Available: http://calcofi.org/publications/calcofireport/v55/Vol_55_CalCOFIREport.pdf. (June 2021).
- Helaouët, P., & Beaugrand, G. (2009). Physiology, ecological niches and species distribution. *Ecosystems*, 12(8), 1235-1245.
- Heller-Shipley, M. A., Stockhausen, W. T., Daly, B. J., Punt, A. E., & Goodman, S. E. (2021). Should harvest control rules for male-only fisheries include reproductive buffers? A Bering Sea Tanner crab (*Chionoecetes bairdi*) case study. *Fisheries Research*, 243, 106049.
- Hempel, G. (1979). *Early life history of marine fish: the egg stage*. Washington Sea Grant: distributed by University of Washington Press.
- Hijmans, Robert J., et al. "Package 'geosphere'." Spherical trigonometry 1.7 (2017).
- Hodgson, E. E., Essington, T. E., & Kaplan, I. C. (2016). Extending Vulnerability Assessment to Include Life Stages Considerations. *PloS one*, 11(7), e0158917.
- Holland, D. S., Abbott, J. K., & Norman, K. E. (2020). Fishing to live or living to fish: job satisfaction and identity of west coast fishermen. *Ambio*, 49(2), 628-639.

- Hollowed, A. B., Barange, M., Beamish, R. J., Brander, K., Cochrane, K., Drinkwater, K., ... & Yamanaka, Y. (2013). Projected impacts of climate change on marine fish and fisheries. *ICES Journal of Marine Science*, 70(5), 1023-1037.
- Holsman, K. K., Haynie, A. C., Hollowed, A. B., Reum, J. C. P., Aydin, K., Hermann, A. J., ... & Punt, A. E. (2020). Ecosystem-based fisheries management forestalls climate-driven collapse. *Nature communications*, 11(1), 1-10.
- Houde, E. D., & Hoyt, R. (1987). Fish early life dynamics and recruitment variability. *Trans. Am. Fish. Soc.*
- Hunsicker ME, Ciannelli L, Bailey KM, Zador S, Stige LC (2013) Climate and Demography Dictate the Strength of Predator-Prey Overlap in a Subarctic Marine Ecosystem. *PLoS ONE* 8(6): e66025. doi:10.1371/journal.pone.0066025
- Hunt Jr, G. L., Coyle, K. O., Eisner, L. B., Farley, E. V., Heintz, R. A., Mueter, F., ... & Stabeno, P. J. (2011). Climate impacts on eastern Bering Sea foodwebs: a synthesis of new data and an assessment of the Oscillating Control Hypothesis. *ICES Journal of Marine Science*, 68(6), 1230-1243.
- Hurst, T. P., Abookire, A. A., & Knoth, B. (2010). Quantifying thermal effects on contemporary growth variability to predict responses to climate change in northern rock sole (*Lepidopsetta polyxystra*). *Canadian Journal of Fisheries and Aquatic Sciences*, 67(1), 97-107.
- Hurst, T. P., Fernandez, E. R., & Mathis, J. T. (2013). Effects of ocean acidification on hatch size and larval growth of walleye pollock (*Theragra chalcogramma*). *ICES Journal of Marine Science*, 70(4), 812-822.
- IPCC, 2021: Climate Change 2021: The Physical Science Basis. Contribution of Working Group I to the Sixth Assessment Report of the Intergovernmental Panel on Climate Change [Masson-Delmotte, V., P. Zhai, A. Pirani, S.L. Connors, C. Péan, S. Berger, N. Caud, Y. Chen, L. Goldfarb, M.I. Gomis, M. Huang, K. Leitzell, E. Lonnoy, J.B.R. Matthews, T.K. Maycock, T. Waterfield, O. Yelekçi, R. Yu, and B. Zhou (eds.)]. Cambridge University Press, Cambridge, United Kingdom and New York, NY, USA, In press, doi:10.1017/9781009157896.
- Jewell, E.D., (1968). SCUBA diving observations on lingcod spawning at a Seattle breakwater. Wash. Dept. Fish., Fish. Res. Pap., 3(1): 27-34.
- Johnson, T. R., Henry, A. M., & Thompson, C. (2014). Qualitative indicators of social resilience in small-scale fishing communities: an emphasis on perceptions and practice. *Human Ecology Review*, 97-115.

- Jordaan, A., Hayhurst, S. E., & Kling, L. J. (2006). The influence of temperature on the stage at hatch of laboratory reared *Gadus morhua* and implications for comparisons of length and morphology. *Journal of Fish Biology*, 68(1), 7-24.
- Kamler, E. (2008). Resource allocation in yolk-feeding fish. *Reviews in Fish biology and Fisheries*, 18(2), 143.
- Kempf, A., Stelzenmüller, V., Akimova, A., & Floeter, J. (2013). Spatial assessment of predator–prey relationships in the North Sea: the influence of abiotic habitat properties on the spatial overlap between 0-group cod and grey gurnard. *Fisheries Oceanography*, 22(3), 174-192.
- King, J. R., & Withler, R. E. (2005). Male nest site fidelity and female serial polyandry in lingcod (*Ophiodon elongatus*, Hexagrammidae). *Molecular Ecology*, 14(2), 653-660.
- Kingsolver, J. G. (2009). The Well-Tempered Biologist: (American Society of Naturalists Presidential Address). *The American Naturalist*, 174(6), 755-768.
- Kortsch, S., Primicerio, R., Fossheim, M., Dolgov, A. V., & Aschan, M. (2015). Climate change alters the structure of arctic marine food webs due to poleward shifts of boreal generalists. *Proceedings of the Royal Society B: Biological Sciences*, 282(1814), 20151546.
- Koslow, J. A., & Allen, C. (2011). The influence of the ocean environment on the abundance of Market Squid, *Doryteuthis (Loligo) opalescens*, paralarvae in the Southern California Bight. *CalCOFI Rep*, 52, 205-213.
- Langbehn, T. J., & Varpe, Ø. (2017). Sea-ice loss boosts visual search: Fish foraging and changing pelagic interactions in polar oceans. *Global Change Biology*, 23(12), 5318-5330.
- Latham, A. D. M., Latham, M. C., Knopff, K. H., Hebblewhite, M., & Boutin, S. (2013). Wolves, white-tailed deer, and beaver: implications of seasonal prey switching for woodland caribou declines. *Ecography*, 36(12), 1276-1290.
- Laurel, B. J., & Blood, D. M. (2011). The effects of temperature on hatching and survival of northern rock sole larvae (*Lepidopsetta polyxystra*). *Fishery Bulletin*, 109(3), 282-291.

- Laurel, B. J., & Rogers, L. A. (2020). Loss of spawning habitat and prerecruits of Pacific cod during a Gulf of Alaska heatwave. *Canadian Journal of Fisheries and Aquatic Sciences*, 77(4), 644-650.
- Laurel, B. J., Copeman, L. A., Spencer, M., & Iseri, P. (2018). Comparative effects of temperature on rates of development and survival of eggs and yolk-sac larvae of Arctic cod (*Boreogadus saida*) and walleye pollock (*Gadus chalcogrammus*). *ICES Journal of Marine Science*, 75(7), 2403-2412.
- Leo, E., Dahlke, F. T., Storch, D., Pörtner, H. O., & Mark, F. C. (2018). Impact of Ocean Acidification and Warming on the bioenergetics of developing eggs of Atlantic herring *Clupea harengus*. *Conservation physiology*, 6(1), coy050.
- Llanos-Rivera, A., & Castro, L. R. (2006). Inter-population differences in temperature effects on *Engraulis ringens* yolk-sac larvae. *Marine Ecology Progress Series*, 312, 245-253.
- Longo, G. C., Lam, L., Basnett, B., Samhoury, J., Hamilton, S., Andrews, K., ... & Nichols, K. M. (2020). Strong population differentiation in lingcod (*Ophiodon elongatus*) is driven by a small portion of the genome. *Evolutionary applications*, 13(10), 2536-2554.
- Love, M. S. (2011). *Certainly more than you want to know about the fishes of the Pacific Coast: a postmodern experience*. Really Big Press.
- Low, C. J., and R. J. Beamish. (1978). A study of the nesting behavior of lingcod (*Ophiodon elongatus*) in the strait of Georgia, British Columbia. *Can. Fish. Mar. Serv. Tech. Rep.* 843.
- Low, N. H., Micheli, F., Aguilar, J. D., Arce, D. R., Boch, C. A., Bonilla, J. C., ... & Woodson, C. B. (2021). Variable coastal hypoxia exposure and drivers across the southern California Current. *Scientific reports*, 11(1), 1-10.
- Lynn, K. (2008). Status of the Fisheries Report 2008. California Department of Fish and Wildlife. 12 pp.
- Lønning, S., Kjørsvik, E., & Falk-petersen, I. B. (1988). A comparative study of pelagic and demersal eggs from common marine fishes in northern Norway. *Sarsia*, 73(1), 49-60.
- Mason, J. G., Eurich, J. G., Lau, J. D., Battista, W., Free, C. M., Mills, K. E., ... & Kleisner, K. M. (2022). Attributes of climate resilience in fisheries: From theory to practice. *Fish and Fisheries*, 23(3), 522-544.

McGarigal, K., S. A. Cushman, M. C. Neel, and E. Ene. 2002. FRAGSTATS: Spatial Pattern Analysis Program for Categorical Maps. Computer software program produced by the authors at the University of Massachusetts, Amherst.

Miller, D. J., & Geibel, J. J. (1973). *Summary of Blue Rockfish and Lingcod Life Histories, a Reef Ecology Study, and Giant Kelp, Macrocystis Pyrifera, Experiments in Monterey Bay, California* (Vol. 158). State of California, Resources Agency, Department of Fish and Game.

Miller, G. M., Watson, S. A., Donelson, J. M., McCormick, M. I., & Munday, P. L. (2012). Parental environment mediates impacts of increased carbon dioxide on a coral reef fish. *Nature Climate Change*, 2(12), 858-861.

Miller, T. J., Crowder, L. B., Rice, J. A., & Marschall, E. A. (1988). Larval size and recruitment mechanisms in fishes: toward a conceptual framework. *Canadian Journal of Fisheries and Aquatic Sciences*, 45(9), 1657-1670.

Moore, A. M., Arango, H. G., Broquet, G., Edwards, C., Veneziani, M., Powell, B., Foley, D., *et al.* 2011. The Regional Ocean Modeling System (ROMS) 4-dimensional variational data assimilation systems. Part II - Performance and application to the California Current System. *Progress in Oceanography*, 91: 50–73. Elsevier Ltd. <http://dx.doi.org/10.1016/j.pocean.2011.05.003>.

Morley, J. W., Selden, R. L., Latour, R. J., Frölicher, T. L., Seagraves, R. J., & Pinsky, M. L. (2018). Projecting shifts in thermal habitat for 686 species on the North American continental shelf. *PloS one*, 13(5), e0196127.

Mote, P. W., & Mantua, N. J. (2002). Coastal upwelling in a warmer future. *Geophysical research letters*, 29(23), 53-1.

Mueter, F. J., & Litzow, M. A. (2008). Sea ice retreat alters the biogeography of the Bering Sea continental shelf. *Ecological Applications*, 18(2), 309-320.

Mueter, F. J., Bond, N. A., Ianelli, J. N., & Hollowed, A. B. (2011). Expected declines in recruitment of walleye pollock (*Theragra chalcogramma*) in the eastern Bering Sea under future climate change. *ICES Journal of Marine Science*, 68(6), 1284-1296.

Munday, P. L., Donelson, J. M., Dixon, D. L., & Endo, G. G. (2009). Effects of ocean acidification on the early life history of a tropical marine fish. *Proceedings of the Royal Society B: Biological Sciences*, 276(1671), 3275-3283.

Munday, P. L., Watson, S. A., Parsons, D. M., King, A., Barr, N. G., Mcleod, I. M., ... & Pether, S. M. (2016). Effects of elevated CO₂ on early life history development of the yellowtail kingfish, *Seriola lalandi*, a large pelagic fish. *ICES Journal of Marine Science*, 73(3), 641-649.

Murphy, J. T. (2020). Climate change, interspecific competition, and poleward vs. depth distribution shifts: Spatial analyses of the eastern Bering Sea snow and Tanner crab (*Chionoecetes opilio* and *C. bairdi*). *Fisheries Research*, 223, 105417.

Nagelkerken, I., Goldenberg, S. U., Ferreira, C. M., Ullah, H., & Connell, S. D. (2020). Trophic pyramids reorganize when food web architecture fails to adjust to ocean change. *Science*, 369(6505), 829-832.

Neveu, E., Moore, A. M., Edwards, C. A., Fiechter, J., Drake, P., Crawford, W. J., Jacox, M. G., *et al.* 2016. An historical analysis of the California Current circulation using ROMS 4D-Var: System configuration and diagnostics. *Ocean Modelling*, 99: 133–151. Elsevier Ltd.

NMFS [National Marine Fisheries Service] (2018) Fisheries economics of the United States 2016. NOAA, US Department of Commerce

NMFS [National Marine Fisheries Service] (2022) Fisheries Economics of the United States, 2019. U.S. Dept. of Commerce, NOAA Tech. Memo. NMFS-F/SPO-229A, 236 p.

NOAA Fisheries (2020, October 20). *Species Directory: Pacific Halibut*. Retrieved from <https://www.fisheries.noaa.gov/species/pacific-halibut>

NOAA Fisheries (2022a, April 21). *Species Directory: Alaska Pollock*. Retrieved from <https://www.fisheries.noaa.gov/species/alaska-pollock>

NOAA Fisheries (2022b, June 22). *Species Directory: Pacific Cod*. Retrieved from <https://www.fisheries.noaa.gov/species/pacific-cod>

NOAA Fisheries (2022c, May 17). *Species Directory: Arrowtooth Flounder*. Retrieved from <https://www.fisheries.noaa.gov/species/arrowtooth-flounder>

Olito, C., White, C. R., Marshall, D. J., & Barneche, D. R. (2017). Estimating monotonic rates from biological data using local linear regression. *Journal of Experimental Biology*, 220(5), 759-764.

Olsen, E., Aanes, S., Mehl, S., Holst, J. C., Aglen, A., & Gjørseter, H. (2010). Cod, haddock, saithe, herring, and capelin in the Barents Sea and adjacent waters: a review of the biological value of the area. *ICES Journal of Marine Science*, 67(1), 87-101.

- Ortiz, I., Aydin, K., Hermann, A. J., Gibson, G. A., Punt, A. E., Wiese, F. K., ... & Boyd, C. (2016). Climate to fish: synthesizing field work, data and models in a 39-year retrospective analysis of seasonal processes on the eastern Bering Sea shelf and slope. *Deep Sea Research Part II: Topical Studies in Oceanography*, 134, 390-412.
- Oseid, D. M., & Smith Jr, L. L. (1971). Survival and hatching of walleye eggs at various dissolved oxygen levels. *The Progressive Fish-Culturist*, 33(2), 81-85.
- Pacifici, M., Foden, W. B., Visconti, P., Watson, J. E., Butchart, S. H., Kovacs, K. M., ... & Corlett, R. T. (2015). Assessing species vulnerability to climate change. *Nature Climate Change*, 5(3), 215-224.
- Paine, R. T., Tegner, M. J., & Johnson, E. A. (1998). Compounded perturbations yield ecological surprises. *Ecosystems*, 1(6), 535-545.
- Palumbi, S. R. (2004). Why mothers matter. *Nature*, 430(7000), 621-622.
- Pankhurst, N. W., & Munday, P. L. (2011). Effects of climate change on fish reproduction and early life history stages. *Marine and Freshwater Research*, 62(9), 1015-1026.
- Papaioannou, E. A., Selden, R. L., Olson, J., McCay, B. J., Pinsky, M. L., & St. Martin, K. (2021). Not All Those Who Wander Are Lost—Responses of Fishers' Communities to Shifts in the Distribution and Abundance of Fish. *Frontiers in Marine Science*, 8.
- Parker, L. M., Ross, P. M., O'Connor, W. A., Borysko, L., Raftos, D. A., & Pörtner, H. O. (2012). Adult exposure influences offspring response to ocean acidification in oysters. *Global change biology*, 18(1), 82-92.
- Pauly, D., & Christensen, V. (1995). Primary production required to sustain global fisheries. *Nature*, 374(6519), 255-257.
- Peck, M. A., Reglero, P., Takahashi, M., & Catalán, I. A. (2013). Life cycle ecophysiology of small pelagic fish and climate-driven changes in populations. *Progress in Oceanography*, 116, 220-245.
- Pecl, G. T. & G. D. Jackson. 2008. The potential impacts of climate change on inshore squid: biology, ecology and fisheries. *Rev. Fish Biol. Fish.* 18:373–385.
- Peers, M. J., Wehtje, M., Thornton, D. H., & Murray, D. L. (2014). Prey switching as a means of enhancing persistence in predators at the trailing southern edge. *Global change biology*, 20(4), 1126-1135.

- Peña, R., Dumas, S., Zavala-Leal, I., & Contreras-Olguín, M. (2014). Effect of incubation temperature on the embryonic development and yolk-sac larvae of the Pacific red snapper *Lutjanus peru* (Nichols & Murphy, 1922). *Aquaculture Research*, 45(3), 519-527.
- Pepin, P. (1991). Effect of temperature and size on development, mortality, and survival rates of the pelagic early life history stages of marine fish. *Canadian Journal of Fisheries and Aquatic Sciences*, 48(3), 503-518.
- Perry, A. L., Low, P. J., Ellis, J. R., & Reynolds, J. D. (2005). Climate change and distribution shifts in marine fishes. *science*, 308(5730), 1912-1915.
- Peterson Williams, M. J., Robbins Gisclair, B., Cerny-Chipman, E., LeVine, M., & Peterson, T. (2022). The heat is on: Gulf of Alaska Pacific cod and climate-ready fisheries. *ICES Journal of Marine Science*, 79(2), 573-583.
- Pfeiffer, L., & Gratz, T. (2016). The effect of rights-based fisheries management on risk taking and fishing safety. *Proceedings of the National Academy of Sciences*, 113(10), 2615-2620.
- Piggott, J. J., Townsend, C. R., & Matthaei, C. D. (2015). Reconceptualizing synergism and antagonism among multiple stressors. *Ecology and evolution*, 5(7), 1538-1547.
- Pikitch, E. K., Santora, C., Babcock, E. A., Bakun, A., Bonfil, R., Conover, D. O., & Houde, E. D. (2004). Ecosystem-based fishery management. *Science*, 305, 346–348. <https://doi.org/10.1126/science.1098222>
- Pimentel, M. S., Faleiro, F., Dionísio, G., Repolho, T., Pousão-Ferreira, P., Machado, J., & Rosa, R. (2014). Defective skeletogenesis and oversized otoliths in fish early stages in a changing ocean. *Journal of Experimental Biology*, 217(12), 2062-2070.
- Politis, S. N., Dahlke, F. T., Butts, I. A., Peck, M. A., & Trippel, E. A. (2014). Temperature, paternity and asynchronous hatching influence early developmental characteristics of larval Atlantic cod, *Gadus morhua*. *Journal of Experimental Marine Biology and Ecology*, 459, 70-79.
- Poloczanska, E. S., Burrows, M. T., Brown, C. J., García Molinos, J., Halpern, B. S., Hoegh-Guldberg, O., ... & Sydeman, W. J. (2016). Responses of marine organisms to climate change across oceans. *Frontiers in Marine Science*, 3, 62.

- Pomeroy, C., Hunter, M., & Los Huertos, M. (2002). *Socio-economic profile of the California wetfish industry*. California Seafood Council.
- Pörtner, H. O., & Farrell, A. P. (2008). Physiology and climate change. *Science*, 690-692.
- Pörtner, H. O., & Peck, M. A. (2010). Climate change effects on fishes and fisheries: towards a cause-and-effect understanding. *Journal of fish biology*, 77(8), 1745-1779.
- Pörtner, H. O., Langenbuch, M., & Michaelidis, B. (2005). Synergistic effects of temperature extremes, hypoxia, and increases in CO₂ on marine animals: From Earth history to global change. *Journal of Geophysical Research: Oceans*, 110(C9).
- Pörtner, H. O. (2012). Integrating climate-related stressor effects on marine organisms: unifying principles linking molecule to ecosystem-level changes. *Marine Ecology Progress Series*, 470, 273-290.
- Powell, F., Levine, A., & Ordonez-Gauger, L. (2022). Climate adaptation in the Market Squid fishery: fishermen responses to past variability associated with El Niño Southern Oscillation cycles inform our understanding of adaptive capacity in the face of future climate change. *Climatic Change*, 173(1), 1-21.
- Pozo Buil, M., Jacox, M. G., Fiechter, J., Alexander, M. A., Bograd, S. J., Curchitser, E. N., ... & Stock, C. A. (2021). A dynamically downscaled ensemble of future projections for the California current system. *Frontiers in Marine Science*, 8, 612874.
- Quinn, T. J., & Deriso, R. B. (1999). *Quantitative fish dynamics*. Oxford University Press.
- Ralston, S., Dorval, E., Ryley, L., Sakuma, K. M., & Field, J. C. (2018). Predicting Market Squid (*Doryteuthis opalescens*) landings from pre-recruit abundance. *Fisheries Research*, 199, 12-18.
- Ramirez-Sanchez, S., and E. Pinkerton. 2009. The impact of resource scarcity on bonding and bridging social capital: The case of fishers' information-sharing networks in Loreto, BCS, Mexico. *Ecology and Society* 14: 22.
- realistic versus climatological forcing. *J. Geophys. Res.* 114:4774. doi: 10.1029/2008jc004774
- Recksiek, C. W. & Frey, H.W. (1978). Biological, oceanographic, and acoustic aspects of the Market Squid, *Loligo opalescens* Berry. State of California, The Resources Agency, Department of Fish and Game Fish Bulletin, 169.

- Reiss, C. S., Maxwell, M. R., Hunter, J. R., & Henry, A. N. N. E. T. T. E. (2004). Investigating environmental effects on population dynamics of *Loligo opalescens* in the Southern California Bight. *California Cooperative Oceanic Fisheries Investigation Report*, 45, 87.
- Reum, J. C., Alin, S. R., Harvey, C. J., Bednaršek, N., Evans, W., Feely, R. A., ... & Sabine, C. L. (2016). Interpretation and design of ocean acidification experiments in upwelling systems in the context of carbonate chemistry co-variation with temperature and oxygen. *ICES Journal of Marine Science*, 73(3), 582-595.
- Rindorf, A., Gislason, H., & Lewy, P. (2006). Prey switching of cod and whiting in the North Sea. *Marine Ecology Progress Series*, 325, 243-253.
- Rogers, L. A., Griffin, R., Young, T., Fuller, E., St Martin, K., & Pinsky, M. L. (2019). Shifting habitats expose fishing communities to risk under climate change. *Nature Climate Change*, 9(7), 512-516.
- Rogers, L. A., Wilson, M. T., Duffy-Anderson, J. T., Kimmel, D. G., & Lamb, J. F. (2021). Pollock and “the Blob”: Impacts of a marine heatwave on walleye pollock early life stages. *Fisheries Oceanography*, 30(2), 142-158.
- Rombough, P. J. (1997). The effects of temperature on embryonic and larval development. In ‘*Global Warming: Implications for Freshwater and Marine Fish*’. (Eds C. M. Wood and D. G. McDonald.) pp. 177–223.
- Rooper, C. N., Ortiz, I., Hermann, A. J., Laman, N., Cheng, W., Kearney, K., & Aydin, K. (2021). Predicted shifts of groundfish distribution in the Eastern Bering Sea under climate change, with implications for fish populations and fisheries management. *ICES Journal of Marine Science*, 78(1), 220-234.
- Rosa, R., & Seibel, B. A. (2008). Synergistic effects of climate-related variables suggest future physiological impairment in a top oceanic predator. *Proceedings of the National Academy of Sciences*, 105(52), 20776-20780.
- Sakuma, K.M., Field, J.C., Mantua, N.J., Ralston, S., Marinovic Carrion, B.B.C.N., 2016. Anomalous epipelagic micronekton assemblage patterns in the neritic waters of the California current in spring 2015 during a period of extreme ocean conditions. *Calif. Coop. Ocean. Fish. Invest Rep.* 57, 163–183.
- Sampaio, E., Santos, C., Rosa, I. C., Ferreira, V., Pörtner, H. O., Duarte, C. M., ... & Rosa, R. (2021). Impacts of hypoxic events surpass those of future ocean warming and acidification. *Nature Ecology & Evolution*, 5(3), 311-321.

Schweiger, O., Settele, J., Kudrna, O., Klotz, S., & Kühn, I. (2008). Climate change can cause spatial mismatch of tropically interacting species. *Ecology*, 89(12), 3472-3479.

Selden, R. L., Batt, R. D., Saba, V. S., & Pinsky, M. L. (2018). Diversity in thermal affinity among key piscivores buffers impacts of ocean warming on predator–prey interactions. *Global Change Biology*, 24(1), 117-131.

Shei, M., Mies, M., & Olivotto, I. (2017). Other demersal spawners and mouthbrooders. *Marine ornamental species aquaculture*, 223-250.

Shelbourne, J. E. (1955). Significance of the subdermal space in pelagic fish embryos and larvae. *Nature*, 176(4485), 743-744.

Shumway, D. L., Warren, C. E., & Doudoroff, P. (1964). Influence of oxygen concentration and water movement on the growth of steelhead trout and coho salmon embryos. *Transactions of the American Fisheries Society*, 93(4), 342-356.

Siefert, R. E., Carlson, A. R., & Herman, L. J. (1974). Effects of reduced oxygen concentrations on the early life stages of mountain whitefish, smallmouth bass, and white bass. *The Progressive Fish-Culturist*, 36(4), 186-190.

Silberberg, K. R., Laidig, T. E., Adams, P. B., & Albin, D. (2001). Analysis of maturity in lingcod, *Ophiodon elongatus*. *California Fish and Game*, 87(4), 139-152.

Silver, S. J., Warren, C. E., & Doudoroff, P. (1963). Dissolved oxygen requirements of developing steelhead trout and chinook salmon embryos at different water velocities. *Transactions of the American Fisheries Society*, 92(4), 327-343.

Somero, G. N. (2010). The physiology of climate change: how potentials for acclimatization and genetic adaptation will determine ‘winners’ and ‘losers’. *Journal of Experimental Biology*, 213(6), 912-920.

Song, H., Kemp, D. B., Tian, L., Chu, D., Song, H., & Dai, X. (2021). Thresholds of temperature change for mass extinctions. *Nature communications*, 12(1), 1-8.

Spies, I., Aydin, K., Ianelli, J. N., & Palsson, W. (2017). Assessment of the arrowtooth flounder stock in the Gulf of Alaska.

Spies, I., Gruenthal, K. M., Drinan, D. P., Hollowed, A. B., Stevenson, D. E., Tarpey, C. M., & Hauser, L. (2020). Genetic evidence of a northward range expansion in the eastern Bering Sea stock of Pacific cod. *Evolutionary applications*, 13(2), 362-375.

- Stabeno, P. J., Bell, S. W., Bond, N. A., Kimmel, D. G., Mordy, C. W., & Sullivan, M. E. (2019). Distributed biological observatory region 1: physics, chemistry and plankton in the northern Bering sea. *Deep Sea Research Part II: Topical Studies in Oceanography*, 162, 8-21.
- Stauffer, G. (compiler). 2004. NOAA Protocols for Groundfish Bottom Trawl Surveys of the Nation's Fishery Resources. U.S. Dep. Commerce, NOAA Tech. Memo. NMFS-F/SPO-65, 205 p.
- Stevenson, D. E., & Lauth, R. R. (2019). Bottom trawl surveys in the northern Bering Sea indicate recent shifts in the distribution of marine species. *Polar Biology*, 42(2), 407-421.
- Stewart, R. I., Dossena, M., Bohan, D. A., Jeppesen, E., Kordas, R. L., Ledger, M. E., ... & Woodward, G. (2013). Mesocosm experiments as a tool for ecological climate-change research. *Advances in ecological research*, 48, 71-181.
- Sunday, J. M., Bates, A. E., & Dulvy, N. K. (2012). Thermal tolerance and the global redistribution of animals. *Nature Climate Change*, 2(9), 686-690.
- Sundby, S., & Kristiansen, T. (2015). The principles of buoyancy in marine fish eggs and their vertical distributions across the world oceans. *PloS one*, 10(10), e0138821.
- Szeche Lam, L. (2019). Geographic and Habitat-Based Variation in Lingcod (*Ophiodon Elongatus*) Demography and Life-History Along the US West Coast. [Master's Thesis].
- Thorne, L. H., & Nye, J. A. (2021). Trait-mediated shifts and climate velocity decouple an endothermic marine predator and its ectothermic prey. *Scientific reports*, 11(1), 1-14.
- Tsenkova, S., & Youssef, K. (2014). Resource-based communities. *Encyclopedia of Quality of Life and Well-Being Research*, 5531-34.
- Tsoukali, S., Visser, A. W., & MacKenzie, B. R. (2016). Functional responses of North Atlantic fish eggs to increasing temperature. *Marine Ecology Progress Series*, 555, 151-165.
- Van Noord, J. E., & Dorval, E. (2017). Oceanographic influences on the distribution and relative abundance of Market Squid paralarvae (*Doryteuthis opalescens*) off the southern and central California coast. *Marine Ecology*, 38(3), e12433.
- Veneziani, M., Edwards, C. A., Doyle, J. D., and Foley, D. (2009). A central

- Visser, M. E., & Gienapp, P. (2019). Evolutionary and demographic consequences of phenological mismatches. *Nature ecology & evolution*, 3(6), 879-885.
- Vojkovich, M. 1998. The California fishery for Market Squid (*Loligo opalescens*). CalCOFI (California Cooperative Oceanic Fisheries Investigations) Reports 39:55–60.
- Wang, X., Song, L., Chen, Y., Ran, H., & Song, J. (2017). Impact of ocean acidification on the early development and escape behavior of marine medaka (*Oryzias melastigma*). *Marine environmental research*, 131, 10-18.
- Watson, S. A., Allan, B. J., McQueen, D. E., Nicol, S., Parsons, D. M., Pether, S. M., ... & Munday, P. L. (2018). Ocean warming has a greater effect than acidification on the early life history development and swimming performance of a large circumglobal pelagic fish. *Global change biology*, 24(9), 4368-4385.
- Wespestad, V. G., Fritz, L.W., Ingraham, W. J., & Megrey, B. A. (2000). On relationships between cannibalism, climate variability, physical transport, and recruitment success of Bering Sea walleye pollock (*Theragra chalcogramma*). *ICES Journal of Marine Science*, 57(2), 272-278.
- Wilby G.V. (1937) The Lingcod, *Ophiodon elongatus* Girard. Fisheries Resource Board of Canada Bulletin 54(24).
- Wilderbuer, T.K., Nichol, D.G., Aydin, K. (2010) Arrowtooth Flounder. In Stock Assessment and fishery evaluation report for the groundfish resources of the Bering Sea and Aleutian Islands regions. North Pacific Fishery Management Council, Anchorage, AK.
- Wilkinson, D. P., Golding, N., Guillera-Arroita, G., Tingley, R., & McCarthy, M. A. (2021). Defining and evaluating predictions of joint species distribution models. *Methods in Ecology and Evolution*, 12(3), 394-404.
- Wilson, J. R., Broitman, B. R., Caselle, J. E., & Wendt, D. E. (2008). Recruitment of coastal fishes and oceanographic variability in central California. *Estuarine, Coastal and Shelf Science*, 79(3), 483-490.
- Wing, B. L., and R. W. Mercer. 1990. Temporary northern range extension of the squid *Loligo opalescens* in Southeast Alaska. *Veliger* 33:238–240.
- Wood, S. N. (2011). Fast stable restricted maximum likelihood and marginal likelihood estimation of semiparametric generalized linear models. In *Journal of the Royal Statistical Society (B)* (Vol. 73, Issue 1, pp. 3–36).

Wyllie-Echeverria, T. I. N. A., & Wooster, W. S. (1998). Year-to-year variations in Bering Sea ice cover and some consequences for fish distributions. *Fisheries Oceanography*, 7(2), 159-170.

Yaremko, M. 2002. California Market Squid. In Leet, W., C. Dewees, R. Klingbeil, and E. Larson, eds. *California's Living Marine Resources: A Status Report*. California Department of Fish and Game.

Zeidberg, L. D., Butler, J. L., Ramon, D., Cossio, A., Stierhoff, K. L., & Henry, A. (2012). Estimation of spawning habitats of Market Squid (*Doryteuthis opalescens*) from field surveys of eggs off Central and Southern California. *Marine Ecology*, 33(3), 326-336.

Zeidberg, L.D., G. Isaac, C.L. Widmer, H. Neumeister and W.F. Gilly. 2011. Egg capsule hatch rate and incubation duration of the California Market Squid, *Doryteuthis (Loligo) opalescens*: insights from laboratory manipulations. *Mar. Ecol.* doi:10.1111/j.1439-0485.2011.00445.x.

Zeidberg, L. D., W. Hamner, K. Moorehead & E. Kristof. 2004. Egg masses of *Loligo opalescens* (Cephalopoda: Myopsida) in Monterey Bay, California following the El Niño event of 1997–1998. *Bull. Mar. Sci.* 74:129–141.